PDGF signalling during Neural Crest Cell migration

PDGF controls contact inhibition of locomotion by regulating N-cadherin during neural crest cell migration

Isabel Bahm

Submitted in partial fulfilment of the requirements for the degree of Doctor of Philosophy at University College London

March 2017

I, Isabel Bahm confirm that the work presented in this thesis is my own. Where information has been derived from other sources, I confirm that this has been indicated in the thesis.

Abstract

Neural crest cells are a transient cell population, which migrates through the vertebrate embryonic body, and eventually gives rise to a many different cell types in the adult. Contact inhibition of locomotion (CIL) is a fundamental property of the collective migrating neural crest cells. CIL describes a process by which colliding cells change their direction upon collision and move away from each other, which has been linked to cell dispersion, boundary formation and metastasis. CIL is acquired in neural crest cells during Epithelial-to-Mesenchymal-Transition (EMT), by a switch in the expression of cadherins, from E to N-cadherin. To examine what governs this change I study PDGF signalling during *Xenopus laevis* cranial neural crest migration. Here I show that PDGFRα and its ligand PDGF-A are expressed in pre-migratory and migrating cranial neural crest cells. Inhibition of PDGF-A/PDGFRα impairs neural crest migration *in vivo* and cell dispersion *in vitro*. I find that PDGFRα inhibition leads to a decrease of N-cadherin levels in neural crest cells. Further, I demonstrate that PDGFRα signalling controls N-cadherin dependent CIL. This cellular response is controlled by the PI3K/AKT signalling pathway as a downstream effector of the PDGFRα cellular response in cranial neural crest cells. This data lead me to propose a novel mechanism by which PDGF signalling as a tissue-autonomous regulator of EMT is regulating N-cadherin dependent CIL during cranial neural crest cell migration in *Xenopus laevis*.

Acknowledgement

First, I would like to thank Professor Roberto Mayor for his supervision and great science discussions during my PhD project. In addition, I would like to thank Dr. Paul Frankel for his collaborative interactions and discussions, which gave an important contribution to the development of this project. I would also like to thank Claire Scott who I had the opportunity to teach and also helped with *in situ* hybridization experiments. Further, I have to thank R. Winkelbauer, K. Symes, W. Richardson and M. Tada for sharing the PDGFRαw37, mouse PDGF-A and PI3K-CAAX, ph-AKT-GFP clones, respectively.

Special thanks go to the members of the Mayor lab from 2013 to 2017, who provided their help, support and excellent scientific discussions.

On a more personal side, I would like all my family for their constant and unwavering support. I would also like to thank my friends at UCL for their support, the fun and the scientific and sometimes un-scientific discussions. Finally, I would like to thank my partner David for his understanding, support and love.

Table of content

Abstract **3**

Acknowledgement **4**

Table of figures **8**

List of tables **11**

List of supplementary movies **12**

List of abbreviations **13**

Chapter 1 Introduction **15**

1.1 The Neural Crest **16**

1.1.1 Neural crest cell induction 18

1.1.2 Delamination and Epithelial-to-mesenchymal transition 18

1.1.3 Neural crest migration 22

1.2 PDGF signalling **37**

1.2.1 PDGF and PI3K signalling pathway 37

1.2.2 PDGF signalling in migrating cells 44

1.2.3 PDGF signalling and neural crest cells 48

1.3 Contact Inhibition of locomotion **53**

1.3.1 CIL in general 54

1.3.2 Study of contact inhibition of locomotion - *assays* 56

1.3.3 Molecular mechanism of contact inhibition of locomotion 59

1.3.4 Contact inhibition in embryonic development 66

1.4 Hypothesis **69**

1.4.1 Hypothesis background 69

1.4.2 Hypothesis 70

Chapter 2 Experimental Procedures **71**

2.1 Embryological and Histological Procedures **72**

2.1.1 In vitro fertilization and embryo collection of Xenopus laevis embryos 72

2.1.2 Microinjection of Xenopus laevis embryos 72

2.1.3 Microdissection and neural crest cells culture 76

2.1.4 Whole mount *in situ* hybridisation 76

2.2 Molecular biology and biochemistry **78**

2.2.1 Amplification of plasmid DNA clones 78

2.2.2 Synthesis of mRNA for microinjection 78
2.2.3 Synthesis of mRNA probe for in-situ hybridisation 80
2.2.4 Immunostaining 81
2.2.5 Morpholinos 82
2.2.6 Inhibitors 83
2.2.7 RT-PCR 83
2.2.8 Western blot 86
2.3 Microscopy and imaging 87
2.3.1 Time lapse imaging of neural crest cells 87
2.3.2 Confocal microscopy of neural crest cells 87
2.4 Analysis 88
2.4.1 *In vivo* migration assay 88
2.4.2 Single cell motility assay 90
2.4.3 Chemotaxis assay 91
2.4.4 Dispersion assay 91
2.4.5 Single cell collision assay 92
2.4.6 Explant Invasion assay 92
2.4.7 Analysis of cell-cell adhesion protein 93
2.4.8 Analysis of ph-AKT-GFP distribution 93
2.4.9 Protrusion analysis 94
2.4.10 Statistical Analysis 94
Chapter 3 Results 95
3.1 Co-expressed PDGFRα and PDGF-A are required for neural crest cell migration *in vivo* and *in vitro* 96
3.1.1 PDGF-A and PDGFRα are co-expressed in Xenopus laevis neural crest cells 96
3.1.2 PDGF-A/PDGFRα signalling is required for neural crest cell migration ... 102
3.1.3 PDGF-A/PDGFRα signalling controls neural crest cell dispersion *in vitro* 109
3.2 PDGF-A/PDGFRα controls N-cadherin dependent contact inhibition of locomotion 119
3.2.1 PDGF-A/PDGFRα controls cell-cell adhesion via N-Cadherin regulation . 119
3.2.2 N-cadherin dependent CIL is regulated by PDGF-A/PDGFRα signalling .. 126
3.3 PI3K/AKT signalling downstream of PDGFRα during neural crest cell migration 133

3.3.1 PDGF-A/Rα controls neural crest cell migration via PI3K/AKT pathway 133
3.3.2 N-cadherin dependent CIL is regulated via PI3K/AKT signalling downstream of PDGF-A/PDGFRα signalling 146
Chapter 4 Discussion 150
4.1 Model overview 151
***4.2* PDGF-A/PDGFRα signalling is required for neural crest migration in *Xenopus laevis* 152**
4.3 PDGF-A/PDGFRα and N-cadherin dependent Contact inhibition of locomotion 156
4.4 PDGF-A/PDGFRα and PI3K/AKT signalling 159
4.5 PDGF-A/PDGFRα signalling in the context of other modes of NC migration 160
4.6 Concluding Remarks 162
References 164

Table of figures

Figure 1-1 Adult neural crest cell derivatives 17

Figure 1-2 Neural crest cell migration 23

Figure 1-3 Cell polarity and Cytoskeletal organization in migratory cell. 28

Figure 1-4 Neural crest cell migration integrates EMT, CIL and co-attraction..... 36

Figure 1-5 PDGF signalling: receptor and ligands. 40

Figure 1-6 PDGF signalling pathways. 41

Figure 1-7 PI3K signalling 43

Figure 1-8 Four phases of contact inhibition of cell locomotion 55

Figure 1-9 Contact inhibition of locomotion type classification 56

Figure 1-10 Methods to study contact inhibition of locomotion..... 58

Figure 1-11 Contact inhibition *in vivo* 69

Figure 2-1 mRNA and Morpholino neural crest targeting injection scheme 74

Figure 2-2 Neural Crest migration measurement scheme..... 89

Figure 2-3 Directionality calculation scheme..... 91

Figure 3-1 PDGF-A and PDGFRα are expressed in pre-migratory and migrating neural crest cells 98

Figure 3-2 RT-PCR of microdissected neural crest cells for PDGF-A and PDGFRα 99

Figure 3-3 PDGFRα is expressed in neural crest cells 100

Figure 3-4 PDGF-A/PDGFRα inhibition impairs collective neural crest cell migration *in vivo*..... 104

Figure 3-5 PDGF-A/PDGFRα inhibition might not affect neural crest cell induction 106

Figure 3-6 PDGF-A and PDGFRα Morpholino rescue. 107

Figure 3-7 PDGFRα does not affect single cell motility. 112

Figure 3-8 PDGFRα signalling is not required for SDF-1 chemotaxis. 113

Figure 3-9 PDGF-A/PDGFRα required for neural crest cell dispersion. 115

Figure 3-10 PDGFRα MO, PDGF-A MO and PDGF-AA protein dispersion titration. 117

Figure 3-11 Cell-Cell Sorting assay: PDGFRα MO in neural crest cells show adhesion differences 121

Figure 3-12 PDGFRα depletion affects N-cadherin level by western blot 122

Figure 3-13 Immunostaining: PDGFRα signalling regulates N-cadherin level..... 123

Figure 3-14 Immunostaining E-cadherin: PDGFRα signalling perturbation does not affect E-cadherin level 125

Figure 3-15 PDGFRα required for contact inhibition of locomotion..... 128

Figure 3-16 PDGFRα depleted neural crest cells are able to invade each other 130

Figure 3-17 PDGFRα depletion affects protrusion formation..... 132

Figure 3-18 PDGF-AA addition leads to ph-AKT translocation to the plasma membrane 137

Figure 3-19 dominant active PI3K and PDGFRα inhibition and ph-AKT translocalisation..... 138

Figure 3-20 PDGFRα depletion decreased phosphorylated AKT in neural crest cells 140

Figure 3-21 PI3K and AKT pharmacological inhibition impairs neural crest cell migration *in vivo* 141

Figure 3-22 neural crest cell dispersion and small molecule inhibition of PI3K/AKT signalling 143

Figure 3-23 pharmacological inhibition leads to reduction of phosphorylated AKT by western blot..... 145

Figure 3-24 N-cadherin mRNA co-injection rescues PDGFRα dispersion inhibition 147

Figure 3-25 PI3K inhibition decreases N-cadherin protein level..... 149

Figure 4-1 Model Overview 152

List of tables

Table 2-1 List of injected mRNA and Morpholinos 75

Table 2-2 List of antisense *in situ* hybridisation probes 81

Table 2-3 List of primary antibodies for immunostaining 82

Table 2-4 List of secondary antibodies immunostaining 82

Table 2-5 List of pharmaceutical inhibitors 83

Table 2-6 Reverse transcriptase PCR Primer and Program 84

Table 2-7 Reverse transcriptase reaction mix 84

Table 2-8 Reverse transcriptase cycle program 85

Table 2-9 RT-PCR PCR reaction Mix 85

Table 2-10 List of primary antibodies for western blot 86

Table 2-11 List of secondary antibodies for western blot 87

List of supplementary movies

Movie 1 PDGFRα MO chemotaxis assay

PDGFRα MO injected explants migrate towards SDF-1 protein beads compared to control neural crest cell explants. No chemotaxis was observed towards PBS only beads. Scale bar 50 μM (5 minutes frame $^{-1}$).

Movie 2 PDGF-A/ α dispersion assay

PDGF-A MO and PDGFRα MO explants have decreased dispersion compared to control neural crest cell cluster. Addition of PDGF-AA protein can rescue PDGF-A MO, but PDGFRα MO dispersion, scale bar 150 μM (25 minutes frame $^{-1}$).

Movie 3 ph-AKT-GFP with and without PDGF-AA protein

Ph-AKT-GFP mRNA injected neural crest cells with and without PDGF-AA protein (50 ng mL^{-1}) at t=300sec. PH-AKT-GFP translocates to the Plasma membrane after protein addition, no effect was observed in untreated neural crest cells, scale bar 10 μM (15 seconds frame $^{-1}$).

Movie 4 PDGFRα MO and N-cadherin mRNA dispersion

N-cadherin mRNA can rescue PDGFRα MO inhibition of dispersion, scale bar 150 μM (10 minutes frame $^{-1}$).

List of abbreviations

ba	Branchial arch
BAD	Bcl-2-associated death promoter
BMP	Bone morphometric protein
CDC42	Cell division control protein 42 homolog
CIL	Contact inhibition of locomotion
Crk	CT10 (chicken tumor virus number 10) regulator of kinase
CoA	Co-attraction
CUB	Complement C1r/C1s, Uegf, Bmp1
CXCR4	C-X-C chemokine receptor type 4
dn	dominate negative
ECM	Extra-cellular matrix
EMT	Epithelial-to mesenchymal-transition
ERK	Extracellular signal–regulated kinases
FGF	Fibroblast growth factor
FGFR	Fibroblast growth factor receptor
FKHR	Forkhead box protein
GAP	GTPase-activating protein
GEF	Guanine nucleotide exchange factors
GSK-3	Glycogen synthase kinase *3*
Hif1	Hypoxia inducible factor 1
HSPG	Heparan sulphate proteoglycan
IRS	Insulin receptor substrate
JNK	Jun N-terminal kinases
MAPK	Mitogen-activated protein kinase
MDM2	Mouse double minute 2
MEPM	mouse embryonic palate mesenchymal
Mirn140	MicroRNA 140
MO	Morpholino
Npn	Neuropilin
NF-κB	nuclear factor-κB
pAKT	phosphorylated AKT
Par-3	Partitioning defective protein 3
PCP	planer cell polarity
PDGF-A	Platelet derived growth factor A
PDGFRα	Platelet derived growth factor receptor alpha
PDK	phosphoinositide-dependent kinase
PI3K	Phosphatidylinositol-3-kinase
PIP2	Phosphatidylinositol biphosphate
PIP3	Phosphatidylinositol triphosphate
PKC	Protein kinase C
PLC-γ	Phosphoinositide phospholipase C γ
PTEN	Phosphatase and tensin homolog
RA	Retinoic Acid
RAC1	Ras-related C3 botulinum toxin substrate 1

RasGAP	Ras GTPase activating protein
ROCK	Rho-associated protein kinase
RU	relative units
SDF1	Stromal cell-derived factor 1
SGK	Serum and glucocorticoid-inducible kinase
Sem	Semaphorin
Shc	SHC-transforming protein
SH2	Src Homology 2
STAT	Signal transducer and activator of transcription
tAkt	Total AKT
tPA	Tissue plasminogen activator
VEFGR	Vascular endothelial growth factor receptor
VEGF	Vascular endothelial growth factor

Chapter 1 Introduction

1.1 The Neural Crest

The neural crest is a transient, migratory cell population unique to the vertebrate embryo. Also referred to as the fourth germ layer, the neural crest is a vertebrate synapomorphy that divides vertebrates from other metazoans (Gans and Northcutt, 1983). Swiss embryologist Wilhelm His (1986) was the first to described the neural crest in the chick embryo calling it the "the intermediate cord" (German: Zwischenstrang). He was referring to a thin band of cells at the interface between the neural epithelium and surface ectoderm. After induction neural crest cells delaminate from the neural tube and undergo an extensive migration through the embryonic body. At their target destination they differentiate and give rise to an array of different cell types, including cartilage and bone of craniofacial structures, neurons and glia of the peripheral nervous system, pigment cells, cardiac structures and endocrine cells (Figure 1-1; reviewed in Theveneau and Mayor, 2012). Due to this wide-ranging set of derivatives, their stem cell properties, and their extensive migratory capabilities scientists have used neural crest cells extensively as a model system (Theveneau and Mayor, 2012).

The neural crest is comprised of several populations that are determined by their rostral-caudal location and thus their migratory path along the embryonic body. The different neural crest cell populations are termed: cranial, vagal and trunk neural crest cells. The subpopulation of cranial neural crest cells migrates along a dorso-lateral route through the pharyngeal arches and gives rise to craniofacial structures as cartilage, bone, cranial neurons and glia, and connective tissue. The vagal neural crest cells specified at the caudal hindbrain level, form part of the enteric nervous system and contribute to the heart. The trunk neural crest cells give rise to sensory and sympathetic ganglia and cells of the adrenal medulla among other derivatives (reviewed in Barembaum and Bronner-fraser, 2005). Due to this wide variety of neural crest cell contributions throughout the embryonic body, disruption of neural crest cell development can lead to congenital defects termed neurocristopathies, which include craniofacial abnormalities, hearing loss, heart malformations and missing enteric ganglia (Mayor, Roberto; Theveneau, 2013). Furthermore,

similarities between neural crest cell development and cancer metastasis, as well as wound healing, have proven it to be interesting model that may contribute to an understanding of these pathological conditions and future therapeutic strategies (Mayor, Roberto; Theveneau, 2013; Theveneau and Mayor, 2012).

This thesis focuses on cranial neural crest cell migration in *Xenopus laevis*. Therefore this part of the introduction will concentrate on cranial neural crest cell delamination, epithelial to mesenchymal transition and migration.

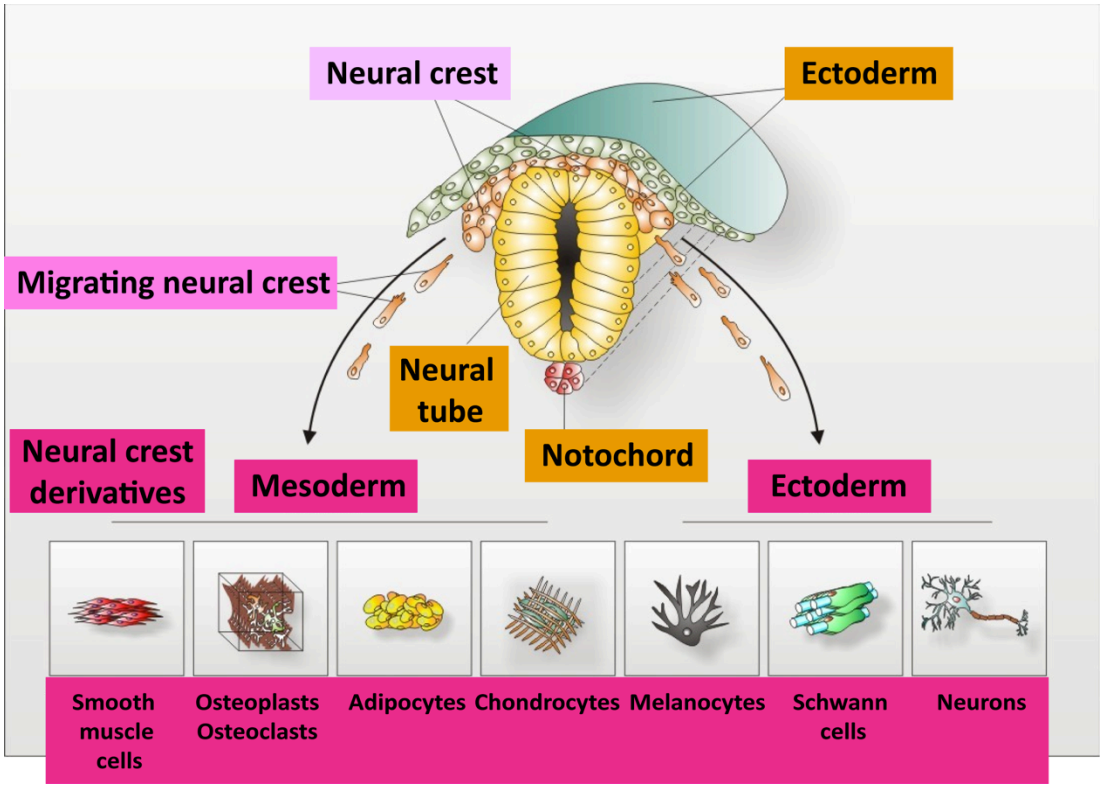

Figure 1-1 Adult neural crest cell derivatives

The neural crest becomes specified between the surface ectoderm and the neural tube. Neural crest migrate away from the neuroepithelium and give rise to different cell types as depicted in the image (neural crest cell derivatives in pink). Adapted from Kaltschmidt et al., 2012.

1.1.1 Neural crest cell induction

The neural crest is induced in a two-step process, which includes an initial induction step followed by a so-called maintenance step. Induction of the neural crest is a complex process and beyond the focus of the research described in the thesis, therefore I will only give a brief introduction; for more detailed description please refer to the following reviews (Bronner and LeDouarin, 2012; Duband et al., 2015; Milet and Monsoro-Burq, 2012; Sauka-Spengler and Bronner-Fraser, 2008)). In brief, neural crest cell induction is initiated in the ectoderm by a combination of instructive signals between the presumptive neural plate and epidermis during gastrulation. These involve intermediate levels of BMP4 and BMP7 signalling and high levels of WNT6/8 or 10a, FGF3 and FGF8 and RA signalling. This induction step leads to the co-expression of a set of transcription factors called *"neural plate border specifiers"* including Msx, Pax3/7 and Zic1, whose co-expression define the neural plate border territory. Once the neural crest cells are induced they are maintained by signals from the intermediate mesoderm and adjacent ectoderm, which together with the first set of transcription factors activates the "*neural crest specifiers".* This set of transcription factors includes Snail/Slug, FoxD3, Id, cMyc and Sox9/10 which maintain and further direct neural crest cell development towards delamination, EMT and migration (Bronner and LeDouarin, 2012; Duband et al., 2015; Milet and Monsoro-Burq, 2012; Sauka-Spengler and Bronner-Fraser, 2008).

1.1.2 Delamination and Epithelial-to-mesenchymal transition

Delamination

Delamination is the process of physical segregation of the neural crest cells from the neural tube. It is also been referred to as emigration, individualization or segregation and is seen as the final step of specification and transition into migration (Duband et al., 2015). It should be noted that delamination cannot be interchanged with Epithelial-to-mesenchymal transition (EMT), a process of molecular changes orchestrating the transition from epithelial to mesenchymal cell state (Thiery et al., 2009; discussed in detail at the end of this section). Neural crest undergo EMT in order to acquire their mesenchymal migratory properties, but

delamination, the segregation from the neural tube, does not match the timing of EMT completion (Theveneau and Mayor, 2012). That both are distinctive processes is for example shown in trunk neural crest cells, where entering into S-phase is required for delamination. However inhibition of G1/S-phase transition by noggin overexpression impairs delamination but does not disrupt EMT (Burstyn-Cohen et al., 2004). Though, both processes cannot be seen independently of each other, as for example Sox9, which alone controls neural crest cell specification but no EMT. However Sox9 together with Snail2 can start EMT process (Cheung and Briscoe, 2003; Cheung et al., 2005).

Cranial neural crest cells delaminate all at once (Theveneau and Mayor, 2012), and in chick embryos onset of delamination overlaps with the closure of the neural tube (Duband and Thiery, 1982; Le Douarin and Kalcheim, 1999; Théveneau et al., 2007). In *Xenopus* and mouse cranial neural crest cell delamination happens while the neural tube is still open (Nichols, 1981; Nichols, 1987; Sadaghiani and Thibaud, 1987). In contrast, trunk neural crest cell delamination starts in all animal models after neural tube closure and the cells leave the neural tube over time as single cells in rostral-caudal wave (Ahlstrom and Erickson, 2009; Berndt et al., 2008; Clay and Halloran, 2010; Duband, 2010). It should be noted that closure of the neural tube and start of neural crest cell delamination are not functionally coupled (Copp et al., 2003).

On the molecular level delamination is orchestrated by “neural crest specifier” transcription factors, including Snail2, Sox9 and FoxD3 (Sauka-Spengler and Bronner-Fraser, 2008). When overexpressed, these factors are able to induce ectopic neural crest cells (Cheung et al., 2005). Additionally, a recent report shows that temporary and reversible Wnt inhibition is required for delamination in *Xenopus* and chick embryos (Rabadán et al., 2016).

Epithelial-to- mesenchymal transition

In the neuroepithelial sheet the neural crest displays epithelial characteristics with apical basal polarity and strong intracellular adhesion supported by a basal lamina.

In order to start their migration neural crest cells need to undergo a change from this steady epithelial to a migratory mesenchymal state. To achieve this, neural crest cells undertake a molecular process termed EMT. This program includes a loss of apical-basal polarity, reduction of intercellular adhesion and acquisition of migratory and invasive properties (Theveneau and Mayor, 2012; Thiery and Sleeman, 2006). To start their migration neural crest cells undergo a complete or partial EMT allowing them to emerge from the neural tube and ectoderm. Complete EMT, is a type of EMT where all cells of an epithelium undergo a full transition, which is mainly observed in cell culture. In contrast, partial, progressive EMT, is most common during developmental processes, as trunk neural crest cell delamination (Duband, 2010). It is not quite clear whether cranial neural crest cells undergo a complete, or a partial EMT. Partial EMT occurs when one or more of the key features of complete-EMT are not shown, such as loss of cell-cell contact. The collective mode of cranial neural crest cell migration suggests a mixed trait of epithelial and mesenchymal character, also called hybrid state. Hereby cells only undergo a partial transition into the mesenchymal fate, instead of completing mesenchymal cell fate transition. (Friedl and Gilmour, 2009). Not only the mode of EMT in neural crest cells may differ between subpopulations and species, but also the onset of the process varies. In *Xenopus laevis* EMT occurs after delamination, permitting migration as a group (Theveneau and Mayor, 2012).

A hallmark of EMT is the diminution of epithelial **cell-cell junction** proteins, like E-cadherin, gap and tight junction molecules (Thiery et al., 2009). E-cadherin is a central component of cell-cell adhesions and is prerequisite for the formation of epithelia. In neural crest cells a change from the strong adhesion type I cadherin, E-cadherin to weaker adhesion type II N-cadherin occurs at the end of neural induction (Dady et al., 2012; Nandadasa et al., 2009; Theveneau and Mayor, 2012). On a molecular level transcription factors of the “neural crest specifier” set, including Slug/Snail and Twist, repress expression of E-cadherin and other junction components (Carl et al., 1999; Kang and Massagué, 2004; Nieto et al., 1994; Taneyhill et al., 2007). Therefore, neural crest cells that start migrating express N-cadherin (Bronner-Fraser et al., 1992; Theveneau et al., 2010; Xu et al., 2001) and

low levels of E-cadherin (Barriga et al., 2013). However this change is followed by another switch, from high to low N-cadherin expression and overlaps with the onset of expression of weaker type II cadherins (6/7/11) (Chalpe et al., 2010; Cheung and Briscoe, 2003; Cheung et al., 2005; Dottori et al., 2001; Kashef et al., 2009; Nakagawa and Takeichi, 1995; Nakagawa and Takeichi, 1998). This change is controlled by an additional set of transcription factors in cranial neural crest cells including Snail/Slug, Foxd3, Sox9/10, Ets1, and p53 (Cheung et al., 2005; McKeown et al., 2013; Perez-Alcala et al., 2004; Rinon et al., 2011; Théveneau et al., 2007). The timed expression of cadherins does not only decrease cell adhesion but is also required for change in cell polarization. For example, Cadherin6B expression is needed to polarize Rho GTPases and actomyosin in zebrafish trunk neural crest cells (Clay and Halloran, 2014). Likewise, N-cadherin has been reported to polarize the small GTPase Rac1 at the leading edge in emigrating neural crest cells (Theveneau et al., 2010). Not only does the expression of cadherin during neural crest cells EMT change, neural crest cells also express metalloproteases, such as ADAM 10 and ADAM13, capable of cleaving cadherins. This further reduces the cell-cell adhesion properties of delaminating neural crest cells and increases their invasiveness into surrounding tissue (Neuner et al., 2009; Shoval et al., 2007). Furthermore the cytoplasmic fragment of the metalloproteases cleaved N-cadherin translocates to the nucleus and supports survival and delamination (Shoval et al., 2007). In addition to the metalloproteases, a endogenous inhibitor of matrix metalloproteases TIMP2 is also required for neural crest cell migration in chick embryos (Cantemir et al., 2004)

Besides the regulation of cell-cell adhesion, the transcription factor set also promotes the acquisition of migratory capabilities in neural crest cells by inducing expression of β_1-Integrin and the small GTPase RhoB (Cheung et al., 2005; McKeown et al., 2013). Exogenous upregulation of β_1-Integrin may lead to emigration through integrin-to-cadherin negative crosstalk. In addition inhibition of integrin function in chick neural crest cells, with RGD fibronectin-derived peptides or antibodies against β_1-Integrin and β_3-Integrin, increases N-cadherin levels at the cell junction and induces cell clustering (Monier-Gavelle and Duband, 1997).

Moreover, the acquisition of a migratory phenotype involves the cytoskeletal re-organisation, including expression of intermediate filament proteins, the change to a flatter rear-front polarity and the ability to generate lamellipodia and filopodia (Theveneau and Mayor, 2012). For example, in zebrafish trunk neural crest cells onset of migration is characterized by myosin II and Rho-kinase (ROCK) activity blebbing. Once migrating, neural crest cells start to produce robust lamellipodia and filopodia that create the traction required for migration (Berndt et al., 2008)

Overall the EMT process is a complex event that requires cell changes driven by cell junction alterations, cytoskeletal re-organisation, remodelling of the extracellular matrix and cellular polarity (Thiery et al., 2009). Interestingly EMT is also a hallmark in cancer which shows similarities to the process acquired in neural crest cells (Theveneau and Mayor, 2012).

1.1.3 Neural crest migration

After delamination and EMT, neural crest cells start their dorso-ventral migration to reach their target location. In this section I will specifically discuss mechanisms of **collective cranial neural crest cell migration**. These include restriction of the migrating neural crest cells into discrete streams, cell-substrate interactions, chemotaxis, co- attraction and contact inhibition of locomotion (Figure 1-2).

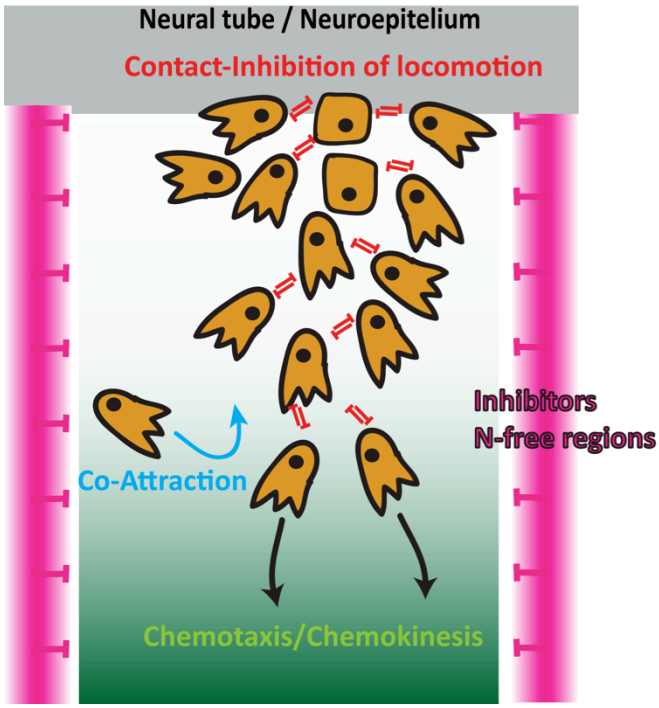

Figure 1-2 Neural crest cell migration

Collaborative actions of physical restraints, contact inhibition of locomotion (CIL), co-attraction, cell-cell interactions, cell-substrate interactions and chemotaxis control cranial neural crest cell migration in *Xenopus laevis*. Physical restraints inhibitory signals guide neural crest cell into streams. CIL orientates protrusions towards the neural crest cell free space and promotes directionality. Co-attraction prevents dispersion and promotes clustering of the stream, thus developing collectivity. Chemotactic signals directs migration of the stream towards the target regions (figure adapted from Theveneau and Mayor, 2012).

Physical restraint of the neural crest cell streams

Cranial neural crest cells in Xenopus embryos migrate away from the neural tube in three defined streams, mandibular, brachial and hyoid, towards the pharyngeal arches (Sadaghiani and Thibaud, 1987; Theveneau and Mayor, 2012). Permissive spaces in the pharyngeal arches might support splitting of the neural crest cell populations (Theveneau and Mayor, 2012). For example the extracellular matrix

with proteins like fibronectin and laminin has been suggested to have a permissive role (Perris and Perissinotto, 2000; see also section 1.1.3 Cell substrate interaction). An additional mechanism, defined as “chase and run”, has been suggested to be involved in the coordination of neural crest cell into streams. The “chase and run” mechanism requires chemotaxis of the neural crest towards the placodes and contact inhibition of locomotion of the placodes after neural crest cell contact (Theveneau et al., 2013). For a thorough discussion of the chase and run mechanism see next sections of this chapter.

Nevertheless, the exact subdivision of the streams seems to be more due to negative and positive external regulators. The tissue surrounding the neural crest expresses non-permissive ligands, which restrict ectopic neural crest cell migration. This exchange is mediated by a set of reciprocally expressed receptor-ligand systems, whereby the receptors are expressed in the neural crest cells and corresponding ligands in the surrounding tissue. So far three main receptor-ligand groups mediating the restrictive signal have been described, namely- Eph receptors and ephrin, Neuropilin receptors and Semaphorin, Robo receptors and Slit. These all work via induction of cell protrusion collapse to ensure stream formation (Theveneau and Mayor, 2012).

Ephs are tyrosine kinase receptors, which bind to their corresponding cell-surface associated ephrin ligands, on neighbouring cells, thus triggering bidirectional signalling (Lisabeth et al., 2013). The Ephs and ephrins expressed by cranial neural crest cell and surrounding tissues, vary across different animal models (Adams et al., 2001; Davy et al., 2004; Mellott and Burke, 2008a; Smith et al., 1997). However they function, as restrictive signal, mediating neural crest cell stream formation, seems to be conserved. Indeed, the Eph/ephrin bidirectional signalling is required for proper formation of neural crest cell streams in mouse, chick and *Xenopus* embryos (Theveneau and Mayor, 2012). For example in Xenopus embryos ephrin-B2 is expressed in the second branchial arch and acts as a negative cue for neural crest cells that are set to migrate into the third and fourth brachial arch, as they express the corresponding receptor EphrinA4 and EphrinB1 (Smith et al., 1997).

Indeed, in Xenopus embryos where this Eph/Ephrin signalling is inhibited neural crest cells show ectopic migration outside their normal routes and a mixing of neural crest cell from different streams occurs (Smith et al., 1997). This indicates that Eph/Ephrins not only have a non-permissive role, but also a sorting function of neural crest cell into their separate streams depending on their rostro-caudal location. Inhibition of Ephrins, specifically of EphrinB1 leads to ectopic neural crest cell migration in normally non-permissive areas in mouse and chick embryos (Davy et al., 2004; Mellott and Burke, 2008b). Additionally, to their role cranial neural crest cell migration, Eph/Ephrins are also essential to limit migration of trunk neural crest cells to the anterior part of the somites (Krull et al., 1997; Santiago and Erickson, 2002).

Similar to the Eph/Ephrins are the neuropilin/plexin receptors and their ligands semaphorins expressed in a reciprocal way in the neural crest cells and surrounding tissue and exert restrictive signals to the neural crest cell. Neuropilins have to associate with members of the plexinA family to convey the intracellular signalling after binding of the semaphorin ligand (Jackson and Eickholt, 2009). Also neuropilins and semaphorins are expressed in a reciprocal way. Class 3-semaphorin family members (3A, 3F and 3G), are expressed in tissues adjacent to the cranial neural crest cell streams. Their correlated neuropilin receptors (Npn1 and Npn2) are expressed by the cranial neural crest cells (Eickholt et al., 1999; Gammill et al., 2007; Koestner et al., 2008; Osborne et al., 2005; Yu and Moens, 2005). Indeed, mutation of Npn2 or Sem3F in mouse embryos causes ectopic migration of cranial neural crest cells into normally non-permissive areas (Gammill et al., 2007). Interestingly, in *Xenopus* embryos Neuropilins and Semaphorins are both expressed in the cranial neural crest cells and surrounding tissue (Koestner et al., 2008). So far, no functional studies of semaphorin-neuropilin interactions in Xenopus laevis have been done so far. However, the complementary expression patterns of both Sema3A/Nrp1 and Sema3F/Nrp2 are preserved in vertebrates across hundreds of millions of years, possibly showing a conserved role in the guidance of migrating neural crest cells (Koestner et al., 2008).

The third receptor-ligand system that restricts the neural crest cell migration to their streams is the Robo/Slit system. Hitherto a role for Robo/Slit has been only investigated in trunk neural crest cells. Here, Slit/Robo signalling was found to be necessary to confine neural crest cells to the ventral-medial migratory pathway, thus preventing premature dorso-lateral migration (Giovannone et al., 2012; Jia et al., 2005).

Polarization of migrating cells: Rho GTPases

In general collective cell migration is driven by lamellipodia and filopodia in the leading front and suppression of these protrusions in the follower cells. To establish this cellular polarity a central role has been attributed to members of Rho GTPases family, specifically -RhoA, Rac 1 and Cdc42. Small GTPases of the Rho family are main regulators of the actin and microtubule cytoskeletal dynamics and their activity needs to be tightly regulated to coordinate the complex cytoskeletal machinery that is required for efficient cell migration (Mayor and Etienne-Manneville, 2016; Ridley, 2015). Small GTPases of the Rho family are molecular switches, which change from an active GTP-bound and to an inactive GDP-unbound state. The GDP/GTP exchange is mediated by Guanine Exchange Factors (GEFs), such as SCRIB, TIAM1 or PAR3, which mediate small GTPase activation. GTPase Activating Proteins (GAPs) on the other side can mediate inactivation of the GTPases (Bos et al., 2007; Ridley, 2015).

In general, Rho GTPases, Rac and Cdc42 induce cytoskeletal rearrangements that polarize a single migrating cell. Rac and Cdc42 induce membrane protrusions at the front, by inducing actin polymerization and promotion of protrusion engagement with integrins and the ECM (Ridley, 2015; Ridley et al., 1992). In order to regulate cytoskeletal rearrangement Rac1 controls protein complexes such as the Scar/Wave complex, which induces actin polymerization via N-WASP-Arp2/3 actin nucleation complex (Ridley, 2015). Cdc42, however is controlling actin polymerization at the very front of the cell during filopodium formation (Itoh et al., 2002). At the rear Rho induces stress-fibre formation and activates the Rho-associated kinase (ROCK), which promotes acto-myosin contraction and protrusion collapse, via triggering of

phosphoinositides phosphatase (PTEN) activation (Chrzanowska-Wodnicka and Burridge, 1996; Ridley, 2015; Ridley and Hall, 1992; Ridley et al., 1992). In general this mutual exclusive activity establishes a front to rear polarity and consequently allows directional migration (Mayor and Etienne-Manneville, 2016; Ridley, 2015). Mutual exclusion of Rac1 and RhoA is a complex process but in a simplified model, Rac1 inhibits RhoA at the front, by triggering p190RhoGAP activity (Bustos et al., 2008). At the rear of the cell RhoA inhibition of Rac1 is mediated via ROCK phosphorylation of FilGAP, which inactivates Rac1 (for overview see Figure 1-3; Ohta et al., 2006). Although, a transient activity of RhoA, associated with cycles of protrusion collapses has also been observed at the cell front (Machacek et al., 2009; Pertz et al., 2006).

A similar mechanism as for single cell migration is used for collective migration, however cellular contacts change the classical Rho GTPase distribution. The contacts involve the leader cells at front of the cluster and follower cells at back and middle. Follower cells are exposed to different cues as leader cells, for example chemoattractants and ECM of surrounding cells (Krause and Gautreau, 2014; Mayor and Etienne-Manneville, 2016). Depletion of small Rho GTPases in neural crest cells in various animal models lead to inhibition of migration, indicating their requirement (Berndt et al., 2008; Clay and Halloran, 2013; Groysman et al., 2008; Liu and Jessell, 1998; Matthews et al., 2008; Phillips et al., 2012; Rupp and Kulesa, 2007; Shoval and Kalcheim, 2012; Stewart et al., 2007; Thomas et al., 2010). Analysis of their activity distribution *in Xenopus* and Zebrafish neural crest cells showed the mutual exclusive behaviour of both, increased Rac1 activity at the front and increased RhoA activity at the back (Carmona-Fontaine et al., 2011; Clay and Halloran, 2013; Matthews et al., 2008; Theveneau et al., 2010). In *Xenopus* collective neural crest cell migration, Rac1 activity is polarized to the leading edge, where it has been shown to promote lamellipodia formation (Matthews et al., 2008; Scarpa et al., 2013; Theveneau et al., 2010). Indeed, the localized activation of Rac1 in a neural crest cell-cell duplets at the free edge leads to protrusion formation and increased separation. Whereas the activation of a dominant negative form inhibits protrusion formation and impairs separation (Scarpa et al., 2015). As RhoA

and Rac1 mutually inhibit each other, RhoA is active at the cell-cell contact in neural crest cells (Mayor and Etienne-Manneville, 2016). This inhibition is dependent upon the activation of the non-canonical Wnt-planar cell polarity (PCP) pathway by the cell-cell contact via the process called contact inhibition of locomotion (CIL) (Carmona-Fontaine et al., 2008b; Matthews et al., 2008; Mayor and Theveneau, 2014). Notably, the cell–cell contact during CIL of neural crest cells leads to RhoA stimulation and Rac inhibition at the site of cell contact (Matthews et al., 2008; Teddy and Kulesa, 2004; Theveneau et al., 2010). The connection and regulation between Wnt-PCP and CIL will be discussed in detail later in this chapter (see Contact inhibition of locomotion).

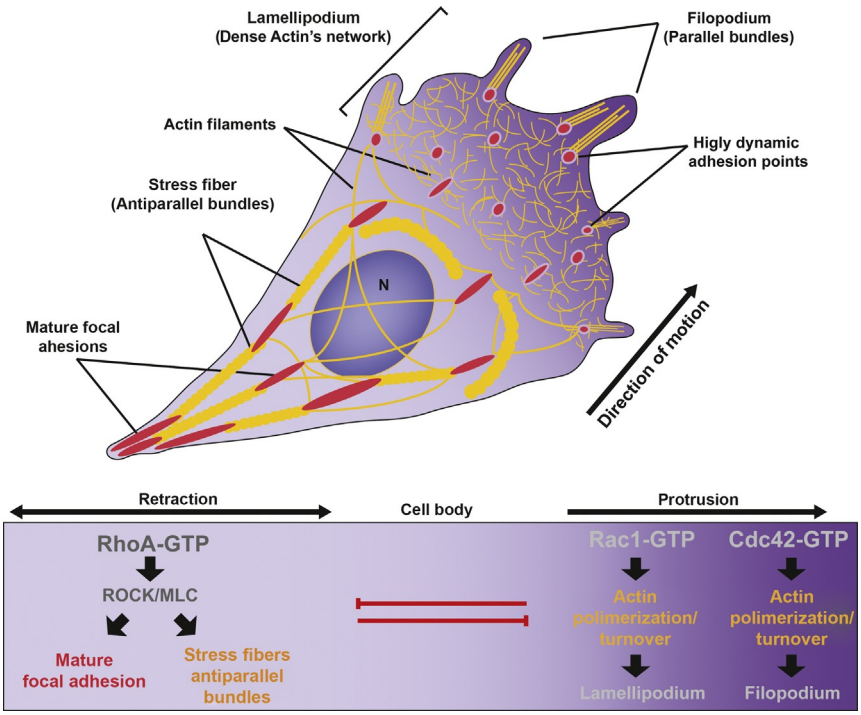

Figure 1-3 Cell polarity and Cytoskeletal organization in migratory cell.

A migratory cell has polarised distribution of small GTPases Cdc42, Rac1, and RhoA. At the protrusion front, Rac1 activity regulates lamellipodium formation by promoting actin assembly (yellow lines). Cdc42-GTP controls actin polymerisation in the filopodium. Rac1 and Cdc42 at the front regulate the formation of cell–substrate adhesions (red dots). At the back of the cell, RhoA activity promotes actin-

myosin contractility via the formation of stress fibres and mature cell–substrate adhesions. Adapted from Barriga and Mayor, 2015.

Cell substrate interaction

During migration, interaction with the underlying ECM is crucial to allow traction. At the leading edge lamellipodia are associated with the ECM, which leads to the stabilization of actin flow and eventually cell protrusion formation. At the rear, anchoring cell–ECM contacts, allow actin-myosin mediated cell-retraction. These cell-substrate contacts are mediated via specific protein complexes named **focal** contacts (Abercrombie and Dunn, 1975; Izzard and Lochner, 1976; Mui et al., 2016). At the cell front, focal contacts stabilize the protrusions, whereby Rac1 is required for the assembly of the focal complex. Focal contact points with the ECM have a high turnover during migration. However, in the back of the cell focal contact points can develop into larger structures, named focal adhesions, connected to RhoA stimulated stress-fibers. Focal adhesions are complex cell-substrate protein complexes including extra cellular-adhesion molecules, like integrins and intracellular adaptor proteins that connect the cytoskeleton to the focal adhesion (Ridley, 2015).

Thus, in order to allow migration, ECM components need to support cell-substrate interactions. Indeed it has been shown that neural crest cells move along permissive ECM routes mainly supported by integrin interaction (Theveneau and Mayor, 2012). In avian trunk neural crest cells ECM components involved in migration include fibronectin, collagen, laminin and integrins (Delannet et al., 1994; Dufour et al., 1988; Newgreen, 1982; Perris and Perissinotto, 2000; Rovasio et al., 1983; Testaz and Duband, 2001). Especially fibronectin has been shown to be expressed in neural crest cell migratory pathways (Newgreen and Thiery, 1980). In *Xenopus* cranial neural crest cells fibronectin is required for migration, at least *in vitro* (Alfandari et al., 2003; Epperlein et al., 1988). Fibronectin contains multiple binding sites that that can interact with integrin receptors. The integrins, expressed

by cranial neural crest cells, include the β1- and α5-integrin subunits (McKeown et al., 2013) and integrin α5β1 is required for avian and amphibian cranial neural crest cell migration on fibronectin in culture (Alfandari et al., 2003; Kil et al., 1998; Lallier et al., 1993). Indeed, using a function blocking antibody against α5β1-integrin on *Xenopus* cranial neural crest cells inhibits migration *in vivo* (Alfandari et al., 2003). Additional depletion of β1-integrin subunit in chick has been shown to lead to inhibition of cranial neural crest cell migration (Boucaut et al., 1984; Bronner-Fraser, 1986). Conversely, β1-integrin subunit conditional depletion in mouse using Wnt1-cre driver did not show any impairment of cranial neural crest cell migration (Turlo et al., 2012). However recent research also showed that conditional knockdown of fibronectin and integrin α5 in mouse cranial neural crest cells leads to a decreased number of cells due to increased apoptosis and decreased proliferation (Mittal et al., 2010). This suggests that fibronectin and integrin α5 are critical for the survival of mouse cranial neural crest cells.

Next to integrin, cranial neural crest cells express also the proteoglycan syndecan-4 which binds to fibronectin (Matthews et al., 2008). Syndecan-4 has been proposed as a key regulator of RhoA and Rac activities and focal adhesion formation (Alexopoulou et al., 2007). Indeed, Syndecan-4 is expressed in Xenopus cranial neural crest cells and has been shown to regulate the migration through localized inhibition of Rac1 at the cell contact (Matthews et al., 2008).

Chemotaxis and co-attraction

The front–rear polarization of cells or clusters can be stimulated by chemical signals gradient such as chemokines (Mayor and Etienne-Manneville, 2016). Thus directional migration towards a gradient is called chemotaxis. In detail, the target tissue needs to express and secrete the chemotaxing signal or ligand and the responding cell has to express an appropriate receptor to allow chemotaxis. Consequently, depletion of both, chemoattraction signal or receptor, should impair directional migration towards its target region. Further, ectopic chemoattractant should lead to diversion of normal migration *in vivo* and loss of the chemoattractant should be able to be rescue by localized exogenous ligand (Cai and Montell, 2012;

Shellard and Mayor, 2016). The validation of these criteria is fundamental to prove that a given signal is exerting chemotaxing behaviour. If no *in vivo* chemotaxis driven directional migration can be proven, changed migration could be also be due to chemokinesis, a process which only supports and maintains migration but gives no directional information (Kay et al., 2008; Shellard and Mayor, 2016). So far, none of the published chemotaxing signals have been shown to fulfil all above-mentioned criteria. Nevertheless there is amounting evidence that vascular endothelial growth factors (VEGFs) (McLennan et al., 2010), platelet-derived growth factors (PDGFs) (Eberhart et al., 2008; He and Soriano, 2013), and stromal cell-derived factor 1 (SDF-1) (Kasemeier-Kulesa et al., 2010; Saito et al., 2012; Theveneau et al., 2010) could function as neural crest cell chemoattractant.

VEGF signalling has been implicated to work as a chemoattractant during chick cranial neural crest cell migration into the second branchial arch (ba2) (McLennan et al., 2010). Indeed, VEGF is expressed in the ectodermal lining of ba2 and its corresponding receptor VEGFR2 and co-receptor neuropilin1 in avian neural crest cells (McLennan and Kulesa, 2007; McLennan and Kulesa, 2010; McLennan et al., 2010). Inhibition the of receptor leads to impairment in migration and ectopic VEGF source is able to divert neural crest cells from there normal path (McLennan et al., 2010). Further, some experimental data is implicating VEGF as an intracellular polarization cue. Whereby VEGF expression and behaviour of neural crest cells at the leading edge, is thought to drive directional migration by a self-generated gradient regulated by the endocytosis of the ligand (McLennan et al., 2012; McLennan et al., 2015).

The PDGF receptor a (PDGFRα) is expressed in migrating neural crest cells (Eberhart et al., 2008; Ho et al., 1994; Orrurtreger and Lonai, 1992; Schatteman et al., 1992; Takakura et al., 1997) and its corresponding ligands PDGF-A and PDGF-C in the surrounding tissue (Ding et al., 2000; Eberhart et al., 2008; He and Soriano, 2013; Ho et al., 1994; Tallquist et al., 2000). Depletion of PDGF signalling in mouse and zebrafish leads to impairment in neural crest cell migration *in vivo* (for more detailed discussion see section 1.2.3 PDGF signalling during neural crest cell

migration). Further neural crest cell derivatives can undergo chemotaxis towards PDGF-A *in vitro* (He and Soriano, 2013) and a exogenous PDGF-A source was shown to attract mouse cranial neural crest cells *in vivo* (Kawakami et al., 2011). Although, it has not yet been fully established if PDGFRα signalling can act as a chemotactic signal during neural crest cell migration.

Another potential chemo-attractive cue for cranial neural crest cells is SDF-1. While the ligand SDF1 is expressed in the pharyngeal arch and ectoderm, the corresponding receptor Cxcr4 is expressed in cranial neural crest cells in zebrafish and *Xenopus* embryos (Olesnicky Killian et al., 2009; Theveneau et al., 2010). Moreover, SDF-1-Cxcr4 signalling is required for the migration of neural crest cells around the optic stalk and into the branchial arches (Olesnicky Killian et al., 2009; Theveneau et al., 2010). SDF-1 has been proposed to work via increasing Rac1 activity towards the chemoattractant and thus stabilizing the protrusion at the free edge (Theveneau et al., 2010). Additionally, the hypoxia inducible factor 1 (Hif-1) and its ability to promote Cxcr4 expression have been shown to be essential for chemotaxis towards SDF-1 (Barriga et al., 2013). During pre-migratory stages SDF-1 is expressed in the epibranchial placodes in *Xenopus*, a tissue that lies adjacent to the neural crest cells (Theveneau et al., 2013). Cranial neural crest cell explants are attracted to placode explants *in vitro* and it is assumed that SDF-1 could provide a short range attractive signal stimulating the directional migration of the neural crest *in vivo* (Theveneau et al., 2013).

Next to long-range chemotaxis neural crest cells maintain a collective during migration via short-range chemotaxis process, also called co-attraction. Co-attraction promotes mutual attraction between neural crest cells (Carmona-Fontaine et al., 2011; Theveneau et al., 2010). This process of co-attraction is seen when two *Xenopus* neural crest cell explants in close vicinity, attract each other. Complement factors of the innate immune response, the ligand C3a and receptor C3aR, have been shown to be required for co-attraction in *Xenopus neural crest cells.* Both ligand and receptor are expressed in neural crest cells and C3a secretion by the neural crest cells leads to a short-range gradient towards higher cell density.

Thus if a cell detaches from a cluster, it consistently move back towards the higher C3a concentration, to re-join the group. Indeed, inhibition of C3a/C3aR signalling leads to neural crest cell dispersion *in vitro* and inhibition of migration *in vivo*, as the neural crest cells can no longer migrate as a collective (Carmona-Fontaine et al., 2011; Woods et al., 2014). The C3a/C3R signalling response has been found to be mediated via Rac1 activation by the C3a/C3aR signalling and repolarization towards the C3a source (Carmona-Fontaine et al., 2011).

Contact inhibition of locomotion and collective migration

Constraint into streams, cell substrate adhesion, chemotaxis and co-attraction provide means that support migration of cranial neural crest cells (see Figure 1-4). A). Nevertheless, they are not sufficient to drive directional collective migration. An additional process, termed contact inhibition of locomotion (CIL), is needed to convene appropriate polarity to the migrating neural crest cells. Here, I will only discuss CIL of cranial neural crest cells, please refer to section 1.3 Contact Inhibition of locomotion for a broader description of the CIL. CIL is the process by which cells in contact break down their protrusions towards each other and polarise away from the contact (Mayor and Carmona-fontaine, 2010; Roycroft and Mayor, 2015; Theveneau et al., 2010). That the CIL process between neural crest cells is required for them to exert their directional migration has been shown in *in vitro, in vivo* and *in silico* (Carmona-Fontaine et al., 2008b; Scarpa et al., 2015; Theveneau et al., 2010; Theveneau et al., 2013; Woods et al., 2014). *In vitro* CIL has been first characterized using an explant invasion assay by Abercrombie (1954). Here two chick heart fibroblast cultures were plated in close proximity and outgrowing cells were undergoing contact inhibition. Thus the two cultures were inhibited to invading each other (Abercrombie and Heaysman, 1954). Indeed, direct confrontation of two neural crest cell cluster using an explant invasion assay did show CIL behaviour in *Xenopus* cranial neural crest cells (Carmona-Fontaine et al., 2008b; Moore et al., 2013; Scarpa et al., 2015; Theveneau et al., 2010). Additionally, CIL of *Xenopus* neural crest cells *in vitro* was also shown by random migration in 2D culture of dissociated neural crest cells and analysis of the angle of migration before and after collision. This randomized collision analysis showed that neural crest cells

change their direction of migration after contact with another neural crest cell (Carmona-Fontaine et al., 2008b; Moore et al., 2013; Scarpa et al., 2015; Theveneau et al., 2013). Moreover, neural crest cell CIL behaviour has been demonstrated using micro-pattern lanes, which restrict the collision angle to a head to head collision (angle of 180 degrees). Using this confinement assay colliding neural crest cells undergo CIL and completely repolarize away from each other (Scarpa et al., 2013). *In vivo*, neural crest cell CIL was shown in Zebrafish were cells undergoing collisions were shown to have comparable trajectories, than those of CIL events *in vitro* (Carmona-Fontaine et al., 2008b). Furthermore, a computational model of neural crest cell migration found that CIL is required for collective neural crest cell migration (Woods et al., 2014). In the neural crest collective CIL is thought to promote migration by preventing formation of protrusions toward the cell-cell contact in the cluster and promotion of protrusions at the leading edge (Carmona-Fontaine et al., 2008b; Stramer and Mayor, 2016). Consequently CIL in a cluster of neural crest cells has also been described as "*contact dependent polarity*" (Theveneau et al., 2010). Inhibition of protrusive activity at the cell-cell contact has been shown to be dependent on the non-canonical Wnt-planar cell polarity (PCP) pathway and RhoA activation (Carmona-Fontaine et al., 2008b; De Calisto et al., 2005; Matthews et al., 2008; Theveneau et al., 2013). This interaction leads to an asymmetric distribution of RhoA at the cell-cell contact and Rac1 at the free edge of the cluster. This promotes a change in polarity towards the direction of neural crest cell migration (see Polarization of migrating cells: Rho GTPases). Indeed, inhibition of the Wnt-PCP pathway in Xenopus leads to an inhibition of cranial neural crest cell migration *in vivo* and a loss of CIL behaviour *in vitro* (Carmona-Fontaine et al., 2008b; De Calisto et al., 2005). However, the PCP signalling pathway is not the only controller of CIL in cranial neural crest cells; Syndecan-4, Par3 and N-cadherin have also been implicated in the process (Matthews et al., 2008; Moore et al., 2013; Theveneau et al., 2010). Syndecan-4, as the Wnt-PCP, has also been shown to control contact dependent protrusion inhibition at the side of cell-cell contact, in a RhoA-dependent manner (Matthews et al., 2008). Par3, a tight junction complex protein, similarly plays a role in CIL in the neural crest by promoting microtubule catastrophe at the site of cell-cell contact (Moore et al., 2013). Moreover the cell-

cell adhesion molecule N-cadherin has been shown to be required for CIL during neural crest cell migration. Although additional signalling pathways/molecules have been implicated in CIL (for a more detailed overview see 1.3.3 Molecular mechanism of contact inhibition of locomotion), all converge on the regulation of cell polarity via small GTPases.

Besides the discussed homotypic CIL between neural crest cells, heterotypic CIL has been shown between the neural crest and placodal cells (Theveneau et al., 2010). As described in chapter 1.1.3 Chemotaxis and co-attraction, placodes express the chemokine SDF-1 and attract neural crest cells with it (Theveneau et al., 2010). However if they collide, CIL occurs and the protrusion of both placodal and neural crest cells collapse. The placodes then repolarizes and migrate away from the contact, thus creating a “chase and run” mechanism by which the neural crest is attracted towards the placode, but upon contact CIL occurs and the placode moves away again (Theveneau et al., 2010).

To ensure directional and collective neural crest cell migration the process of CIL is balanced by the process of co-attraction (see Figure 1-4 A, B). Thus, both, CIL and Co-attraction, are intrinsic neural crest cell forces that are required for neural crest cell migration.

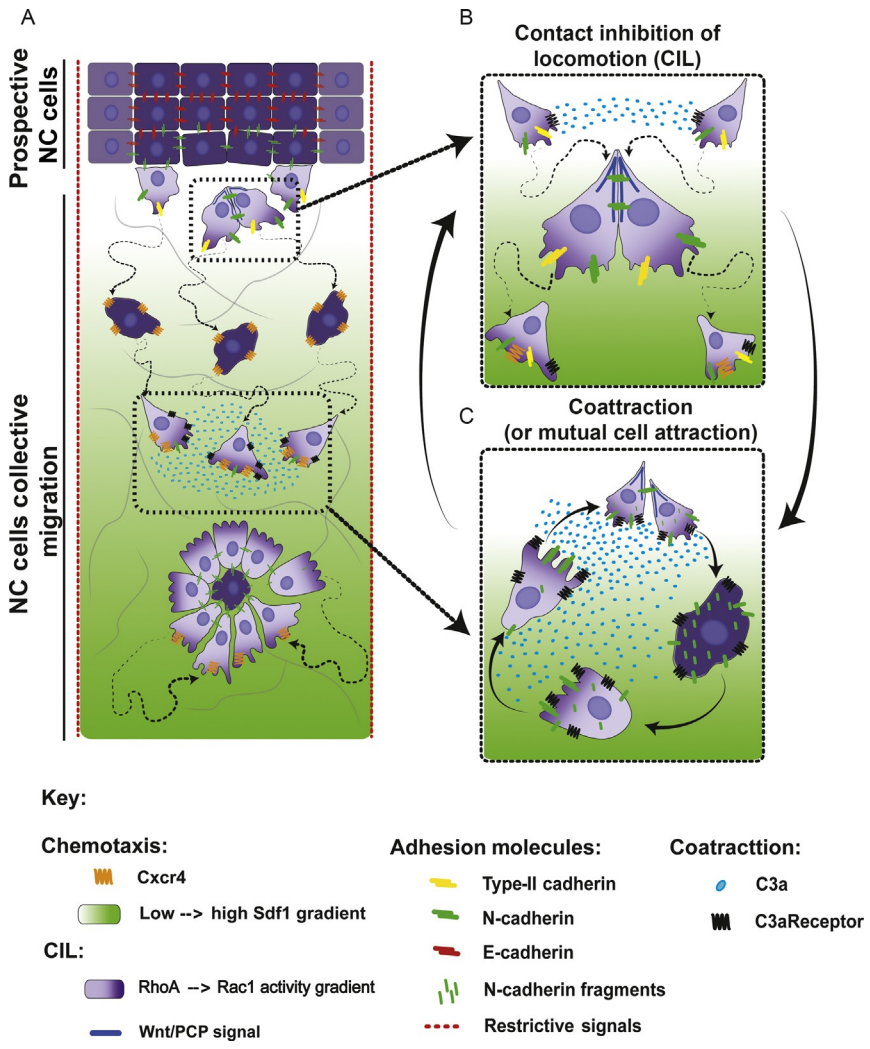

Figure 1-4 Neural crest cell migration integrates EMT, CIL and co-attraction

(A) Induced neural crest cells undergo EMT at the neural tube and acquire CIL behaviour and disperse. Co-attraction maintains the cohesive stream and chemotactic cues (green) guide through the migration pathway. Restrictive signals in surrounding tissues (red dotted line) prevent divergent migration.

(B) CIL is a cellular phenomenon by which cells upon contact, halt their migration and repolarize in opposing directions. When two neural crest cells collide transient N-cadherin-based cell–cell adhesions (green lines) are formed and produce local Wnt/PCP signals (blue). Wnt/PCP activates RhoA and represses Rac1 at the contact.

(C) Co-attraction is a process whereby neural crest cells mutually attract one another by secretion of C3a (light blue dots). CIL and co-attraction counterbalance each other Adapted from (Barriga and Mayor, 2015).

1.2 PDGF signalling

Platelet-derived growth factor (PDGF) was first found as a serum component to stimulate proliferation of vascular smooth muscle cells (Ross et al., 1974). By now the repertoire of known PDGF signalling cellular mechanisms has been expanded as diverse as proliferation, survival, cell migration, EMT, ECM production, and differentiation. During vertebrate development, PDGF signalling has been shown to play a role in neural/oligodendrocyte, vascular and hematopoietic, organogenesis, somitogenesis, skeletogenesis and neural crest cell development (Smith and Tallquist, 2010). In the following section I will discuss the PDGF signalling pathway and its components, its role in cell migration and its role neural crest cell development and migration.

1.2.1 PDGF and PI3K signalling pathway

Studies in different model mechanisms of PDGF- and PDGFR-related forms imply that some developmental roles are conserved (Hoch and Soriano, 2003). For example PDGFs role in neural development is conserved from *Drosophila* to Humans (Duchek et al., 2001; Jeibmann et al., 2015; Learte et al., 2008; Lui et al., 2014; Mellström et al., 1983; Richardson et al., 1988), similarly its role in neural crest cell development has been shown to be conserved between vertebrates (Cebra-Thomas et al., 2013; Eberhart et al., 2008; Ho et al., 1994; Klinghoffer et al., 2001; Morrison-Graham et al., 1992). Additionally PDGFs are related to VEGF, with the PDGFs being most likely evolved through divergent evolution from a common PDGF/VEGF ancestor present in *C. elegans* and *Drosophila*, by gene duplication (Andrae et al., 2008b; Grassot et al., 2006; Holmes and Zachary, 2005).

So far four different PDGF ligand variants have been described, PDGF-A, PDGF-B, PDGF-C and PDGF-D. In general, PDGFs build homodimeric ligands via two cysteine bridges, although one heterodimer PDGF-AB has been described *in vitro* (see Figure 1-5; Demoulin and Essaghir, 2014; Heldin, 2004). The PDGF-AA ligand exists in two, a “short” and “long” from, produced by alternative splicing. In the long from the ligand retains a C-terminal basic retention motif, which binds to extracellular matrix

components, a positively charged motive which is missing in the short isoform. This motif does not restrain binding to the receptor but confines diffusion (Demoulin and Essaghir, 2014). The consequence of this retention motif was highlighted during *Xenopus laevis* gastrulation. Here, the spreading and intercalation of mesoderm requires long-range signal from the short splicing isoform of PDGF-A, but not the long matrix-binding isoform (Damm and Winklbauer, 2011). The long form has been found to bind directly to fibronectin and require heparin sulphate proteoglycans (HSPGs) for this interaction (Smith et al., 2009). However a physiological role for the long form has so far not been reported. The PDGF-BB ligand similarly to the PDGF-AA ligand can have a C-terminal retention motif. However, in contrast to the A from, PDGF-BB gets translated with the retention motif and intracellular or extracellular proteases can convert it to a short, soluble from (Demoulin and Essaghir, 2014). Studies in mice with a deletion mutation in the retention motif of PDGF-B have shown its requirement for proper recruitment and organization of pericyte migration towards microvessels (Lindblom et al., 2003). More recently the PDGF-C and PDGF -D ligands were described in mouse and human (Bergsten et al., 2001; Lee et al., 2016; Li et al., 2000). In contras to both other PDGF ligands, PDGF-C and PDGF-D, are secreted in an inactive form and are only activated by proteolytic removal of the extracellular matrix binding CUB (complement subcomponent C1r/C1s, Uegf, Bmp1) domain (Demoulin and Essaghir, 2014). The protease plasmin is able to activate both PDGF-C and –D (Bergsten et al., 2001; Li et al., 2000), whereas the serine protease, tissue plasminogen activator (tPA) is exclusively activating PDGF-CC (Fredriksson et al., 2004).

All PDGFs exercise their biological tasks through the activation of dimeric receptors made up of two, structurally alike protein-tyrosine kinase receptor subunits, PDGFRα and/or PDGFRβ. Whilst PDGFRαα can be activated by PDGF-AA, -AB, -BB, or -CC, the PDGFRββ form is only activated by PDGF-BB or -DD. The heterodimeric αβ receptor has been reported to bind and be activated by PDGF- AB, -BB and possibly -CC and –DD (Figure 1-5; Demoulin and Essaghir, 2014). Additionally to PDGF ligand binding, it has been reported that the PDGFR signalling can be triggered in an indirect way, via several G protein-coupled receptors, for example angiotensin II

(Demoulin and Essaghir, 2014; Heeneman et al., 2000). Furthermore it has been shown that ligand VEGF-A can bind to PDGF receptors, agonize PDGF binding and activate mesenchymal cell migration (Ball et al., 2007; Pennock and Kazlauskas, 2012). To activate the conventional signalling pathway dimeric PDGFs bind to two receptor molecules. The receptor is build up of an extracellular ligand binding domain, consisting of five immunoglobulin-like motifs and an intracellular tyrosine kinase domain. If there is no signalling activation through a ligand, the activation loop conformation does not allow substrate access to the catalytic pocket and thus no signalling activation happens. In the presence of the ligand, receptor dimerization and conformational changes trigger auto-phosphorylation of tyrosine residues. These auto-phosphorylation sites work as docking sites for signalling proteins containing Src homology 2 (SH2) domains, leading to a relocalization of signalling molecules from the cytosol to the plasma membrane. These proteins are themselves phosphorylated on tyrosine residues, generating further docking sites or inducing conformational changes that transform their activity (Demoulin and Essaghir, 2014; Ostman and Heldin, 2007). The activated PDGFR can bind SH2 domain containing molecules at to specific phosphorylation residues, including Src tyrosine kinases, phosphatidylinositol kinase (PI3K), the Grb2/Sos1 complex that activates MAP kinase (MAPK) pathway, phospholipase C γ (PLCγ), GTPase - activating protein for Ras (RasGAP), the tyrosine phosphatase SHP-2, and STAT family transcription factors (see Figure 1-6). Next to those direct downstream activators, the receptor can bind some SH2 domain containing adaptor molecules, as Nck, Shc, and Crk, whose function it is to mediate between the receptor and further effector molecules (Ostman and Heldin, 2007). Several signalling pathways have been described downstream of PDGFR signalling, including MAPK, PI3K, JNK, PKC and Rac related pathways (Demoulin and Essaghir, 2014). However PI3K and PLC downstream of PDGF signalling have been mainly linked to PDGF induced actin reorganization and chemotaxis, while the MAPK and Src pathway have been found as major contributors to cell proliferation (Ostman and Heldin, 2007). Nevertheless, wide-ranging cross talk between the downstream signalling pathways and the cellular effect of the pathway changes from cell type to cell type.

In the following only the PI3K pathway will be discussed in detail, please refer to the following reviews for more information on other PDGF downstream signalling pathways (Demoulin and Essaghir, 2014; Heldin and Westermark, 1999; Ostman and Heldin, 2007).

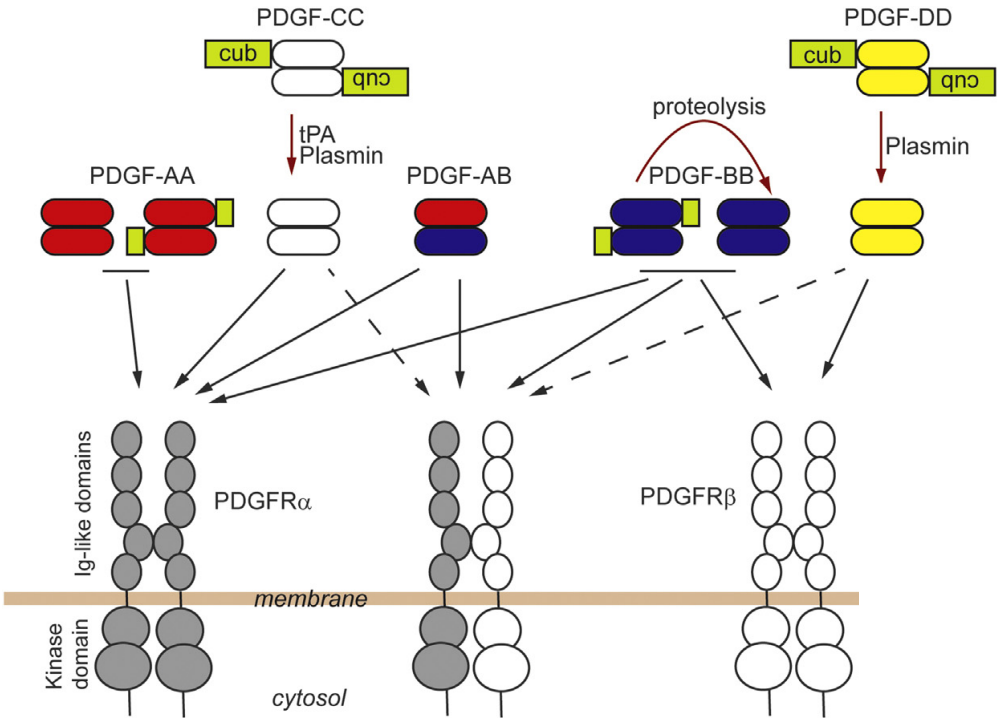

Figure 1-5 PDGF signalling: receptor and ligands.

PDGF-A, -B, -C and - D, PDGFs are secreted as homodimeric or heterodimeric proteins (PDGF-AA, -BB, -CC, -DD and –AB) linked by two cysteine bridges. PDGF-AA (red) exits in two splice variations a short and a long isoform. The long isoform posses a C-terminal basic retention motif (green box), which does not inhibit binding to the receptor, but restricts diffusion. Also PDGF-BB (blue) has a C-terminal basic retention motif (green box), which can be removed by intracellular or extracellular proteases. PDGF-CC and -DD are secreted as inactive precursors, due to the N-terminal CUB domain (green box). The CUB domain is removed by proteases (plasmin or tissue plasminogen activator (tPA)) releasing the active soluble ligand. The two RTKs PDGFRα and/or PDGFRβ build active receptor complexes containing two receptor chains. PDGFRα is activated by all PDGF

isoforms except PDGF- DD, while PDGFRβ is activated by PDGF-BB and -DD. A heterodimeric PDGFR-α/β receptor has been reported, and binds to PDGF-AB (Figure adapted from Demoulin and Essaghir, 2014.)

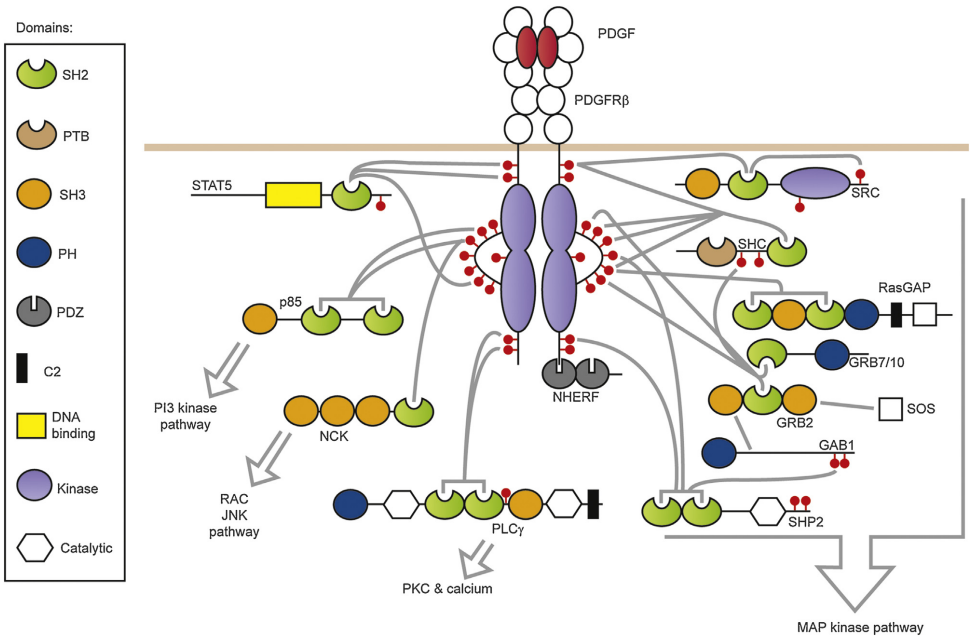

Figure 1-6 PDGF signalling pathways.

Upon ligand binding multiple phosphorylation sites (red circles) at the PDGF receptor convey different downstream signalling pathways via adaptor proteins. PDGF signalling downstream pathways include the PI3K, RAC-JNK, PKC and MAPK pathway. Domains of adaptor proteins depicted on the right side; SH2 (Src Homology 2), PTB (phosphotyrosine-binding), PH (Pleckstrin homology). (Figure adapted from Demoulin and Essaghir, 2014).

PI3K signalling pathway

Phosphatidylinositol-3 kinase (PI3K), pathway is named after its signalling effector, PI3K a heterodimeric lipid kinase that consists of a regulatory and a catalytic subunit. P85 is the regulatory subunit, which binds, upon receptor activation, to specific phosphorylation sites at the receptor tyrosine kinase (RTK). Activation of

p85 leads to membrane localization and catalytic activity of the second subunit p110. P110 is the catalytic subunit, which mediates the phosphorylation of the second messenger phosphatidylinositol- 4,5-triphosphate (PIP2) to phosphatidylinositol- 3,4,5-triphosphate (PIP3) (Demoulin and Essaghir, 2014; Vivanco and Sawyers, 2002). Additionally, PI3K has also been indicated to regulate other cellular targets than PIP3, such as the serum and glucocorticoid-inducible kinase (SGK) (Park et al., 1999), the small GTP-binding proteins RAC1 and CDC42 (Jiang et al., 2000; Liliental et al., 2000; Welch et al., 1998), and protein kinase C (PKC) (Fan et al., 2009). The PIP3 lipid second messenger triggers a cascade of effector kinases, beginning with the activation and translocalisation of 3-phosphoinositide-dependent protein kinase-1 (PDK1), which binds to PIP3 with its pleckstrin homology (ph) domain. Membrane bound PDK1 activates further downstream kinases by phosphorylation of AKT/PKB, the p70 S6 kinase and atypical protein kinase C isoforms (see Figure 1-7; Hanada et al., 2004; Heldin et al., 1998). All these kinases have been linked to PDGF signalling (Heldin et al., 1998). Additionally there are several PIP3 phosphatases known which negatively regulate PI3K signalling, the best studied is PTEN (Demoulin and Essaghir, 2014; Hanada et al., 2004). Interestingly, AKT might be the only vital effector of PIP3 signalling. A study in *Drosophila* found that of Pten could be rescue-able by a PH-domain mutant of AKT that cannot bind PIP3 (Stocker et al., 2002).

In general, AKT has different downstream effectors it can activate. AKT can block cell death by inhibition of pro-apoptotic BAD and Forkhead or NF-κβ transcription factors (Brunet et al., 1999; Datta et al., 1997; Peso et al., 1997; Romashkova and Makarov, 1999). Moreover, AKT can also stimulate the cell cycle by phosphorylation of MDM2 and subsequent inhibition of pro-apoptotic p53 (Mayo and Donner, 2001; Zhou et al., 2001) and has been shown to regulate glucose metabolism (Cho et al., 2001).

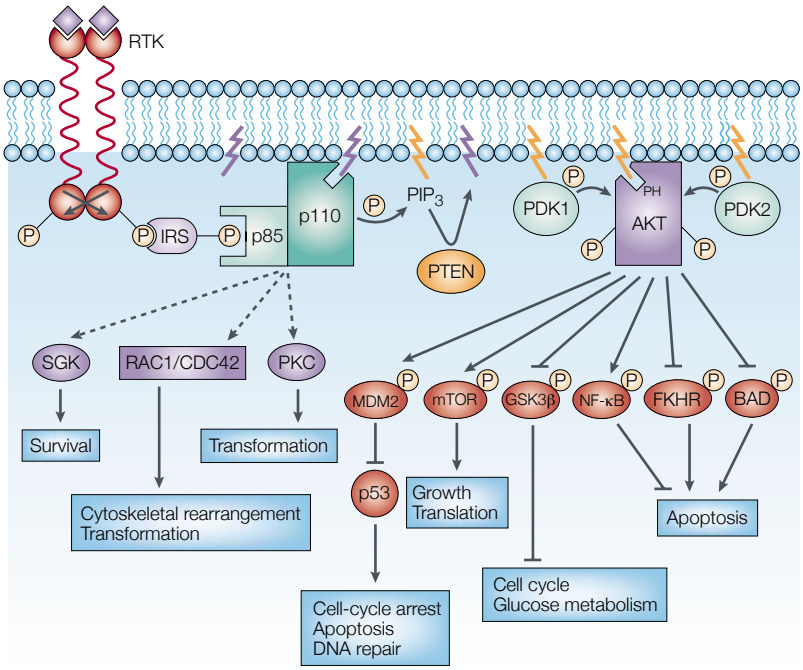

Figure 1-7 PI3K signalling

Schematic representation of PI3K signalling pathway. Upon ligand binding the receptor dimer autophosphorylates specific tyrosine residues (see Figure 1-7). IRS (Insulin receptor substrate) adaptor protein facilitates activation and translocation of PI3K, comprising a regulator (p85) and catalytic subunit (p110). Translocated PI3K mediates phosphorylation of PIP2 to PIP3. The PIP3 lipid second messenger activates and translocalisation PDK1/2, which further activates AKT/PKB by phosphorylation. Activates AKT/PKB can trigger different downstream signalling effectors and cellular events. PI3K has also been indicated to regulate (SGK) the small GTP-binding proteins RAC1 and CDC42 and PKC. *(Adapted from Vivanco and Sawyers, 2002)*

1.2.2 PDGF signalling in migrating cells

In this section I will discuss PDGF signalling in migrating cells *in vitro* and *in vivo,* with a particular focus on the effector PI3K/AKT. PDGF signalling and its specific role in neural crest cell development and migration will be discussed in the following section (see section 1.2.3 PDGF signalling and neural crest cells).

PDGF signalling and cell migration *in vitro*

The PDGFRα and PDGFRβ signalling roles have been extensively studied in *in vitro* and have been associated with regulation of proliferation, cell migration and chemotaxis in response to PDGF ligands (Demoulin and Essaghir, 2014). Especially PI3K downstream signalling has been implicated in this process. (Bazenet and Kazlauskas, 1994; Brachmann et al., 2005; Joly et al., 1994; Kundra et al., 1994; Valius and Kazlauskas, 1993). Indeed, *in vitro* studies using pharmacological inhibitors, PDGFR-PI3K binding site mutants or mouse fibroblasts from PI3K subunit knock-downs have shown that PI3K dependent downstream signalling is required for PDGF mediated cell ruffling and chemotaxis (Brachmann et al., 2005; Kundra et al., 1994; Severinsson et al., 1990; Wennstrom et al., 1994; Wennström et al., 1994)

As discussed in chapter 1.1.2 Polarization of migrating cells: Rho GTPases polarization of migrating cells is mediated by small GTPases. In cell culture assays PDGFs have been shown to strongly activate the small GTPase Rac1 which leads to reorganization and protrusion formation in the leading edge (Nimnual et al., 2003; Pertz et al., 2006; Ridley and Hall, 1992; Sander et al., 1999). Furthermore, mutual inhibition between Rac1 and RhoA has been suggested as a prominent role during migration in the leading edge of a PDGF-AA treated cells (Pertz et al., 2006). Indeed, inhibition of RhoA activity has been especially observed in randomly migrating fibroblast cells. These cells have a small stripe of RhoA activity in the leading edge, which has been associated with peripheral ruffles and pinocytic vesicles production. However, if fibroblasts are treated with PDGF-AA the RhoA activity vanishes from the leading edge potentially by inhibition via Rac1 (Pertz et al., 2006). Interestingly, the Rac1 activity is though to be regulated by downstream PI3K signalling. PI3K and as a consequence PIP3 get concentrated at the leading edge and recruit Rac GEFs,

as Tiam1 and Dock4, to the plasma membrane to trigger Rac (Buchanan et al., 2000; Goicoechea et al., 2014; Han et al., 1998; Kawada et al., 2009). Although AKT, another PI3K downstream effector, has been implicated in cell polarity establishment via small GTPases (Xue and Hemmings, 2013). Dominant negative mutation of AKT was able to decrease PDGF-Rac1 mediated cell migration in fibroblasts (Higuchi et al., 2001). Interestingly polarizing PI3K/Rac1 activity has been shown to be inhibited by N-cadherin junctions in cell clusters (Charrasse et al., 2002; Dupin et al., 2009; Haÿ et al., 2009; Theveneau et al., 2010). A recent study found that N-cadherin in cell-cell adhesions of cell doublets plated on fibronectin micropatternstripes, promotes the activation of PDGF dependent PI3K and Rac localization at the free edge. This is thought to work via inhibition of integrin at the cell-cell contact by N-cadherin bound p120, while integrin-PI3K-Rac activation is supported at the free edge (Ouyang et al., 2013). Moreover direct integrin-PDGFR interaction has been shown to influence receptor activation and downstream signalling. Thus adhesion to fibronectin via integrin have been shown to strongly potentiate PDGF-induced PDGFR signalling (Amano et al., 2008; Borges et al., 2000; Minami et al., 2007; Schneller et al., 1997; Woodard et al., 1998; Zemskov et al., 2009). A recent publication in mesenchymal stem cells found that PDGFRβ mediated PI3K/AKT activation as well as actin assembly and migration is controlled by fibronectin and integrin α5β1 interactions (Veevers-Lowe et al., 2011). They found that adhesion to ECM, specifically fibronectin, induces PDGFRα and PDGFβ phosphorylation in a α5β1-integrin dependent manner. And this leads to downstream activation of PI3K/AKT signalling pathway and actin assembly and finally migration. Thus, they conclude that the synergistic interactions between integrin and PDGFR are fundamental for cell migration (Veevers-Lowe et al., 2011).

Moreover a recent study showed that uniform PDGF can induce rapid, uni-directional, and persistent migration in fibroblasts, if the cells are polarized by adhesion on a fibronectin line. This unidirectional migration was not observed if the PDGF ligand was not applied or the cells were plated on uniform fibronectin substrate (Martin et al., 2014). This suggests that cells can independently integrate chemical (PDGF) and physical cues (fibronectin line) and indicates that PDGF-

induced, directional fibroblast migration might not be essentially required as a chemotactic cue, rather more as a chemokinetic factor.

PDGF signalling *in vivo*

PDGF signalling has been implicated in plethora of developmental processes and wound healing, tissue homeostasis and cancer metastasis in the adult. Here I will focus on its developmental role. Please refer to the following reviews on roles of PDGF in the adult (Demoulin and Essaghir, 2014; Heldin, 2012; Ostman and Heldin, 2007).

As described in the section before, cell migration is a highly investigated consequence of PDGF stimulation *in vitro* (Andrae et al., 2008a; Heldin, 2012), however the knowledge about PDGF-dependent cell migration *in vivo* is restricted. PDGF signalling in developmental processes have been strongly implicated in cell spreading of different populations, such as oligodendrocyte or glia spreading in the spinal cord, neural crest cell spreading towards its migratory pathways and targets, pericyte spreading along newly building vasculature and mesoderm spreading during gastrulation.

One early role of PDGF signalling has been shown during *Xenopus* gastrulation. Here PDGF-A and PDGFRα have been implicated in mesoderm migration and spreading over the fibronectin covered blastocoel roof in a PI3K-dependent mechanism. PDGF-A is expressed by the ectodermal cells in the blastocoel roof and works as a gradient that drives mesodermal cell movements along the blastocoel roof (Ataliotis et al., 1995; Nagel et al., 2004; Symes and Mercola, 1996; Winklbauer et al., 1996). Thus PDGFRα expressing mesoderm cells migrate directionally over a matrix bound gradient, of the PDGF-A long form, over the blastocoel roof. The PDGF-A gradient is generated by the fibronectin binding of the PDGF-A long isoform via its retention motif. Indeed, PDGF-A signalling gradient impairment leads to depletion of persistent migration in direction of the animal pool in *Xenopus laevis embryos* (Nagel et al., 2004). A more recent publication found that also that the short isoform of PDGF-A is required during *Xenopus* gastrulation (Damm and Winklbauer,

2011). Here the short-form of PDGF-A was found to be important as a long range guidance cue for protrusion orientation and radial intercalation of the deep mesoderm prechordal cells (Damm and Winklbauer, 2011).

Additionally to its role in Xenopus, PDGFR and PI3K have also been linked to collective mesoderm migration in zebrafish (Dumortier et al., 2012; Kai et al., 2008; Montero et al., 2003). This role was first shown in leading cells during mesoderm migration, using a dominant negative form of PI3K and showed that leading edge cells need a PDGF/PI3K pathway for protrusion formation and cell polarization (Montero et al., 2003). However, Dumortier et al. (2012) showed that all plate mesoderm cells require PI3K signalling for proper protrusion formation (Dumortier et al., 2012). By using a ph-AKT-mcherry biosensor, which binds to PIP3 in the plasma membrane, they also found that active PI3K signalling in mesodermal cells orient towards the anterior, that means towards their direction of migration (Dumortier et al., 2012; Montero et al., 2003). However, no effect on directionality was observed by PDGF signalling depletion, as prechordal mesoderm cells still migrated towards the animal pole. Moreover no source of PDGF has been described in the zebrafish embryo so far, thus suggesting the presence of other process that might ensure directionality (Montero et al., 2003).

In *Drosophila* PVF1 and PVR, the PDGF/VEGF and PDGFR/VEGFR homologues, respectively, are required for directional border cell migration in the egg chamber (Duchek et al., 2001). In general the role of PVR signalling has many similar characteristics to *Xenopus* gastrulation. Likewise, the receptor is expressed in the migrating tissue, in this case the border cells, and the ligand is expressed in tissue over which the cells migrate, here the egg chamber. The border cells migrate as a collective, whereby a single cell acts as the leader, extending a long protrusion towards the target region. Knockdown of either PVR or PVF1, by dominant negative form or a homozygous mutant, respectively, leads to the inhibition of border cell migration (Duchek et al., 2001). Similarly, ectopic expression of the ligand leads to migration of boarder cells to their endogenous path. Moreover uniform overexpression of PVF1 impairs protrusion formation and thus directional migration

of border cells (McDonald et al., 2006). Thus the directional, collective migration of border cells depend on the PV1 gradient towards the oocyte (Fulga and Rørth, 2002), similar to the PDGF gradient in the blastocoel roof required mesoderm migration in *Xenopus* (Nagel et al., 2004). Likewise in *Xenopus,* disruption of the gradient by overexpression of PDGF-A in the whole blastocoel roof leads to inhibition of mesoderm migration. However, migration of *Drosophila* border cells require EGF signalling together with PVR signalling which has so far not been linked to *Xenopus* mesoderm migration (McDonald et al., 2006). Only Ras and a homologue of the vertebrate GEF Dock180, seem to be required for boarder cell migration in *Drosophila* (Duchek et al., 2001). In contrast to the role of PI3K described in Xenopus and Zebrafish mesoderm migration, inhibition or ectopic activation of the PI3K subunit p110 homologue does not affect border cell migration (Duchek and Rørth, 2001).

Thus, the ability to control collective cell migration via PDGF/VEGF gradients in the extracellular space appears to be a conserved mechanism between vertebrates and invertebrates (Andrae et al., 2008a; Scarpa and Mayor, 2016)

1.2.3 PDGF signalling and neural crest cells

PDGF signalling plays essential roles during development from gastrulation to the development of neural crest cell, gonads, lung, intestine, skin, central nervous system, vasculature, and skeleton (Heldin and Lennartsson, 2013; Hoch and Soriano, 2003). This section will mainly focus on PDGF signalling in neural crest cell development.

PDGF signalling during neural crest cell migration

The PDGF receptor α (PDGFRα) is expressed in migrating neural crest cells in, mouse, zebrafish and *Xenopus* (Eberhart et al., 2008; Ho et al., 1994; Orrurtreger and Lonai, 1992; Schatteman et al., 1992; Takakura et al., 1997) and its corresponding ligands PDGF-A and PDGF-C in the surrounding tissue (Ding et al., 2000; Eberhart et al., 2008; He and Soriano, 2013; Ho et al., 1994; Tallquist et al., 2000). Expression of PDGFRβ, PDGF-B and PDGF-D have so far not been reported

during cranial neural crest cell migration in mouse, however PDGF-B and PDGFRβ have been linked to vasculagenesis and are expressed in endothelial cells and some pericytes in the mouse cranium, respectively (Lindahl et al., 1997; Soriano, 1994). PDGF-B expression in Xenopus has been recently shown to be specific to the developing central nervous system, rather than cranial neural crest cells (Giannetti et al., 2016). Although many different PDGFR and PDGF ligand connections have been shown *in vitro* (Figure 1-5), so far *in vivo* interaction studies in mouse development have only demonstrated PDGF-AA or PDGF-CC interaction with PDGFRα (Boström et al., 1996; Ding et al., 2004; Soriano, 1997), whereas PDGF-BB exclusively activates PDGFRβ *in vivo* (Levéen et al., 1994; Soriano, 1994).

Developmental studies of PDGF signalling during neural crest cell migration have mainly been done in mouse so far. In general, PDGFRα signalling has been demonstrated to be essential for both cranial and cardiac neural crest cell development, while a more restricted role in cardiac NCC development has been demonstrated for PDGFRβ (Fantauzzo and Soriano, 2015).

The first connection of a possible role of PDGFRα in neural crest cell development was drawn in the Patched (Ph) mouse mutant (Stephenson et al., 1991). A spontaneous mouse mutant that was studied because of its non-pigmented hair patches in the trunk region, caused by a large deletion of the PDGFRα locus and part of the receptor cKit enhancer (Duttlinger et al., 1995; Grüneberg and Truslove, 1960; Stephenson et al., 1991). Most of the malformations in the Ph mutants could be attributed to the PDGFRα depletion due to the fact that the only phenotype in a cKit mutant is a developmental defect in melanocyte development (Geissler et al., 1981; Wehrle-Haller, 2003). Apart form this the homozygous Ph allele mimicked phenotypes which where generally observed when neural crest cell development was disrupted (Geissler et al., 1981; Grüneberg and Truslove, 1960; Wehrle-Haller, 2003), including severe craniofacial phenotypes as complete clefting of the frontonasal process palate and malformation of the heart septation, and heart valve abnormalities (Grüneberg and Truslove, 1960; Robbins et al., 1999; Schatteman et al., 1992). The first set of phenotypes can be attributed to defects in cranial neural

crest cell development and the heart abnormalities to cardiac neural crest cell development. Notably, the craniofacial malformations could be traced back to different arch regions. However neural derivatives from the same arch developed normally, suggesting that PDGFR mutation might only affect a subset of neural crest cell population (Morrison-Graham et al., 1992). Defects of the Ph mutant were phenocopied in mice having a targeted homozygous mutation in the PDGFRα including clefting of the frontonasal process palate, subepidermal blebbing, vascular abnormalities, cardiac defects, abnormalities in neural tube development, defects in somite pattering, and skeletal defects (Soriano, 1997). Interestingly, those defects could be copied in targeted disruption of PDGF ligands A and C (Ding et al., 2004). This highlights the functional requirement of PDGF-A and PDGF-C for PDGFRα signalling during neural crest cell development. Though PDGF-B is proficient of binding to PDGFRα, functional studies have not shown any part for this interaction so far.

Chimeric analysis of PDGFRα signalling, with PDGFRα deleted embryonic stem cells showed a high exclusion of depleted cells from neural crest cell derived tissue. This suggests that the defects in the PDGFRα null mutants are cell-autonomous and can be accounted to neural crest cell developmental disruptions (Tallquist et al., 2003). Interestingly, the conditional knock down of PDGFRα in neural crest cell tissue, using Wnt1-Cre driver line, showed only a subset of the phenotypes observed in the mutant embryo, including facial clefting, haemorrhaging in the midline, defects in the heart outflow tract and thymus malformations (Tallquist et al., 2003). The fact that only a subset of phenotypes was observed might be due to the use of the Wnt1-Cre line which has been recently found to have ectopic activation of Wnt signalling (Lewis et al., 2013). Further the Wnt1 driver might not be perfect choice for a conditional knock down of PDGFRα, as the expression of Wnt1 is not limited to the neural crest territories in the embryo and the onset of expression might be to late to affect early neural crest cell developmental defects (Barriga et al., 2015; McMahon et al., 1992). Nonetheless, analysis of the cellular mechanism involved in the facial clefting phenotypes in $Pdgfr\alpha^{fl/fl}$; Wnt1-Cre embryos showed that PDGFRα signalling is required for migration of neural crest cells towards medial lateral

prominence and later for the proliferation of the neural crest cell derivative mouse embryonic palatal mesenchymal cells (MEPMs) (He and Soriano, 2013). Indeed, it has been shown that ex vivo culturing of PDGFRα depleted neural crest cell explants showed a decreased emigration from explant cultures. Further analysis of PDGFRα signalling in MEPMs found that the PI3K/Akt and Rac1 to pathway are required for MEPM proliferation (He and Soriano, 2013). However, it has not been established if PI3K/AKT or the small GTPase Rac1 are also required for neural crest cell development and migration.

The PDGFRβ is expressed in mouse embryonic mesenchyme during neural crest cell induction and early migration stages (E 8.5), however the expression is more restricted towards the heart, somite and limb buds at later stages (Soriano, 1994). Targeted disruption of PDGFRβ leads to vascular and kidney defects in mouse embryos (Soriano, 1994). The mouse double knockdown of PDGFRα and PDGFRβ exhibit defects linked with cardiac neural crest cell development (Richarte et al., 2007; Van Den Akker et al., 2008). Interestingly, the conditional knockdown using the Wnt1-Cre driver of both, PDGFRα and PDGFRβ, leads to a more severe phenotype in cardiac neural crest cell derived tissues than each depletion alone (Richarte et al., 2007). This suggests that both receptors are needed for cardiac neural crest cell development. In general, the difference in neural crest cell phenotypes between PDGFRα and PDGFRβ depleted mouse embryos seems to be predominantly caused by differences in their spatiotemporal expression. To study the different signalling capacities of the two receptors Klinghoffer et al. (2001) developed two complementary lines of knock-in mice in which the intracellular signalling domains of one PDGFR was exchanged by those of the other and vice versa (Klinghoffer et al., 2001). Analysis of embryos from these two lines showed a considerable rescue, while the PDGFRβ receptor with a PDGFRα cytosolic domain resulted in vascular malformations (Klinghoffer et al., 2001). Thus showing a strong similarity in signalling capabilities between the two receptor functions.

In zebrafish, PDGFRα and PDGFRβ are both expressed in migrating neural crest cells and pharmacological inhibition using a PDGFR inhibitor showed inhibition of neural

crest cell migration (McCarthy et al., 2016). Interestingly, PDGFRα depletion in zebrafish using a mutant leads to craniofacial abnormalities as observed in mouse (Eberhart et al., 2008). Eberhard et al. (2008) suggested a mechanism by which cranial neural crest cell migration is dependent on PDGFRα level attenuation of microRNA 140 (Mirn140). Indeed, if Mirn140 expression is inhibited or Mirn140 is overexpressed cranial neural crest cell defects including facial clefting were reported. This suggests that this attenuation is needed for cranial neural crest cells to migrate over PDGF-AA expressing cells and reach the oral ectoderm (Eberhart et al., 2008).

Additionally a recent study looked into the requirement of PDGFRβ in mouse and zebrafish development. They showed that the β receptor is replaceable for craniofacial development in zebrafish. Although the double knockdown of both receptors, in mouse and zebrafish, displayed a stronger defect in palatogenesis than the PDGFRα mutant alone (McCarthy et al., 2016). Analysis of the cellular mechanisms in PDGFRα-PDGFRβ mutant zebrafish revealed that the phenotype is due to loss of proper condensation of neural crest cells in the maxillary domain (McCarthy et al., 2016). Overall, this suggests that PDGFRβ has a minor, complementary role and PDGFRα has the major role ensuring proper cranial neural crest cell migration.

Downstream effectors of PDGF signalling in neural crest cell

Investigation of downstream effectors of the PDGFRα receptor, using phosphorylation docking site point mutation for either PI3K, SRC or multiple other pathways in mouse embryo development, revealed the essential requirement for PI3K in PDGFRα signalling (Klinghoffer et al., 2002). While loss of the phospho-docking site for Src and subsequent downstream signalling had no obvious affect on neural crest cell development (Klinghoffer et al., 2002). Homozygous mutation of the PI3K binding site in the PDGFRα receptor leads to some craniofacial defects. Interestingly, only the homozygous double knockdown of PI3K binding sites in both, the PDGFRα and PDGFRβ, embryos mimics the PDGFRα knockout phenotype (Klinghoffer et al., 2002). This suggests a role for PDGFRα/β heterodimers in mouse

neural crest cell development, while PI3K signalling seems to be the downstream effector. Moreover the depletion of the regulatory subunits p85a and p85b, or p110a catalytic subunit of PI3K mimic the phenotype observed in the PDGFRα knock-down (Brachmann et al., 2005).

In vitro experiments suggested that PDGFRα/β heterodimers have different downstream properties than homodimeric receptor complexes (Fantauzzo and Soriano, 2015). For instance, PDGFRα phosphorylation on tyrosine 754, for SHP-2 binding, has been exclusively reported for heterodimeric receptors (Rupp et al., 1994). Moreover, the heterodimeric receptor has been reported to have increased mitogenic properties compared to the homodimeric receptors (Rupp et al., 1994). However the occurrence of these functional differences in heterodimeric signalling and their potential effect on cellular mechanisms compared to the homodimeric receptors has yet to be determined.

More recently Fantauzzo and Soriano (2014) investigated intracellular downstream effectors of the PDGFRα-PI3K-Akt axis in neural crest cell derived palatal mesenchyme. Using a phosphoproteomic mass spectrometry approach they found that downstream effector proteins are involved mainly in cell and proliferation and this to be, at least in part, regulated by the p53 transcription factor (Fantauzzo and Soriano, 2014). However, downstream signalling in earlier stages, as neural crest cell migration, has not been investigated yet.

1.3 Contact Inhibition of locomotion

Abercrombie first described contact inhibition of locomotion during chick heart fibroblast migration (1958). And he describes the process as

> *"…the phenomenon of a cell ceasing to continue moving in the same direction after contact with another cell."*
>
> (Abercrombie, 1978).

CIL by now has been reported during cancer cell metastasis, haemocyte dispersion in *Drosophila* and most important during neural crest cell migration in *Xenopus laevis* and zebrafish. In the following section I will discuss general cellular molecular aspects of CIL, describe its *in vivo* roles and specifically its role in neural crest cell migration and EMT.

1.3.1 CIL in general

CIL is a process by which two colliding cells stop their movement and migrate away in a different direction. Simplified the process of contact inhibition can be subdivided into four distinct phases after collision (Figure 1-8).

1. build up of a transient adhesion between the two colliding cells

2. repolarization of the cell

3. formation of new leading edge

4. moving away from the point of cell-cell contact

(Reig et al., 2014; Stramer and Mayor, 2016).

The process of homotypic CIL, whereby two cells of the same cell type collide, can be subdivided into the following two types (see also Figure 1-9). The first type describes the immobility upon contact, followed by cellular retraction of the leading edge and movement away from the colliding cell, thus an active migration away (Abercrombie, 1970; Abercrombie, 1978; Stramer and Mayor, 2016). The second type describes the inability of a cell to move across another, which leads to either cessation of movement or random diversion of the colliding cell. Thus, compared to the controlled contraction and repolarization of type I, type II is a more inactive reaction controlled by the forces of the cell-cell contact (Abercrombie, 1970; Stramer and Mayor, 2016; Veselý and Weiss, 1973). In comparison type I CIL is most possibly controlled by specific molecular mechanisms, as cell-cell contact receptors and downstream signals which lead to changes in cell polarization and actin

assembly (Stramer and Mayor, 2016). Nonetheless it is noteworthy that the type of CIL a cell population undergoes underlies variability. These variations depend on the orientation of collision, if the cells collide front-to-front or front-to-back. Further also changes in the signalling pathways recognized may lead also to a different type of CIL (Abercrombie, 1967; Abercrombie, 1970; Abercrombie and Dunn, 1975; Desai et al., 2013; Scarpa et al., 2013).

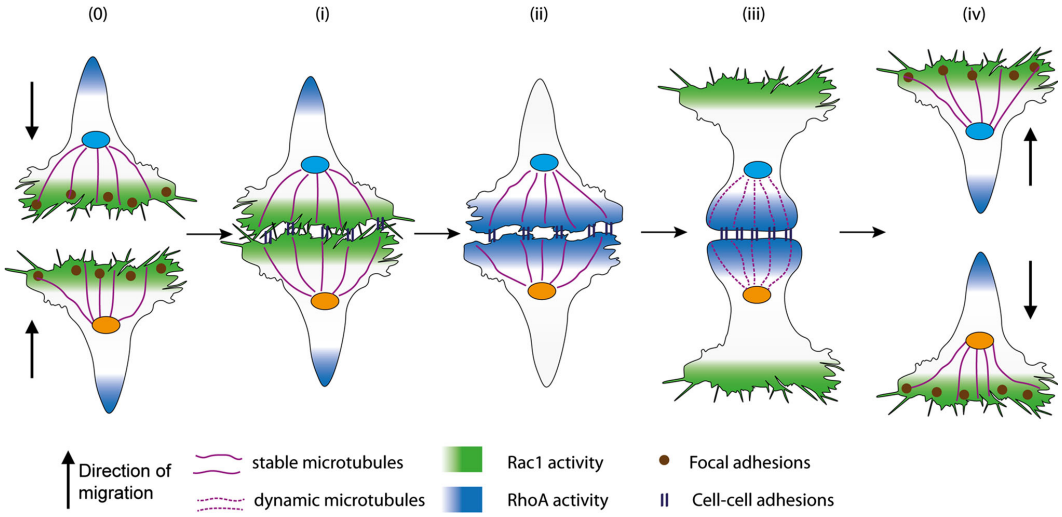

Figure 1-8 Four phases of contact inhibition of cell locomotion

The mechanism of contact inhibition can be subdivided in three different phases. – (1) Colliding cells get into contact. (2) Cell-cell contact inhibits protrusion. (3) Cells repolarise and from protrusion away from point of contract. (4) Cells detached from another and move away. Adapted from Roycroft and Mayor, 2016

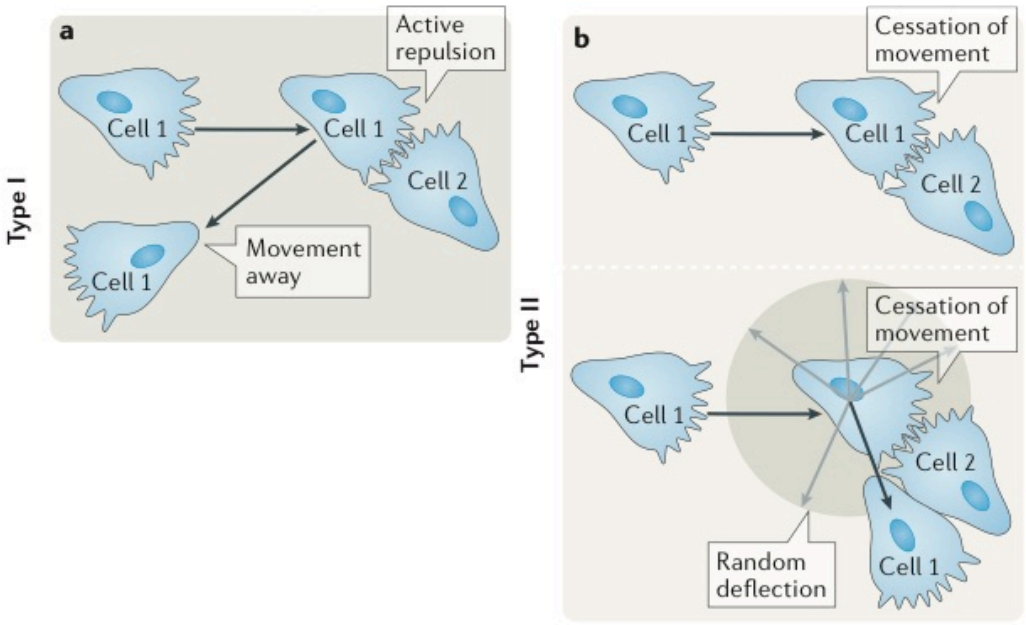

Figure 1-9 Contact inhibition of locomotion type classification

(a) Type I CIL collisions comprise active repulsion and movement away from the colliding cell. (b) Type II CIL collisions do not display repulsion, cells either cease movement after contact or are randomly deflected form the colliding cell. Adapted from Stramer and Mayor, 2016.

1.3.2 Study of contact inhibition of locomotion - *assays*

As described in the section before (section 1.3.1) CIL behaviour underlies variability. To investigate and describe the CIL behaviour of a given cell population, use of multiple assays is generally required to describe the cellular behaviour. Over recent years several approaches have been developed to study and understand CIL including mixing, radial outgrowth, kinematics in 2D and 1D. In the following section they will be described in detail.

Mixing assay

The first assay used to study CIL by Abercrombie is the so called mixing assay (Abercrombie and Heaysman, 1954), sometimes also described as invasion or

explant confrontation assay. Here differently marked explant cultures are plated at a short gap between each other, the outgrowth of cells and their overlapping behaviour was used as readout of CIL. Thus when cells start to overlap they undergo a CIL response and cell migration from the explants stops. However in the case of explants with impaired CIL, explants will overlap and invade each other (Roycroft and Mayor, 2016; Stramer and Mayor, 2016). Abercrombie used this assay to describe CIL of fibroblast and metastatic sarcoma cells, whereby the latter showed an impaired CIL response and the cancer cell explants were able to invade each other (Abercrombie and Heaysman, 1954). This suggested a loss of CIL in metastatic sarcoma cells. Moreover this assay was also used to describe CIL responses in neural crest cell explants in *Xenopus* (Carmona-Fontaine et al., 2008b; Scarpa et al., 2015; Theveneau et al., 2010). A variation of this CIL test was developed, which analyses instead of the overlap of the two explant, the overlap area of protrusions (Moore et al., 2013; Scarpa et al., 2015).

Radial outgrowth assay

The next assay used to study CIL is the so-called radial outgrowth assay. If an explant is cultured alone, CIL behaviour will lead to radial dispersion. Quantification of CIL dispersion is done by measuring the distance between neighbouring cells, using Delaunay nearest neighbour equation (Carmona-Fontaine et al., 2008b; Nawrocki Raby et al., 2001; Scarpa and Mayor, 2016; Theveneau et al., 2010).

Kinematics assay 2D and 1D

CIL behaviour in single cells has mostly been studied using 2D substrates (Roycroft and Mayor, 2016). In the 2D Kinematics assay, cells are plated in a 2D environment of a culture dish, or analysed *in vivo* in cases where 2D dimensions can be applied and monitored using time-lapse microscopy. The Individual cells migrate randomly and stochastic collisions between them are observed (Roycroft and Mayor, 2016; Stramer and Mayor, 2016). This assay is a powerful way to describe many characteristics of changes such as changes in velocity and acceleration during CIL, as

well as the angle of migration after contact (Carmona-Fontaine et al., 2008b; Davis et al., 2012; Davis et al., 2015). One disadvantage of the 2D Kinematics assay is that cells can collide from different angles, such as front-on-front or front-on-side or even front-back. This is especially problematic as it is known for long that front-on-front collisions show a clear CIL behaviour, whereas other cell confrontations, where cell front lamellae do not get in contact, do not (Abercrombie and Dunn, 1975; Davis et al., 2012). To circumvent this, a 1D Kinematic collision assay was developed. Here migration of cells is restricted using striped micropatterns, so more head-on-head collisions are generated, while the angle of repolarization is limited (Desai et al., 2013; Scarpa et al., 2015). Collision in the 1D assay can lead to a type I CIL response, whereby the cells repolarize and move away from each other, or just one cell is repolarizing. If a type II response occurs, the cells remain in contact with each other (Stramer and Mayor, 2016)

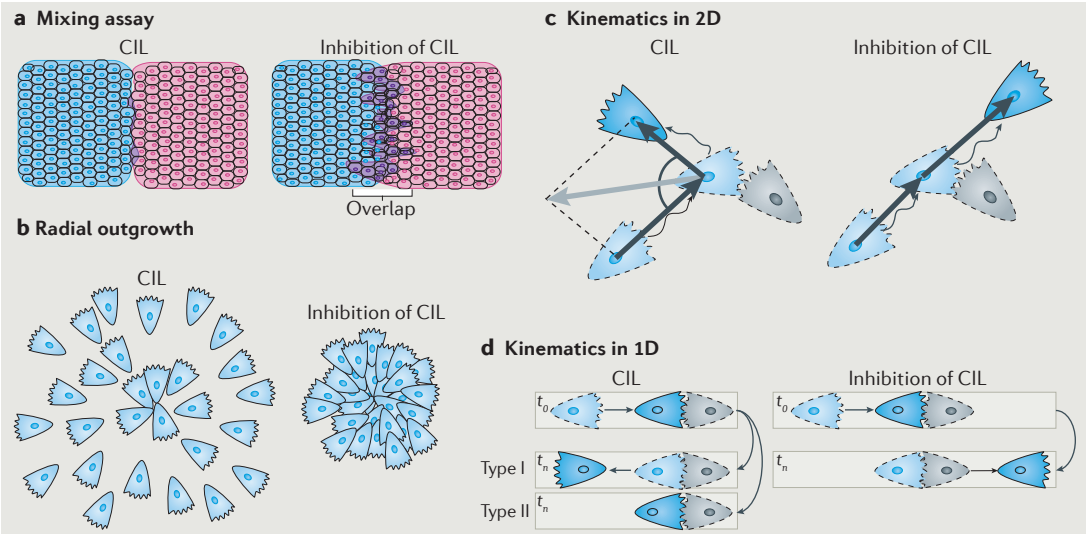

Figure 1-10 Methods to study contact inhibition of locomotion

Different methods to study CIL behaviour. (a) Mixing assay (also called invasion or explant confrontation assay. (b) Radial outgrowth assay (also called dispersion assay). (c) Kinematics in 2D. (d) Kinematics in 1D. t_0 indicates time before collision. t_n indicates time after collision. Adapted from Mayor and Streamer, 2016.

1.3.3 Molecular mechanism of contact inhibition of locomotion

CIL is a diverse process involving four steps (see section 1.3.1 and Figure 1-8); here I will discuss the molecular mechanisms and key components of the CIL response known so far.

(1) Cell-cell contact

The formation of a direct, physical contact between two cells is a requirement for CIL (Roycroft and Mayor, 2016). Moreover it has been shown that an adhesive contact between two colliding cells is needed to build up membrane tension across the area of contact (Abercrombie and Ambrose, 1958; Harris, 1973; Heaysman and Pegrum, 1973). So far cadherin, Ephrin and the Robo-Slit cell-cell adhesion complexes have been shown to be involved in CIL (Stramer and Mayor, 2016). Although these molecular players are known to be required for CIL, they are not of the same adhesion family, thus suggesting that CIL might work trough different mechanisms (Roycroft and Mayor, 2016).

Cadherins comprise a family of transmembrane glycoproteins, which build up calcium-dependent cell-cell adhesion. Classically cadherins were associated with regulation of the actin cytoskeleton in adherents junction of epithelial monolayers (Takeichi, 1988). However more recent publications have suggested that the cell-cell contact during CIL involves transient cadherin-dependent adhesion. It is not known why these adheres junctions are transient, compared to their epithelial counterpart. However, so far E-cadherin, N-cadherin and cadherin 11 have been shown to be involved in the CIL in different cell types during the cell-cell contact process (Becker et al., 2013; Bracke et al., 1997; Chen and Obrink, 1991; Huttenlocher et al., 1998; Omelchenko et al., 2001; Scarpa and Mayor, 2016; Theveneau et al., 2010). Moreover proteins involved in the cadherin-adherent junction complex, as β-catenin, α-catenin, p120 and vinculin, have been found to be important for CIL process (Bracke et al., 1997; Gloushankova et al., 1998; Scarpa et al., 2015). A recent publication in *Xenopus* neural crest cells found that a switch from E-cadherin to N-cadherin is required for the acquisition of CIL during EMT (Scarpa et al., 2015). They found that cells overexpressing E-cadherin remain in

contact and have impaired CIL (Scarpa and Mayor, 2016). A role of E-cadherin which has been described earlier in cell lines, where E-cadherin was been found to immobilizes protrusive activity at the point of cell-cell contact in cell lines (Chen and Obrink, 1991). However N-cadherin has been shown to be required for neural crest cell CIL, inhibition of N-cadherin using either Morpholino or blocking antibody, leading to an impairment of CIL behaviour in neural crest cells, as well as inhibition of neural crest cell migration *in vivo* (Theveneau et al., 2010).

In general, Xenopus neural crest cells in a 2D Kinematic assay show normal CIL behaviour, thus colliding cells collapse their protrusion, stop migrating and then repolarize and migrate away from each other (Carmona-Fontaine et al., 2008b). Once N-cadherin dependent actions are inhibited neural crest cells have an increased protrusive activity at the contact and fail to repolarize away from the contact. This suggested that N-cadherin might control a mechanism termed "contact-dependent polarity" (Theveneau et al., 2010). Apart from neural crest cells, N-cadherin requirement during CIL has been implicated in different cell types as myoblasts and glial cells (Huttenlocher et al., 1998; Tanaka et al., 2012; Theveneau et al., 2010). However, the role of N-cadherin in CIL seems not to be general, as depletion in Schwann cells has been suggested to enhance CIL (Letourneau et al., 1991). Furthermore Cadherin 11 is also essential for CIL in *Xenopus* neural crest cells. Inhibition of cadherin-11 leads to impairment of CIL behaviour and neural crest cell migration *in vivo* (Becker et al., 2013).

Furthermore the Eph tyrosine kinase receptors and their transmembrane ephrin ligands have been linked to the initial cell contact during CIL. The EphA and EphB receptors both have been shown to be required for CIL behaviour in Cajal-Retzius cells and prostate cancer cells. While both have shown to be important for CIL-dependent dispersion of Cajal-Retzius neurons in the mammalian cerebral cortex (Villar-Cerviño et al., 2013). EphA has been shown to be important for homotypic CIL amongst prostate cancer cells (Astin et al., 2010; Batson et al., 2014). Whereas EhpB controls invasiveness of prostate cancer cells by inhibition of heterotypic CIL by suppression of CIL between prostate cancer cells and fibroblasts (Astin et al.,

2010). Moreover EhpB signalling has been implicated in CIL in breast cancer cell lines, where it was able to dominate given EGF chemotactic cues (Lin et al., 2015).

Next to Ephrin signalling the repulsive Slit-Robo ligand-receptor pair has been linked to CIL cell behaviour (Fritz et al., 2015). The ligand slit is normally secreted, but a membrane bound version of Slit2, together with the ROBO4 receptor, was recently found to be employed during fibroblast CIL (Fritz et al., 2015). Interestingly for both, the SLIT-ROBO and Eph-ephrin receptor ligand system have been shown to interact and crosstalk with cadherins (Rhee et al., 2002; Solanas et al., 2011)

Moreover the zyxin cell-cell adhesion molecule has been reported to be required for haemocyte CIL in *Drosophila* development (Davis et al., 2012; Davis et al., 2015), although the molecular details of the zyxin cell-cell adhesion have not been investigated yet.

(2) Protrusion inhibition at the contact site

Following cell-cell contact, protrusion formation is inhibited at the contact side. This protrusive inhibition during CIL is initiated by the family small GTPases which drive cytoskeletal reorganizations (Roycroft and Mayor, 2016; Stramer and Mayor, 2016). Rac1, RhoA and Cdc42 are the best-studied members of the GTPase family. Rac1 and Cdc42 are necessary for actin polymerization in the lamellipodia whereas RhoA is required for actomyosin regulation and thus contraction at the back of the cell (Ridley, 2015) (for more detailed description 1.1.3 Polarization of migrating cells: Rho GTPases).

All three members have been implicated in the CIL response (Astin et al., 2010; Carmona-Fontaine et al., 2008b; Fritz et al., 2015; Moore et al., 2013; Scarpa et al., 2015; Théveneau et al., 2007). In *Xenopus* neural crest cells protrusive activity is repressed by inhibition of RAC1 in a N-cadherin and WNT/PCP signalling dependent way (Carmona-Fontaine et al., 2008a; Moore et al., 2013; Theveneau et al., 2010). Inhibition of N-cadherin, by either Morpholino or blocking antibody, leads to ubiquitous Rac1 activity, a loss of protrusion inhibition at the contact in *Xenopus*

neural crest cells (Theveneau et al., 2010). Additionally, ectopic overexpression of E-cadherin in neural crest cells leads to an increase of Rac1 activity at the contact site, resulting in an overlap of protrusions and impairment of CIL (Scarpa et al., 2015). However the exact molecular mechanism of N-cadherin dependent activation of RhoA and Rac1 is not known, though some interactions have been reported. For example, p120-catenin binds to the intracellular domain of N-cadherin and regulates its turnover (Davis et al., 2003). Unbound cytosolic p120-catenin can increase Rac1-mediated protrusion formation, however if it is bound to N-cadherin, protrusion formation is inhibited (Grosheva et al., 2001; Noren et al., 2000). Hence during CIL N-cadherin could be sequestering p120-catenin and thus inhibiting activation of Rac1 (Roycroft and Mayor, 2016). Moreover, in neural crest cells overexpressing E-cadherin, Rac1 activity is increased at the contact in a p120-catinin dependent manner (Scarpa et al., 2015).

Furthermore the WNT/PCP pathway plays a major role in Rac1 inhibition and activation of RhoA at the site of contact in neural crest cell CIL (Carmona-Fontaine et al., 2008a; Scarpa et al., 2015; Theveneau et al., 2010). After collision Wnt/PCP downstream effectors including Dishevelled, Prickle1 and Strabismus are localized with the receptor Frizzled7 at the site of contact, whereby they inhibit protrusion formation (Matthews et al., 2008; Mayor and Theveneau, 2014). In detail, the triggering of the Wnt/PCP signal leads to the activation of RhoA and its kinase ROCK (Rho-associated protein kinase) which leads to contraction of protrusions in neural crest cell (Carmona-Fontaine et al., 2008a; Matthews et al., 2008). Furthermore Wnt/PCP activity leads to inhibition of Rac1 at the point of contact, followed by a protrusion collapse (Matthews et al., 2008; Scarpa et al., 2015; Theveneau et al., 2010). The inhibition of Rac1 could be due to the antagonistic behaviour between RhoA and Rac1, where the activation of one results in the inhibition of the other (Shoval and Kalcheim, 2012). Nevertheless, the exact molecular mechanism of the Rac1 inhibition and RhoA activation remains to be solved. However the partition defective 3 homologue (PAR3) polarity molecule has been shown to be localized to the point of cell-cell contact during CIL, where it inhibits the Rac1 activator, Trio (Moore et al., 2013). Additionally, it has been reported that Trio is recruited upon

cadherin-11 activation at the cell contact and this inhibition could provide a method for RhoA activation and Rac1 inhibition upon cell-cell contact (Becker et al., 2013; Kashef et al., 2009).

But not only neural crest cells require RhoA/ROCK activation at the contact site for CIL response, depletion of either RhoA or ROCK in chick heart fibroblasts leads to inhibition of protrusive activity upon collision and thus CIL (Kadir et al., 2011). Correspondingly, CIL in pancreatic cancer cells is coordinated by EphA-mediated ROCK and RhoA activation at the contact site (Astin et al., 2010). In addition the impairment of Rac1 by use of either a dominant active or dominant negative form in fibroblasts leads to the loss of CIL behaviour (Anear and Parish, 2012). Besides, it has recently been reported that Rac1 activity in colliding fibroblasts is controlled by the GAP srGAP2 (SLIT-ROBO Rho GTPase-activating protein 2) in the overlapping protrusions (Fritz et al., 2015). They report that slit-robo signalling is stimulated in the overlapping protrusions at the site of contact causing the activation of srGAP2 and thus inhibition of Rac1 activity (Fritz et al., 2015). Likewise CIL between glial cells is regulated by the suppression of Rac1, mediated by the inactivation of the guanine nucleotide exchange factor TIAM1 (T-lymphoma invasion and metastasis-inducing protein 1) (Tanaka et al., 2012).

(3) Repolarization and protrusion formation

The next key step during CIL is the repolarization away from the site of contact, involving a switch of the front-rear polarity. Not only has RhoA to be activated and Rac1 to inhibited at the contact, a new leading edge opposing the contact needs to be formed, depending on changes in adhesions, small Rho GTPases activities and cytoskeletal changes (Roycroft and Mayor, 2016). In order to form a new leading edge, increase in Rac1 activity away from the contact is required for the formation of new protrusions in neural crest cells (Scarpa et al., 2015; Theveneau et al., 2010). FRET analysis of Rac1 activity in *Xenopus* neural crest cells showed that Rac1 is activated in the leading front of the cell, but upon cell-cell contact Rac1 gets inhibited at the contact and becomes activated away from the contact site (Scarpa et al., 2015). Moreover localized photoactivation of Rac1 at the free edge leads to

extension of a protrusion formation and increased separation of cell-cell duplets (Scarpa et al., 2015). In contrast, the photoactivation of a dominant negative form inhibits protrusion formation and impairs separation of a cell-cell duplet in *Xenopus* neural crest cells (Scarpa et al., 2015). Neural crest cell duplets overexpressing E-cadherin do not separate after colliding due to an increased Rac1 activity at the cell-cell contact. However activation of photoactivatable Rac1 away from the contact was able to trigger separation, thus illustrating the importance of Rac1 activity in the leading edge for repolarization (Roycroft and Mayor, 2016; Scarpa et al., 2015).

Not only changes in Rac1 polarity, but also microtubule remodeling has been shown to be required for switch of cell repolarization during CIL (Kadir et al., 2011; Moore et al., 2013; Nagasaki et al., 1992). In general, in a migrating cell, microtubules strengthen polarity and are stabilized in the front of the cell (Bershadsky et al., 1991; Glasgow and Daniele, 1994). After cell collision of neural crest cells microtubules at the site of contact show an increase in microtubule catastrophe at the contact site during CIL (Moore et al., 2013). This increase of dynamic microtubule after collision has been shown to be essential for CIL (Batson et al., 2013; Kadir et al., 2011; Moore et al., 2013; Stramer et al., 2010). As mentioned before in *Xenopus* neural crest cells, this dynamic action of microtubules requires the cell polarity protein, Par3 (Moore et al., 2013). Par3 concentrates to the cell–cell contact upon collision where it stimulates microtubule catastrophe (Moore et al., 2013). The microtubule catastrophe in neural crest cells is trigged through the inhibition of the GEF Trio and following inhibition of Rac1 (Moore et al., 2013). Also in *Drosophila* haemocytes microtubule catastrophe is required for a normal CIL response (Stramer et al., 2010). Additionally it has been shown that microtubule bundles of two colliding haemocytes align before they collapse (Stramer et al., 2010).

(4) Cell separation and migration away from the collision

The next step of CIL, after repolarization, is the separation of the cells and the migration away from the colliding cell. So far the sequence of events during repolarization, protrusion formation and separation during CIL has not resolved yet

(Stramer and Mayor, 2016). In *Drosophila* haemocytes and chick fibroblasts the protrusion collapse at the cell-cell contact, precedes the repolarization and new protrusion formation away from the contact (Abercrombie, 1978; Abercrombie and Ambrose, 1958; Davis et al., 2015). Though, in *Xenopus* neural crest cells, the new protrusion formation, and thus repolarization precedes the loss of cell-cell contact. Moreover the repolarization and protrusion formation have been implicated to generate the tension needed for cell separation in neural crest cells (Scarpa et al., 2015). Since Abercrombie 1958 it has been thought that tension build-up across the contacting lamellae could be essential for the cell separation (Abercrombie and Ambrose, 1958; Davis et al., 2015; Harris, 1973; Heaysman and Pegrum, 1973). Nevertheless, it remains unsolved how this tension is established and if it is sufficient for cell separation. Furthermore how cell separation is started remains controversial. Its been suggested that it could be triggered by the endocytosis or disassembly of adhesion complexes between the cells (Roycroft and Mayor, 2016; Scarpa et al., 2015). However it is also possible that high tension build up by activation of RhoA/ROCK and microtubule disassembly at the contact leads to the cell separation (Astin et al., 2010; Carmona-Fontaine et al., 2008a; Kadir et al., 2011; Matthews et al., 2008; Moore et al., 2013; Roycroft and Mayor, 2016; Stramer et al., 2010). In neural crest cells the cell-cell adhesion is not perturbed if cell protrusion formation is inhibited away from the contact (Scarpa et al., 2015). Thus suggesting that neural crest cells first need to separate before the cell-cell adhesion is disassembled. Moreover, as mentioned before Scarpa et al. (2015) showed that forced protrusion formation by photoactivatable Rac1 in E-cadherin overexpressing cells is sufficient to separate cell neural crest cell duplets. This suggests that neural crest cell separation is mainly regulated by the repolarization and subsequent tension build up across the membrane, then disassembly of cell-cell adhesion complexes.

After repolarization and separation the final step in CIL program is the migration away from the contact site. To allow this migration a reorganization of cell-substrate traction stresses, via the modification of focal adhesions (Stramer and Mayor, 2016). For example, in *Drosophila* CIL-driven macrophage dispersion,

integrin, responsible to link the focal adhesion to the migration substrate, has been shown to be required for normal development (Comber et al., 2013). In *Xenopus* neural crest cells focal adhesion reorganization during CIL has been observed. Cells undergoing CIL reduce their focal adhesions at the cell-cell contact (Scarpa et al., 2015; Theveneau et al., 2013), which could lead to a change in cell-matrix traction stresses away from the contact, and finally cause movement away from the colliding partner. However, Abercrombie did not see any changes in focal adhesion before cell separation during chick embryonic fibroblast CIL (Abercrombie and Dunn, 1975). This might imply that focal adhesion changes during CIL could be cell-type dependent (Stramer and Mayor, 2016).

1.3.4 Contact inhibition in embryonic development

CIL has been implicated more recently in embryonic processes. It has emerged that it is not only a cell-cell interaction *in vitro*, but can instruct development within cell populations *in vivo* (Stramer and Mayor, 2016). Recent developments of *in vivo* imaging have brought CIL into the attention of embryonic development. Processes such as cellular dispersion, cellular tilling and collective migration have been connected to CIL (Roycroft and Mayor, 2016; Stramer and Mayor, 2016) and will be discussed in detail in this section with specific emphasis on neural crest cell development (see also Figure 1-11).

Contact inhibition of locomotion and cellular dispersion

Abercrombie (1962) first described the ability of CIL to disperse a cell cluster as

> "Negative taxis… to promote movement into space where contact inhibition does not operate"

Dispersion of cells via CIL has been widely described in cell culture (see also section 1.3.2 radial outgrowth; Stramer and Mayor, 2016). More recently, *in vivo* and *in vitro* studies of Cajal-Retzius cells described their CIL response to be necessary for their spreading throughout mammalian cerebral cortex (Figure 1-11 a; Villar-Cerviño et al., 2013). Cajal-Retzius are induced in distinct regions of the brain and

spread throughout the cerebral cortex and control the development of cortical layers by regulating migration of other neuronal cells. Thus inhibition of CIL in Cajal-Retzius cells leads to cell clustering and thus severe impairment of cerebral cortex development. The Cajal-Retzius CIL-dependent dispersion was found to be regulated by Eph/ephrin signalling (Villar-Cerviño et al., 2013).

Contact inhibition of locomotion and cellular tiling

Cellular tilling describes the cell dispersion during embryogenesis where cells end up in a highly organized pattern. This process can be regulated by CIL, as shown for the homogenous *Drosophila* macrophage dispersion (Figure 1-11 b; Davis et al., 2012; Davis et al., 2015). Analysis with live imaging and computational modelling in the *Drosophila* embryo revealed that macrophage evenly spaced dispersion is regulated by CIL. The distinction between the above mentioned CIL driven dispersion of Cajal-Retzius and tilling of macrophages, could be related to the more precise coordinated CIL in the latter (Davis et al., 2015; Stramer and Mayor, 2016; Villar-Cerviño et al., 2013). Davis et al. 2015 showed that precise repulsion and patterning involves the coordination of intracellular forces during the CIL response *in vivo*. This CIL tilling is orchestrated by the cell-cell adhesions and subsequent action-myosin networks drive the uniform dispersion of the CIL response (Davis et al., 2015).

Contact inhibition of locomotion and collective cell migration

Contact inhibition as discussed before (1.1.3 Contact inhibition of locomotion and collective migration) has been shown to be necessary for collective migration of neural crest cells (Figure 1-11 c; Carmona-Fontaine et al., 2008b; Moore et al., 2013; Theveneau et al., 2010). Not only has CIL behaviour of neural crest cells been described *in vitro.* Live-imaging *in vivo* experiments have revealed that *Xenopus* and zebrafish neural crest cells undergo a CIL response during their migration comparable to those observed in culture (Carmona-Fontaine et al., 2008b; Theveneau et al., 2010). Different experiments showed that impairment of CIL leads to inhibition of *Xenopus* neural crest cell collective movement *in vivo* (Moore et al., 2013; Scarpa et al., 2015; Theveneau et al., 2010).

A number of molecules have been found to be regulating this process, including Wnt/PCP pathway and N-cadherin (Carmona-Fontaine et al., 2008b; Theveneau et al., 2010). For example N-cadherin based adherents junctions between cells are crucial for CIL in *Xenopus* cranial neural crest cells (Theveneau et al., 2010). If N-cadherin is inhibited, using a Morpholino or blocking antibody, protrusions are no longer repressed at the cell-cell contact and CIL is impaired *in vitro* and *in vivo* (Theveneau et al., 2010). The presence of E-cadherin however suppresses CIL (Scarpa et al., 2015). The switch between the CIL-suppressive cadherin (E-cadherin) and the CIL-supportive cadherin (N-cadherin), has been recently described has a requirement for EMT program. The restrain of protrusions via CIL together with the chemokine cue SDF-1, from the placodes, is thought to give the neural crest cell population polarity and admits collective migration (Theveneau et al., 2010). Thus the authors termed CIL response in a neural crest cell streams also "*contact-dependent-polarity*" (Theveneau et al., 2010).

CIL does not only occur homotypically between neural crest cells, heterotypic CIL response between neural crest cells and the underlying placodes have also been described essential for collective migration (Figure 1-11; Theveneau et al., 2013). Placodes are the source of the chemokine SDF-1 and attract neural crest cells. Though the placodal cells respond with a CIL reaction to neural crest cells, triggering a mechanism termed "*chase-and-run*". Whereby neural crest cells are attracted to the placodal cells, which in turn migrate away (Theveneau et al., 2013). The interplay of CIL and chemotaxis might be a common thing, as a similar behaviour has also been reported in breast melanoma *in vitro* (Lin et al., 2015).

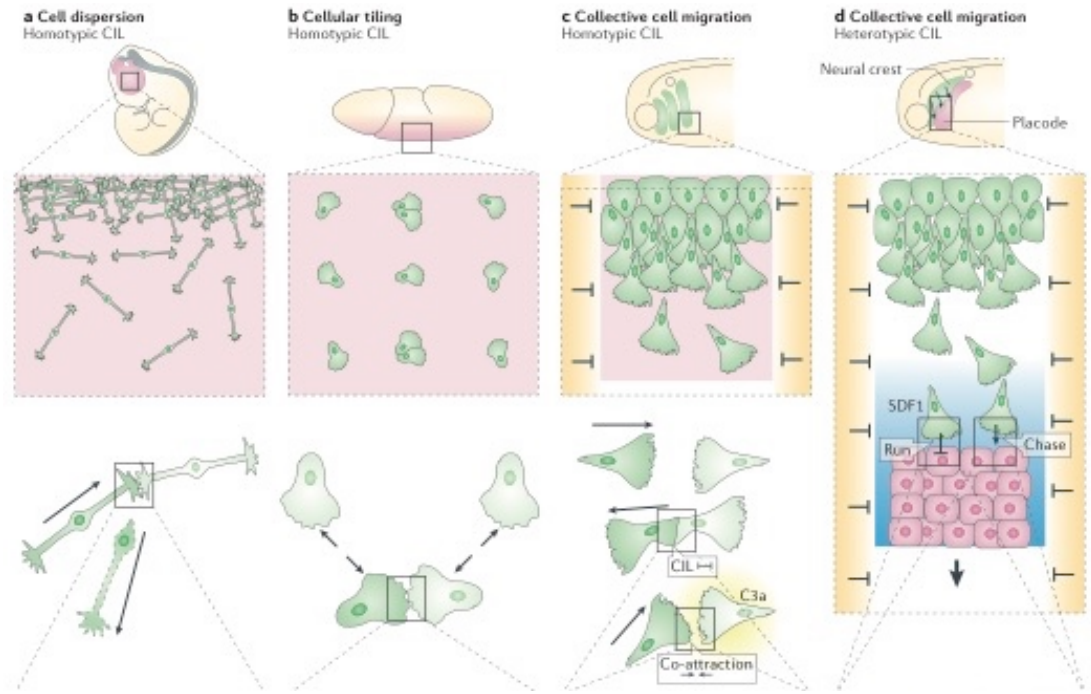

Figure 1-11 Contact inhibition *in vivo*

(a) CIL regulated cell dispersion of Cajal-Retzius cells during mammalian cerebral cortex development, similar to radial outgrowth from an explant. (b) Cellular tilling of *Drosophila* macrophages is controlled by precise CIL responses. (c) Collective migration of neural crest cells is regulated by homotypic CIL interactions, together with Co-attraction. (D) The movement of neural crest cells is also regulated by heterotypic CIL between neural crest cells and placodal cells, in a mechanism where the neural crest cells "chase" towards the placodes (triggered by SDF-1 chemotaxis), leading the placodes to "run" (triggered by CIL) away. Adapted from Stramer and Mayor, 2016.

1.4 Hypothesis

1.4.1 Hypothesis background

The receptor tyrosine kinase pathway Platelet-derived growth factor (PDGF) has been implicated in EMT during cancer invasion (Eckert et al., 2011; Jechlinger et al., 2006a; Thiery and Sleeman, 2006) and it is essential for the correct development of several neural crest cell derivatives (Morrison-Graham et al., 1992; Soriano, 1997;

Tallquist et al., 2003). Perturbations of PDGFRα signalling in mouse and zebrafish lead to severe defects in cranial neural crest cell derived tissues, suggesting developmental role of PDGFRα signalling in neural crest cell development towards its craniofacial targets (Eberhart et al., 2008; He and Soriano, 2013; Morrison-Graham et al., 1992; Soriano, 1997; Tallquist et al., 2003). However, the specific mechanism by which PDGF controls the formation of neural crest cell derivatives has not been completely elucidated, as evidence suggest it is involved in cell migration and proliferation (Eberhart et al., 2008; He and Soriano, 2013; Smith and Tallquist, 2010).

1.4.2 Hypothesis

Thus, I am proposing the following hypothesis:

> ***"PDGF-A/PDGFRα signalling controls collective migration of neural crest cell migration in Xenopus laevis"***

In order to test this hypothesis the following questions will be addressed:

1. Are the ligand PDGF-A and its receptor PDGFRα **expressed** in neural crest cells during *Xenopus laevis* development?

2. Is PDGF-A/PDGFRα signalling required for neural crest cell **migration** *in vivo* and *in vitro*?

3. What are the **cellular activities** controlled by PDGF-A/PDGFRα signalling during neural crest cell migration?

4. Which are the **downstream targets** of PDGF-A/PDGFRα signalling that are required for neural crest cell migration?

5. What are the **signalling pathways** downstream of the PDGF-A/PDGFRα signalling response during neural crest cell migration?

Chapter 2 Experimental Procedures

2.1 Embryological and Histological Procedures

2.1.1 In vitro fertilization and embryo collection of Xenopus laevis embryos

Xenopus laevis were obtained from Portsmouth Animal Facility, UK and Nasco, USA. Ovulation was induced with 100 units of gonadotropic hormone (pregnant mare serum gonadotropin hormone PMSG; Intervet) 2-5 days before the experiment and with 500 units of human chorionic gonadotropin hormone (Chorulon; Intervet) 16 hours before the experiment. During egg laying females were held in modified ringer solution (MMR: 100 mM NaCl, 2 mM KCl, 1 mM $MgS0_4$, 2 mM CaC_2, 5 mM Hepes, 0.1 mM EDTA, pH 7.6) at 17-18 °C, conserving the mature oocytes inactivated until fertilisation. Male *Xenopus laevis* were culled by anaesthetizing in 0.5 % Tricaine solution for minimum of 40 minutes, followed by decapitation and pithing. Testes were dissected and kept in Leibovitz L-15 medium (Invitrogen, 11415-064) with added streptomycin (5 µg mL^{-1}, Sigma, 85886) at 4 °C for up to 4 days. The Oocytes were collected in a petri dish excessive MMR was removed and fertilised with homogenized testes tissue. After an incubation period of 15-30 minutes, NAM1/10 (normal amphibian medium 1/10: 11 mM NaCa, 0.2 mM KCl, 0.1 mM $Ca(NO_3)_2$, 0.1 mM $MgS0_4$, 10 µM EDTA, 0.2 mM NaH_2PO_4, 0.1 mM $NaHCO_3$, pH 7.5, 50 µg mL^{-1} streptomycin) was applied to the fertilisation. After approximately 2 hours cortical rotation and the first division of the embryo was observed. Subsequently the embryos were dejellied by incubation in 2 % L-cysteine (Sigma) solution for 5-10 minutes. Embryos were kept at 14.5 °C in NAM1/10 and staged according to Nieuwkoop and Faber (1967) normal table of *Xenopus* development table.

2.1.2 Microinjection of Xenopus laevis embryos

Xenopus laevis embryos were injected using a Narishige IM300 microinjector under a LeicaMZ6 or a Nikon SMZ645 dissecting microscope. Needles were made from borosilicate glass capillaries (Intracel, 01-001- 06) with 0.58 mm inner diameter by pulling the capillaries on a Narishige PC-10 puller set to 2 step mode; with the first step regulated to 86 % capacity and second step regulated to 99 % capacity.

Subsequently needles were calibrated using an eyepiece graticule to inject a volume of 5 nL or 10 nL per injection. The needles were filled with the solution to be injected, such as mRNA, DNA or antisense Morpholinos (see Table 2-1 List of injected mRNA and Morpholinos) and embryos were injected at either 4-cell or 8-cell stage in a 3 % polysucrose (Sigma) solution in NAM 3/8 (40.7 mM NaCa, 0.74 mM KCl, 0.37 mM $Ca(NO_3)_2$, 0.37 mM $MgSO_4$, 37 µM EDTA, 0.37 mM NaH_2PO_4, 0.1 mM $NaHPO_4$, pH 7.5, 50 µg mL^{-1} streptomycin) at 17 °C. Fluorescein-dextran (FDX; Invitrogen, D1821, 20 ng/10 nL injection) or Rhodamine-dextran (RDX; Invitrogen, D1824, 20 ng/10 nL injection) were used as tracers if needed. For injection of Morpholinos and mRNAs the neural crest cells were targeted by injection at the 8-cell stage, into the dorsal animal blastomere and the ventral animal blastomere (Figure 2-1). Following injection the embryos were left in Ficoll solution for 1 hour to overnight at 14.5 °C, before being transferred to NAM 1/10. Embryos were generally developed at 14.5 °C although temperature could be varied from 14 °C – 18 °C to alter the timing of development and experiments.

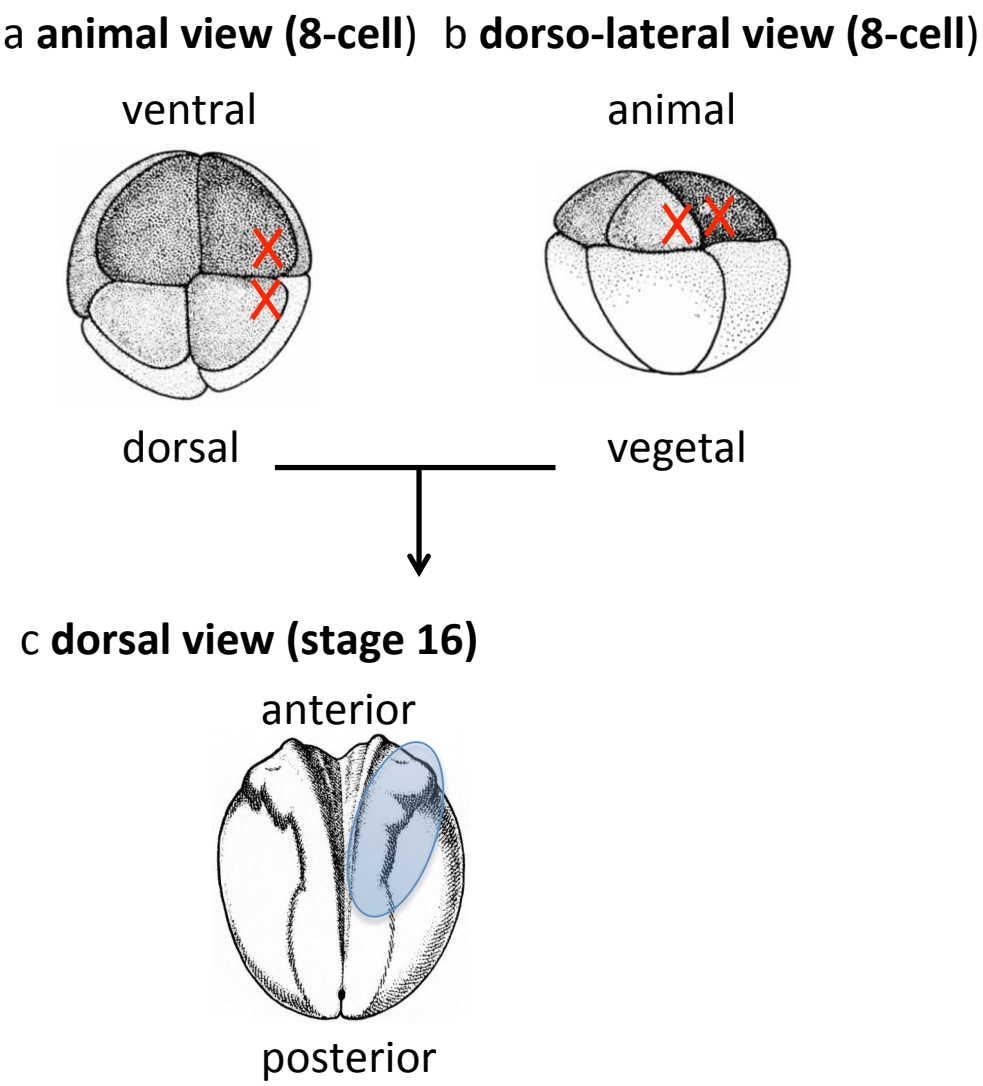

Figure 2-1 mRNA and Morpholino neural crest targeting injection scheme

(A) 8-cell stage *Xenopus laevis* embryo animal view. (B) 8-cell *Xenopus laevis* embryo dorso-lateral view. (A, B) For injection of Morpholinos and mRNAs the neural crest cells were targeted by injection at the 8-cell stage into the dorsal animal blastomere and the ventral animal blastomere (red crosses). (C) *Xenopus laevis embryo stage 16* Neural crest cell target region at stage 18 depicted in blue (images from Nieuwkoop et al., 1994)

Table 2-1 List of injected mRNA and Morpholinos

Construct	Name	Plasmid	Amount (total/ 10 nL injection concentration)
membrane RFP	mRFP mRNA	pCS2+ (Theveneau et al., 2010)	300 pg/ 30 ng μL^{-1}
membrane GFP	mGFP mRNA	pCS2+ (Theveneau et al., 2010)	300 pg/ 30 ng μL^{-1}
nuclear H2B RFP	nRFP mRNA	pCS2+ (Theveneau et al., 2010)	300 pg/ 30ng μL^{-1}
life actin mCherry	liveActin	pCS2+ (Scarpa et al., 2015)	300 pg/ 30 ng μL^{-1}
Xenopus laevis PDGFRαw37	dom. neg. PDGFRα mRNA	pALTER-1 (Ataliotis et al., 1995)	300 pg/ 30 ng μL^{-1}
zebrafish ph-AKT-GFP	ph-AKT-GFP mRNA	pCS2+ (Montero et al., 2003)	500 pg/ 50 ng μL^{-1}
zebrafish PI3K-p110-CAAX	PI3K-CAAX mRNA	pCS2+ (Montero et al., 2003)	300 pg/ 30 ng μL^{-1}
mouse PDGF-A	mouse PDGF-A mRNA	pGEM-1 (Fruttiger et al., 1999)	200 pg/ 20 ng μL^{-1}
mouse PDGFRα	mouse PDGFRα mRNA	pGEM-1 (IMAGE ID 5704645)	300 pg/ 30 ng μL^{-1}
Chick N-cadherin-GFP	N-cadherin mRNA	pCS2+ (Scarpa et al., 2015)	500 pg/ 50 ng μL^{-1}
PDGFRα Morpholino	PDGFRa MO mRNA	-	16 ng/ 16 µg μL^{-1}
PDGF-A Morpholino	PDGF-A MO mRNA	-	16 ng/ 16 µg μL^{-1}

2.1.3 Microdissection and neural crest cells culture

Microdissection was performed as previously described (Theveneau et al., 2010) Briefly, neural crest cells were microdissected with help of an eyebrow knife at stage 17 from *Xenopus laevis* embryos in 3/8 NAM (40.7 mM NaCa, 0.74 mM KCl, 0.37 mM $Ca(NO_3)_2$, 0.37 mM $MgSO_4$, 37 µM EDTA, 0.37 mM NaH_2PO_4, 0.1 mM $NaHPO_4$, pH 7.5, 50 µg mL^{-1} streptomycin) at 17 °C. Before the start of dissection the vitelline membrane was removed with the help of forceps and the embryo was placed at 14.5 °C for at least 15 minutes to heal. To fix the embryos during dissection, embryos were embedded into plasticine and the ectoderm, superficial to the neural crest, cells was removed. Subsequently the neural crest cells were dissected and transferred to a plastic dish containing Danilchick's Medium (DFA, 53 mM NaCl, 5 mM Na_2CO_3, 4.5 mM K-Gluconate, 32 mM Na-Gluconate, 1 mM $MgSO_4$, 1 mM $CaCl_2$, 0.1 % BSA, pH 8.3 , 50 µg mL^{-1} streptomycin). Neural crest explants were further dissected into small clusters and plated on a fibronectin-coated dish. Dishes were coated using 10 µg mL^{-1} or 50 µg mL^{-1} fibronectin (Sigma) for plastic or glass dishes, respectively. For single cell experiments the explants were fully dissociated in calcium and magnesium free DFA for 3-5 minutes before culturing on fibronectin-coated dishes in normal DFA. Cells and explants were incubated for at least 20-30 minutes before imaging. Plastic dishes (single well: Falcon 50 x 9 mm; 4-well: ThermoFischer multidish) and glass bottomed dishes (Greiner bio-one 35 mm 4 compartments or FluoroDish 35 mm) and coverslips (Academy Dia. 13, 0.13-0.16 mm thick) were incubated with fibronectin for 1 hour at 37 °C prior to plating. After coating with fibronectin, the dishes were washed with 1x PBS and subsequently blocked with 0.1 % bovine serum albumin (BSA) in 1x PBS for 15-30 minutes at 37 °C. Afterwards the dishes were washed again with 1x PBS before DFA was added and the dishes were cooled to 17 °C.

2.1.4 Whole mount *in situ* hybridisation

In situ hybridisation was performed as described previously reported (Fawcett and Klymkowsky, 2004; Harland, 1991). If not stated otherwise steps were performed at room temperature. In short, embryos were fixed at the required stage in MEMFA

(100 mM MOPS, 1 mM $MgSO_4$, 2 mM EGTA, 3.7 % formaldehyde) for 1 hour at room temperature or over night at 4 °C. After fixation embryos were dehydrated in 100 % methanol with 3 washes for 5 min and subsequently stored at -20 °C for up to 2 month. To start the *in situ* hybridisation the fixed embryos were rehydrated with successive washes of 5 minutes each, of 75 % methanol in 1x PBS, 50 % methanol in 1 x PBS, 25 % methanol in 1 x PBS. Followed by 3 washes in 1 x PBS. Subsequently embryos were bleached in bleaching buffer (20 % H_20_2, 2.5 % saline-sodium citrate buffer (20 x SSC: 3 M NaCl, 0.3 M tri-sodium citrate, pH 7.0), 5 % formamide) for approximately 20 minutes in the dark. Embryos were then washed 3 times in 1 x PBS and fixed again in 3.7 % formaldehyde in 1 x PBS for 30 minutes, followed by 3 washes in 1 x PBS. Embryos were then transferred into hybridisation buffer (50 % formamide, 5 x SSC, 1 x Denhardt's solution, 1 mg mL^{-1} ribonucleic acid, 100 µg mL^{-1} heparin, 0.1 % CHAPS, 10 mM EDTA, 0.1 % Tween-20, pH 5.5) and incubated at 65-68 °C for 30-60 minutes. Afterwards the hybridisation buffer was replaced hybridisation buffer containing digoxigenin-labelled probe at 65-68 °C and the embryos were incubated over night. After over night hybridisation, the embryos were washed in a series of washes at 65-68 °C for 10 minutes each: washing solution 1 (50 % formamide, 10 % 20 x SSC, 0.1 % Tween-20); washing solution 2 (25 % formamide, 10 % 20 x SSC, 0.1 % Tween-20); washing solution 3 (12.5 % formamide, 10 % 20 x SSC, 0.1 % Tween-20); washing solution 4 (2x SSC, 0.1 % Tween-20). Followed by a last wash in washing solution 5 (0.2 x SSC, 0.1 % Tween-20) for 30 minutes at 65-68 °C. All solutions and buffers used up to this point were made with autoclaved DEPC-treated water (0.1 % diethylpyrocarbonatein in ddH2O) to prevent RNase contamination and thus degradation of the probe. Embryos were then washed twice with 1x PBS and equilibrated for blocking with 3 washes in 1 x MAB (maleic acid buffer 100 mM maleic acid, 150 mM NaCl, 0.1 % Tween-20, pH 7.6). Followed by blocking in 2 % BMBR (Boehringer Mannheim Blocking Reagent; Roche, 11096176001) in 1 x MAB for 2 hours or at 4 °C over night. Embryos were incubated overnight at 4 °C with an anti-digoxigenin-alkaline phosphatase (AP) conjugated antibody (Roche, 11093274910) in a dilution of 1:3000 in 2 % BMBR in 1 x MAB. Subsequently embryos were washed 5 times in 1 x MAB buffer for 30 minutes each. Embryos were then equilibrated to AP buffer (100 mM NaCl, 50 mM

MgCl2, 100 mM Tris-HCL pH 9.8, 0.1 % Tween-20) with 3 washes each 15 minutes. Followed by developing the colorimetric reaction in the dark using 75 µg mL^{-1} 5-bromo-4-chloro-3-indoyl-phosphate (Roche, 11585002001) and 150 µg mL^{-1} 4-nitro blue tetrazolium chloride (Roche, 11383213001). The reaction was stopped by 3 washes in 1 x PBS and background staining was removed by 20 minutes incubation in 100 % methanol. Embryos were then fixed in 3.7 % formaldehyde in 1vx PBS and stored at room temperature until they were photographed. The ribonuclease probes used in this thesis were against *Xenopus laevis* Snail2 (Mayor et al., 1995), *Xenopus laevis* Twist (Hopwood et al., 1989), *Xenopus laevis* PDGFRα (Ataliotis et al., 1995) and *Xenopus laevis* PDGF-A (Nagel et al., 2004).

2.2 Molecular biology and biochemistry

2.2.1 Amplification of plasmid DNA clones

Plasmid DNA was amplified by transforming 50-100 ng of DNA into heat shock competent Escherichia Coli of the DH5α strain (Invitrogen). Briefly, DNA was added to the 30 µL bacteria cells suspension on ice and incubated for 30 minutes. Cells were heat shocked for 45 seconds at 42 °C and subsequently incubated on ice for 2 minutes. Then 500 µL of LB broth (20 g L^{-1} LB Broth, Sigma) was added and bacteria were incubated for 1 hour at 37 °C. Following 100 µL of the bacteria culture were spread on to a preheated LB agar plate with Ampicillin (37 g L^{-1} LB Agar, Sigma; 100 µg mL^{-1} Ampicillin) and incubated over night at 37 °C. Colonies were picked and amplified in 50-100 mL of LB broth supplemented with 50 µg mL^{-1} Ampicillin overnight in a shacking incubator at 37 °C. Following plasmid DNA was purified using a Plasmid Midiprep Kit (Qiagen). DNA was re-suspended in 100 µL of nuclease free H_20 (Ambion) and subsequently quantified using a Nanodrop Spectrophotometer NDL2000.

2.2.2 Synthesis of mRNA for microinjection

For sense mRNA synthesis, plasmid DNA was linearized by restriction digest at a 3' restriction site with an appropriate restriction endonuclease. A restriction digest

with a total volume of 100 µL, containing 10 µg plasmid DNA, 10 µL 10x buffer and 1 µL (10 Units) of enzyme in nuclease free H_20 (Ambion), was incubated for 2 hours at 37 °C. Digested plasmid was purified using Qiaquick PCR Purification kit (Qiagen) and concentration of purified digested plasmid was measured using a Nanodrop spectrophotometer NDL20001. 1 µg purified 3' linearized plasmid DNA was used to transcribe synthetic capped mRNA with the SP6 or T7 Ambion mMessage Machine kit according to manufacturers instructions (Invitrogen, AM1340 and AM1344 respectively). To degrade template DNA 1 µL of the reaction mixture was replaced with 1 µL of Turbo DNase (2 Units, Ambion) and the mixture was incubated for a further 30 minutes at 37 °C. The mRNA was purified using the RNeasy kit following manufactures instructions (Qiagen, 74104) and resuspended in 30 µL nuclease free H_2O (Ambion). RNA concentration was measured using the Nanodrop spectrophotometer NDL20001 and the efficiency of mRNA synthesis, DNase digestion and quality of mRNA transcript was evaluated by agarose gel electrophoresis. Therefore, 1 µL of linearized plasmid DNA, 1 µL of transcription mixture before addition of DNase, 1 µL of purified sense mRNA were run on 1 % agarose (Fisher Scientific, BP1356-100) gel in TAE (20 mM acetic acid, 1 mM EDTA, 40 mM Tris, pH 7.6). For mouse PDGF-A mRNA transcription mouse PDGF-A pGEM-1 (Fruttiger et al., 1999) was linearized with PvuII and transcribed with SP6 RNA polymerase. For transcription of mouse PDGFRα mRNA the mouse PDGFRα pYX-Asc plasmid (IMAGE consortium, 5704645) was linearized with PacI and mRNA was transcribed using RNA T7 polymerase. For N-cadherin mRNA transcription the chick N-cadherin-GFP pCS2+ plasmid was linearized with NotI and mRNA was transcribed using Sp6 RNA polymerase. For ph-AKT-GFP mRNA transcription ph-AKT-GFP pCS2+ plasmid (Montero et al., 2003) was linearized with NotI and was transcribed using Sp6 RNA polymerase. For dominant negative PDGFRα mRNA the PDGFRαw37 pGHE2 (Ataliotis et al., 1995) plasmid was linearized NheI and was transcribed using T7 RNA polymerase. For PI3K-CAAX mRNA transcription PI3K-p110-CAAX pCS2+ plasmid (Montero et al., 2003) was linearized with NotI and was transcribed using Sp6 RNA polymerase. All restriction enzymes and buffers were all obtained from Promega.

2.2.3 Synthesis of mRNA probe for in-situ hybridisation

For *in vitro* transcription of labelled antisense RNA, plasmid DNA was linearized at a 5' restriction site with the appropriate restriction enzyme. Plasmids were linearized and purified as described before (see section 2.2.2 Synthesis of mRNA for microinjection) Antisense RNA transcription mix (total Volume 20 µL) contained 1 µg of linearized DNA, 4 µL of 5 x buffer (Promega), 2 µL of 10 x DTT (Promega), 2 µL of DIG RNA Labelling Mix (Roche, 11277073910), 0.5 µL of ribonuclease inhibitors (Promega) and 1 µL of appropriate RNA polymerase (SP6, T3, T7; 10-20 Units, Promega). This transcription reaction mix was incubated at 37 °C for 2 hours. Following 1 µL of the reaction mix was replaced with 1 µL of DNase (1,000 Units; Promega) to degrade the plasmid DNA template for 30 minutes at 37 °C. The mRNA was purified using the RNeasy kit following manufactures instructions (Qiagen, 74104) and resuspended in 20 µL nuclease free H_2O (Ambion). The efficiency of mRNA synthesis, DNase digestion and quality of mRNA transcript was evaluated by agarose gel electrophoresis as described before (see section 2.2.2 Synthesis of mRNA for microinjection). Probes were diluted in hybridisation buffer to working concentrations see Table 2-2 List of antisense *in situ* hybridisation probes.

Table 2-2 List of antisense *in situ* hybridisation probes

Antisense Probe	Plasmid	Restriction Enzyme	Transcription polymerase	*Working concentration*
Twist	Twist-pCS2+ (Hopwood et al. 1989)	SmaI	T7	1000 ng mL^{-1}
Slug	Slug pSP72 (Mayor et al. 1995)	Kpn	T7	800 ng mL^{-1}
PDGF-A	PDGF-A pGHE2 (Nagel et al. 2004)	NotI	T7	1000 ng mL^{-1}
PDGFRα	PDGFRα pGHE2 (Ataliontis et al. 1995)	NotI	T7	1000 ng mL^{-1}

2.2.4 Immunostaining

Immunofluorescence staining of neural crest cell explant culture was performed as previously described (Theveneau et al., 2010). In short, neural crest cell explants plated on glass coverslips (Academy Dia. 13, 0.13-0.16 mm thick) and allowed to spread for at least 2 hours. Subsequently, the neural crest cell explants were fixed in 4 % paraformaldehyde (PFA; Sigma, P6148) in 1 x PBS for 30 minutes at room temperature, and then washed 3 x in 1 x PBS and permeabilised in 0.1 % Triton-X-100 in 1 x PBS for 10 minutes. After washing the explants thoroughly in PBS, they were blocked in blocking buffer (3 % fetal calf serum (FCS), 5 % BSA in 1 x PBS) for 30 minutes. The primary antibody (see Table 2-3 List of primary antibodies for immunostaining) was diluted in blocking buffer (3 % fetal calf serum (FCS), 5 % BSA in 1 x PBS) and incubated over night at 4 °C in a humidity chamber. The next day the explants were washed 3 x in 1 x PBS and the secondary antibody (see Table 2-4 List of secondary antibodies immunostaining) in blocking buffer was incubated for 1 hour at room temperature. 1 µg mL^{-1} DAPI (4',6- diamidino-2-phenylindole; Sigma, D9542) and 1 µg mL^{-1} phallodin tetramethylrhodamin-b-isothiocyanate (PhR;

P1951) were incubated together with the secondary antibody if appropriate. Following the incubation samples were 3 x washed in 1 x PBS and mounted in Mowiol (Sigma, 81381).

Table 2-3 List of primary antibodies for immunostaining

Antibody	Species	Working conc.	Producer
N-cadherin	rat	6 µg mL^{-1}	DSHB, MNCD-2
E-cadherin	mouse	1.2 µg mL^{-1}	DSHB, 5D3
PDGFRα	rabbit	1:500	Cell signalling, 9271

Table 2-4 List of secondary antibodies immunostaining

Antibody	Species	Working conc.	Producer
Anti-Mouse IgG Alexa Flour 488	goat	1:500	Life Technologies, A-11017
Anti-Rat IgG Alexa Flour 488	donkey	1:500	Life Technologies, A-21208
Anti-Rabbit IgG Alexa Fluor 488	goat	1:500	Life Technologies, A-11034
Anti-Rabbit IgG Alexa Fluor 647	donkey	1:500	Life Technologies, A-31573

2.2.5 Morpholinos

Morpholinos were obtained from GeneTools. Morpholinos against PDGF-A (PDGF-A MO; 8ng, 5'-AGAATCCAAGCCCAGATCCTCATTG-3'; Nagel et al., 2004) and new designed Morpholino against PDGFRα (16ng, 5'-TGCCCTCATGGCAGGCATCATGGAC-3'). Mouse mRNA mismatches for rescue experiments are underlined. Equimolar concentrations of standard control Morpholino (Control MO; 3'-ATATTTAACATTGACTCCATTCTCC - 5') was used.

2.2.6 Inhibitors

Pharmacological inhibitors were all solubilized in DMSO (Sigma) see Table 2-5 List of pharmaceutical inhibitors for an overview. For all experiments DMSO controls, comparable to the amount of DMSO added with the inhibitor, were used. For example, as a control for 10 µL mL^{-1} of AG1296 (diluted in DMSO), 10 µL mL^{-1} DMSO were used as a control. For *in vivo* experiments inhibitors were applied at stage 15-16 and the embryos were allowed to develop until stage 25 before proceeding to *in situ* hybridization or western blot. For *in vitro* experiments inhibitors were applied to neural crest cells after an initial attachment phase of 20-30 minutes and then incubated for 1 hour before imaging or addition of PDGF-AA protein (50 ng mL^{-1}; Peprotech).

Table 2-5 List of pharmaceutical inhibitors

Name	Inhibitor of	Company	Working conc.
AG1296	PDGFR	Merck Millipore, 658551	*in vivo* 20 µM
LY294002	PI3K	Cell Signaling, 9901	*in vivo* 40 µ M *in vitro* 5 µM
MK-2206	AKT	Axon, 1684	*in vivo* 100 µM *in vitro* 5 µM
UO126	MAPK	Cell Signaling, 9903	*in vivo* 100 µM

2.2.7 RT-PCR

RNAs were extracted from neural crest cell explants or ventral non-neural crest cell tissue dissections using RNeasy Mini kit (Qiagen). Amount of purified RNA was measured using the Nanodrop spectrophotometer NDL20001. From the purified RNA cDNA libraries were reverse-transcribed using ImProm II Reverse transcription kit (Promega, A3800) and PCR machine Eppendorf mastercycler Personal. cDNA libraries were transcribed according to manufactures instructions, using a reverse

transcriptase reaction mix and a reverse transcriptase cycle program as described in Table 2-7 and Table 2-8, respectively. Subsequently PCR was performed using GoTaq G2 Hot Start Polymerase (Promega, M7401) using a 10 µL reaction mix (see Table 2-9). PCR cycles were analysed in pilot experiments. PCR reactions were run with 95 °C 15 seconds, temperature dependent on primer pair 30 seconds, 72 °C 30 seconds cycle program started by a 95 °C 5 minutes denaturation and finished with a 72 °C 5 minutes elongation period, see Table 2-6 Reverse transcriptase PCR Primer and Program. 10 µL of RT-PCR were run on 2 % agarose (Fisher Scientific, BP1356-100) gel in TAE buffer (20 mM acetic acid, 1 mM EDTA, 40 mM Tris, pH 7.6).

Table 2-6 Reverse transcriptase PCR Primer and Program

Name	Primer forward/reverse	Cycle	Reference
PDGF-A	5'-GGAATGCACGTGTACAGCAA-3'	60°C, 32x	Damm and Winkelbauer 2011
	5'-CGGGAATGTAACATGGCGTA-3'		
PDGFRα	5'-CTCGCAAATGCCACTACAGA-3'	60°C, 30x	
	5'-CCACAAGGTGT-CATTGTTGC-3'		
ODC	5'-GTCAATGATGGAGTGTATGGATC- 3'	60°C, 25x	
	5'-TCCATTCCGCTCTCCTGAGCAC-3'		
Sox9	5'-AACAGGAGTTCCATCAATCCCC- 3'	55°C, 30x	Monsoro-Burq et al., 2003
	5'-CTTTTGCTAAACCCCGTGTCAC- 3'		
Sox2	5'-CCACACGCCGCCTCGATGT- 3'	55°C, 27x	Sugiura et al., 2004
	5'-TCAGCCCCCAGCCTCTTGC- 3'		
Keratin	5'-CACCAGAACACAGAGTAC- 3'	55°C, 25x	Wilson and Melton, 1994
	5'-CAACCTTCCCATCAACCA- 3'		
Brachyury	5'-GGATCGTTATCACCTCTG- 3'	55°C, 27x	Kuriyama et al., 2014
	5'-GTGTAGTCTGTAGCAGCA-- 3'		

Table 2-7 Reverse transcriptase reaction mix

RT Mix	Total RNA	500 ng
	Oligo DT	1 µL

Up to 5 µL with nuclease free H_2O

Enzyme Mix	50 mM $MgCl_2$	4 µL
	10 mM dNTPs	1 µL
	RNasin 40 u μL^{-1}	0.5 µL
	Improm II (200 u μL^{-1})	1 µL

Up to 15 µL with nuclease free H_2O

Table 2-8 Reverse transcriptase cycle program

Addition of RT Mix		
	Temperature	**Time**
Denaturation	65 °C	5 minutes
Cooling	4 °C	∞
Addition of Enzyme Mix		
Annealing	25 °C	5 minutes
Extension	42 °C	60 minutes
Inactivation RT	70 °C	15 minutes
Cooling	4 °C	∞

Table 2-9 RT-PCR PCR reaction Mix

PCR Mix	cDNA	1-2 µL
	5x Buffer	2 µL
	10 mM dNTPs	0.2 µL
	25 mM $MgCl_2$	0.2 µL
	forward primer (10 µM)	0.2 µL
	reverse primer (10 µM)	0.2 µL
	GoTaq Polymerase (5 u μL^{-1})	1 µL

Up to 10 µL with nuclease free H_2O

2.2.8 Western blot

For immunoblotting, cells were lysed in a lysis buffer containing 100 mM Tris-HCl (pH 8.0), 1 % Triton X-100, 0.01 %SDS, complete Mini protease inhibitor (Roche) and PhosphoStop phosphatase inhibitor (Roche). 20-25 neural crest cell explants in 15 µL lysis buffer per lane, or 1 embryo in 20 µL lysis buffer. The Protein fraction was isolated by centrifugation (13,200 rpm, 4 °C) in two rounds for whole embryo lysates. Neural crest lysates were further processed without the protein purification step. The appropriate amount of 4x SDS Sample Buffer (Millipore 70607-3) was added to the lysate and boiled at 95 °C for 3 minutes. Protein lysates were analysed by SDS-PAGE using 4 to 12 % Bis-Tris gels (NuPAGE; Invitrogen), and subsequent transfer onto Invitrolon polyvinylidene difluoride membranes (Invitrogen). Membranes were blocked with 5 % non-fat dry milk and 0.1 % Tween-20 in 1 x PBS for 1 hour at room temperature, before being probed with the primary antibody (see Table 2-10) by overnight incubation at 4 °C, followed by incubation for 1 hour at room temperature with a horseradish peroxidase-linked secondary antibody (Table 2-11) and detection using ECL reagent (Luminata Forte Western HRP Substrate, Milipore). Band intensity was measured by scanning of films and analysis by densitometry using Image J (NIH).

Table 2-10 List of primary antibodies for western blot

Antibody	Species	Working concentration	Producer
PDGFRα	rabbit	1:2000	Cell Signaling, 3164
pAKT Ser437	rabbit	1:2000	Cell Signaling, 9271
panAKT (total AKT)	rabbit	1:2000	Cell Signaling, 4691
GAPDH-HRP	goat	1:2000	Santa Cruz, sc20357
N-cadherin	rat	380 ng mL^{-1}	DHSB, MNCD-2
E-cadherin	mouse	60 ng mL^{-1}	DHSB, 5D3

Table 2-11 List of secondary antibodies for western blot

Antibody	Species	Working concentration	Producer
Anti-rabbit IgG-HRP	goat	1:10,000	Santa cruz, sc-2004
Anti-rat IgG-HRP	goat	1:10,000	Santa cruz, sc-2006
Anti-mouse IgG-HRP	goat	1:10,000	Santa cruz, sc-2005

2.3 Microscopy and imaging

2.3.1 Time lapse imaging of neural crest cells

Neural crest cells cultured on fibronectin-coated plastic dishes (single well: 50 x 9 mm Falcon 351006; 4-well: Thermo Scientific 179830) and were imaged using a compound upright or inverted microscopes. Images were taken on either upright compound microscopes with motorised stages, either a DM550B Leica Microscope with a DFC 300FX Leica camera, a DMRXA2 Leica Microscope with a Hamamatsu Digital, Nikon camera, a Nikon Eclipse 80i with a Hamamatsu ORCA 05G camera or inverted compound microscope with motorised stage, a Olympus 1X70 with a Hamamatsu ORCA 05G camera. All imaging was performed in a temperature regulated environment at approximately 18 °C. Cells were imaged using a 10 x or 20 x lens. Images were acquired every 3-5 minutes, dependent on the experiments for up to 10-20 hours using either the Las AF or the SimplePCI6 software. Images were exported as .avi or .lif files and analysed as appropriate using the ImageJ software (Schneider et al., 2012).

2.3.2 Confocal microscopy of neural crest cells

For confocal imaging of living cells, neural crest cells were cultured on fibronectin coated glass bottom dishes (single well: world precision instrument Inc. FD35-100; 4-well: Greiner bio-one 627870). Images were acquired using a PerkinElmer

UltraVIEW Vox Spinning Disk system mounted on a Nikon *Ti* Eclipse microscope for high time resolution imaging. Neural crest explants were imaged with a frequency of 10 to 30 seconds performing Z-stacks of a thickness of 1 µm using Nikon 60X oil immersion lenses. Acquired images were exported as TIFF files and further analysed using the Image J free software. For imaging of fluorescently immunostained neural crest cell explants, either an Olympus Fluoview 1000 or a Leica SPE1 confocal microscope were used, with a 60 x or a 63 x oil immersion lens, respectively. Imaging conditions were adjusted according to the characteristics of the specimen.

2.4 Analysis

2.4.1 *In vivo* migration assay

For the analysis of *in vivo* neural crest cell migration *in situ* hybridization for the neural crest cell marker Twist was performed at stage 25 on *Xenopus* embryos (see section 2.1.4 Whole mount *in situ* hybridisation). Embryos were injected with either mRNAs or/and Morpholinos at one side of the embryo and labelled with fluorescein-dextran (FDX Invitrogen D1821) or rhodamine dextran (RDXL Invitrogen D1824). Injected embryos and control embryos were developed until approximately stage25, and processed for *in situ* hybridization. Images of both sides of the embryo, injected and uninjected, were taken with Leica MZFLIII Fluorescence Stereomicroscope with a Leica DFC420 using the Leica IM50 Image Manager. The length of the dorso-ventral (D-V) neural crest cell migration was measured using Twist marker in ImageJ of both sides of the embryo, the injected and uninjected side. Thus *in vivo* Migration (%) was calculated ratio of injected side to the uninjected side per embryo. In order to control for variations the measurements were repeated three times for each embryo and the average calculated. For embryos incubated with inhibitors, neural crest cell migration was estimated by the average proportion of D-V distance of a control population (> 15 embryos) compared to the average of the inhibitor treated embryo population. Following this control embryos were treated, with either mRNA or Morpholino injection, or

inhibitors the migration value calculated by the experimental data should approach 1.

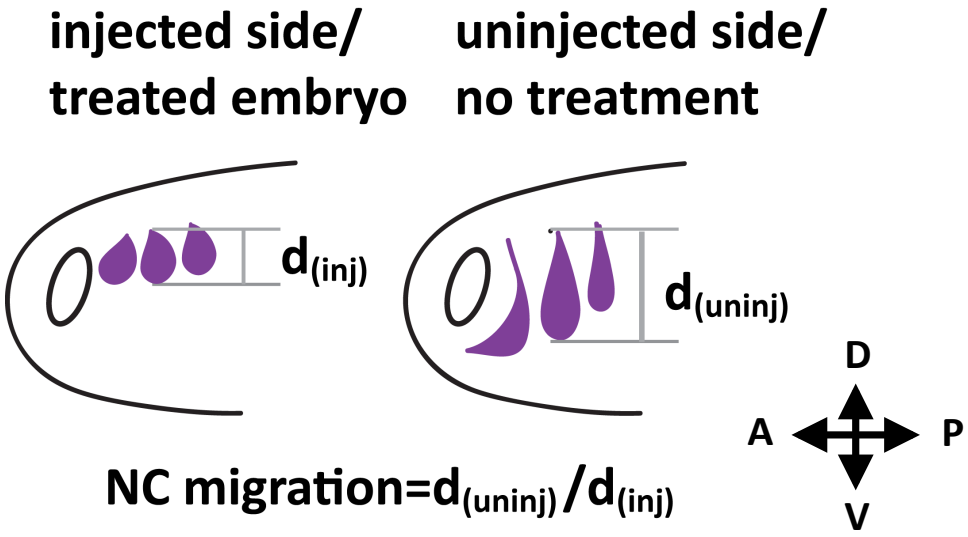

Figure 2-2 Neural Crest migration measurement scheme

Lateral head view of stage 25 *Xenopus laevis* embryo. A= anterior; P= posterior; D= dorsal; V= ventral; inj= injected; uninj= uninjected; d= distance. Neural crest streams depicted in purple.

mRNA or/and Morpholino

In vivo migration = D-V distance injected side/D-V distance uninjected side

Inhibitor treatment

In vivo migration = average D-V distance inhibitor treated embryos/average D-V distance inhibitor treated embryos head length

2.4.2 Single cell motility assay

For neural crest cells single cell motility assays nuclear RFP injected neural crest cell explants were dissociated (see section 2.1.3 Microdissection and neural crest cells culture) and allowed to attach for 30 minutes. Neural crest cell clusters were imaged as described before (see section 2.3.1 Time lapse imaging of neural crest cells), with a compound epifluorescence microscope at a magnification of 20 x for 8 hours and a 3-5 minutes frame rate. Individual cells nuclei were tracked for 5 hours using the ImageJ Manual Tracking plug-in and cells that contacted another cell were not included in the analysis. Following the cell tracks were analysed using the ImageJ Chemotaxis tool plug-in and speed and directionality of cell migration was extracted. The Cell speed by the plug in is estimated based on the equation speed= dx/dt. The distance travelled (dx) within a period of time (dt corresponding to the time between two frames) was calculated using the ImageJ plug-in Chemotaxis Tool using the coordinates dx, dy from the cell tracks. Directionality was calculated as the euclidean or accumulated distance between the start and end point of migration divided by the actual distance migrated (Figure 2-3). The average speed and directionality was calculated per cell, from which the average velocity and persistence of any given population was calculated.

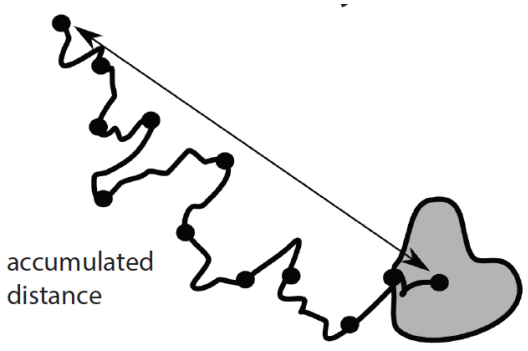

$$V_i = \frac{d_{accum}}{dt}$$

Figure 2-3 Directionality calculation scheme

Directionality was calculated as the euclidean distance or accumulated distance between the start and end point of migration (d_{accum}) divided by the actual distance (dt) migrated.

2.4.3 Chemotaxis assay

The chemotaxis assay was performed as previously described (Theveneau et al., 2010). Briefly, heparin acrylic beads (Sigma H5263, Adar Biotech 6024-1) were incubated with 1 µg mL^{-1} purified human stromal cell-derived factor-1 (Sdf1) protein overnight. Sdf1-beads of a similar diameter (150–200 mm) were immobilized on a fibronectin- coated dish using silicone grease (VWR, 6366082B) and neural crest cell explants were plated at between 250 and 500 mm away from the bead and left to attach for 20-30 minutes. Neural crest cell clusters were imaged as described before (see section 2.3.1 Time lapse imaging of neural crest cells) with a compound epifluorescence microscope at a magnification of 10 x for 15 hours and a 5 minutes frame rate. After imaging the image was rotated so the y-axis of the images goes through the SDF-1 bead at the top and the neural crest cell cluster at the bottom. To calculate the Chemotaxis Index, individual cells nuclei were tracked for 5 hours using the ImageJ Manual Tracking plug-in. Following the tracks were analysed with the ImageJ Chemotaxis tool plug-in and the chemotaxis index was extracted, which resembles the net displacement of a cell divided by the distance travelled by each cell. Thus, with a chemotaxis index of 1 the cell moves directly towards the chemotactic cue and with a chemotaxis index of -1 that the cells move away from the chemotactic source.

2.4.4 Dispersion assay

For dispersion assays nuclear RFP mRNA injected neural crest cell explants were plated on a plastic dish for 20-30 minutes to settle before imaging. When using inhibitors (see section 2.2.6 Inhibitors), they were incubated 60 minutes before

recombinant PDGF-AA protein (50 ng mL $^{-1}$; Peprotech) addition. Neural crest cell clusters were imaged as described before (see section 2.3.1 Time lapse imaging of neural crest cells), with a compound epifluorescence microscope at a magnification of 10 x for 20 hours and a 10 minutes frame rate. Cells within the explant were tracked using their nuclear marker and cell dispersion was analysed by the average triangle area between cells calculated using Delaunay triangulation algorithm as described before (Carmona-Fontaine et al., 2011; Nawrocki Raby et al., 2001) using a ImageJ dispersion tool plugin developed in the lab by András Szabó. The Delaunay algorithm connects each cell (nucleus) in a cluster with its closest two neighbours and determines the triangle area between them. The average triangle area per cluster was used as readout of cell dispersion and calculated 12 hours after imaging had started. In order to control for variations between different experiments the average triangle areas were made relative to the average area of control at the same time point.

2.4.5 Single cell collision assay

For analysis of single cell collisions, neural crest cells derived from embryos injected with membrane GFP and nuclear RFP were dissociated and plated on a fibronectin coated plastic dish. Neural crest cell clusters were imaged as described before (see section 2.3.1 Time lapse imaging of neural crest cells) with a compound epifluorescence microscope at a magnification of 20 x for 10 hours with a 3 minutes frame rate. The time of CIL collision was measured. The start (t_0) of a cell-cell collision event was classified as the first frame in which a contact between the two colliding cells could be observed. The end (tend) of the collision was defined as the last frame of contact between the two colliding cells. Cell collisions, which exceeded 60 minutes, were considered as adhesion events. The average ratio of CIL cell collision time per experiment population was calculated for comparison.

2.4.6 Explant Invasion assay

For Explant Overlap Assays, as previously described (Carmona-Fontaine et al., 2008b), neural crest cell clusters differentially labelled with fluorescein-dextran

(FDX Invitrogen D1821) or rhodamine dextran (RDXL Invitrogen D1824) were plated close to each other and imaged on a 10 x magnification on a compound epifluorescence microscope for 10 hours and a frame rate of 10 minutes. To analyse the extent of overlap between two differentially labelled neural crest cell explants, .avi or .lif movies were imported into ImageJ. Red and green channels were split, converted to 8-bit and each of them thresholded to obtain a binary image. Thresholded images of both channels, red and green, were then merged. The frame showing the maximum overlap (characterized by the area of overlap between the red and green channels) was identified and the overlap area was normalized as the ratio between the area of overlap between the two explants and the area of the smallest of the two.

2.4.7 Analysis of cell-cell adhesion protein

To determine the levels of the endogenous cadherin complex proteins at the cell-cell junction, neural crest cells clusters were plated on fibronectin coated glass coverslips and allowed to spread for at least 2 hours before fixation and immunostaining (see section 2.2.4 Immunostaining). For quantitation, confocal stacks were acquired (see section 2.3.2 Confocal microscopy of neural crest cells) and then analysed on ImageJ. A maximum projection of the Stacks was carried and to measure the intensity profile a straight segment of 10 µm in length was traced across each cell-cell junction and the intensity profile (grey values) retrieved using the Plot Profile function of ImageJ. The measured plot intensity was normalised to the intensity profile of the cell cytoplasmic region.

2.4.8 Analysis of ph-AKT-GFP distribution

For ph-GFP analysis neural crest cell explants injected with ph-AKT-GFP and either membrane RFP or liveActin RFP, were plated on 4-well glass petri dishes in 750 µL DFA and allowed to attach for at least 20 minutes. Images were acquired using a 60 x oil-immersion lens using the Vox Spinning Disk system for 10 minutes with a frame rat of 10-30 seconds (see section 2.3.2 Confocal microscopy of neural crest cells). PDGF-AA protein (200 ng mL-1) was applied diluted in 250 µL DFA, giving a final

concentration of PDGF-AA (50 ng mL-1), after 5 minutes of the start of the image acquisition without stopping the image acquisition. To analyse ph-AKT-GFP membrane localization .tif files were imported into ImageJ. A maximum projection of the Stacks was carried out and to measure the intensity profile a segmented line (width 2 pixel) was drawn at the cell boarder, visualized by mRFP or liveActin RFP. The measured grey value intensity was normalised to the grey value intensity profile of the cell cytoplasmic region. ph-AKT-GFP membrane localization was analysed every 15 seconds for 10 minutes.

2.4.9 Protrusion analysis

For protrusion analysis neural crest cell explants, injected with nuclear RFP and membrane GFP, were plated on glass petri dishes and monitored using a 60 x oil-immersion lens using the Vox Spinning Disk system for 10 minutes with a frame rate of 10 seconds (see section 2.3.2 Confocal microscopy of neural crest cells). Protrusions were defined as the regions devoid of vitelline platelets and measured in ImageJ every 30 seconds for a total of 10 minutes and the average area per cell over 10 minutes period was calculated.

2.4.10 Statistical Analysis

Significant differences between two data sets were considered different (null hypothesis rejected). Data sets (expect Western blot data) were analysed as follows: Normality was evaluated by Kolmogorov-Smirnov's test, d'Agostino and Pearson's test using. Data set were treated normal distributed if found so by all two tests. Normal distributed data was compared using Student's t-test (two-tailed, unequal variances) or using one-way ANOVA with a Dunnett's multiple comparisons post-test. Data sets that were found not to follow normal distribution were compared using Mann-Whitney's test or a non- parametric ANOVA in Prism5 (GraphPad). Normalised western blot data was analysed by one-way ANOVA followed by Student Newman-Keuls test for multiple comparison differences. All analysis was performed in Prism5 (GraphPad).

Chapter 3 Results

3.1 Co-expressed PDGFRα and PDGF-A are required for neural crest cell migration *in vivo* and *in vitro*

3.1.1 PDGF-A and PDGFRα are co-expressed in Xenopus laevis neural crest cells

During late neural crest cell migration in mouse, Zebrafish and *Xenopus* PDGF receptor alpha (PDGFRα) and its corresponding ligand PDGF-A have been reported to be expressed in neural crest cells and surrounding tissues, respectively (Ho et al., 1994; Liu et al., 2002a; Liu et al., 2002b; Orr-Urtreger and Lonai, 1992; Takakura et al., 1997). To address whether the receptor and ligand have the same reciprocal expression pattern during onset and early neural crest cell migration, I first analysed the expression of the receptor (PDGFRα) and its corresponding ligand PDGF-A by *in situ* hybridization. Both expression patterns were compared to either neural crest cell induction marker Slug (Figure 3-1 A) or migrating neural crest cell marker Twist (Figure 3-1 B, C). Interestingly, in this comparative approach I found both, ligand and receptor, to be expressed in pre-migratory (Figure 3-1 D and G) and migrating neural crest cells (Figure 3-1 E, F and H, I). To validate that both receptor and ligand are expressed in neural crest cells, I performed RT-PCR of micro-dissected neural crest cell tissue. Consistent with the previous data, RT-PCR analysis showed specific expression of both, PDGF-A and PDGFRα, in neural crest cells but not in non-neural crest cell tissue (Figure 3-2).

To further verify this I performed immunostaining and western blot analysis of neural crest cell explants for the PDGFRα protein. In line with the expression data (Figure 3-1 and Figure 3-2) I observed the PDGFRα protein in neural crest cell explants with both methods (Figure 3-3 A, B; control lane).

To deplete the levels of PDGFRα, for further experimental approaches, a translation blocking ATG anti-sense Morpholino oligonucleotide (PDGFRα MO), was designed (see experimental procedures 2.2.5 Morpholinos). To verify the specificity of the new Morpholino I tested its depletion capabilities by immunoblotting of PDGFRα MO injected neural crest cell lysates against PDGFRα. This MO showed high efficiency to reduce the protein levels by western blot (Figure 3-3 B,C). Taken together these data suggests that both the receptor PDGFRα and ligand PDGF-A are

expressed in pre-migratory and migratory neural crest cells. Further I was able to verify effective depletion of PDGFRα by use of an antisense Morpholino.

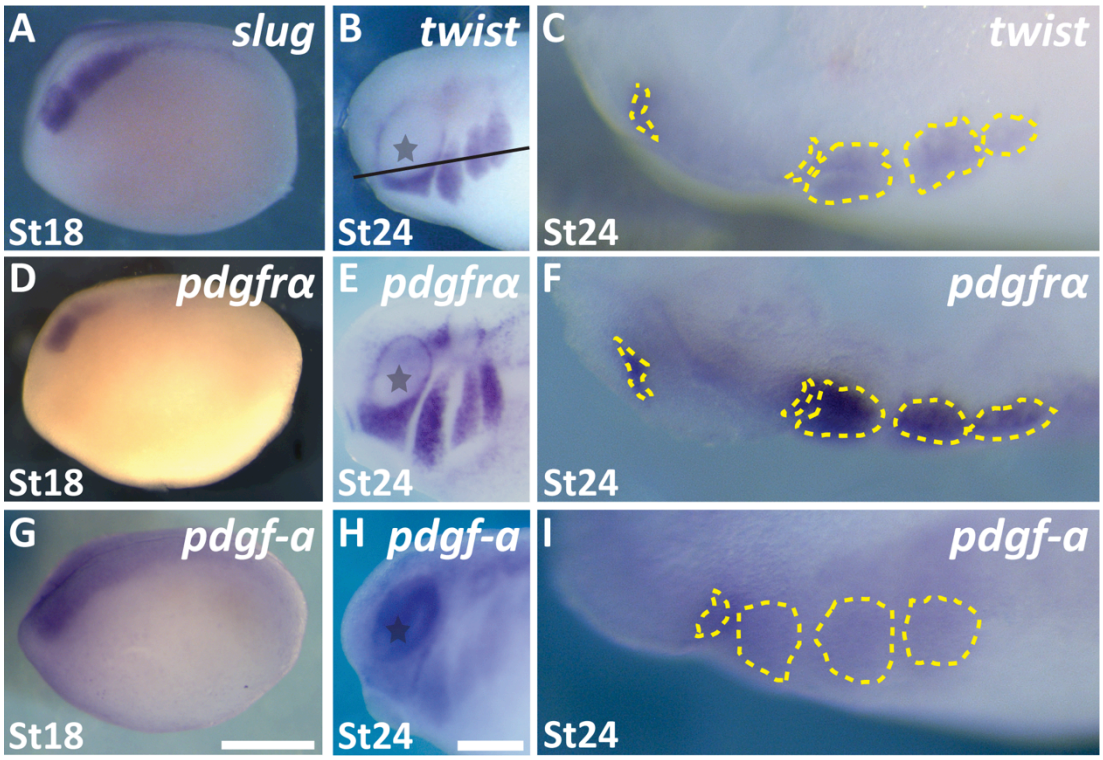

Figure 3-1 PDGF-A and PDGFRα are expressed in pre-migratory and migrating neural crest cells

(A-I) Whole mount *in situ* hybridisation of Xenopus embryos at neural crest cell induction stage 18 (lateral view, scale bar 500 µm) and neural crest cell migration stage 24 (lateral head region, scale bar 1 mm). **(A)** neural crest induction marker *Slug*. **(B)** neural crest migration marker *Twist*. **(D-F)** PDGF-A and **(G-I)** PDGFRα expression. Grey asterisk marks the eye; arrows indicate neural crest cell migration; **(C-F)** line in (B) indicates level of frontal-lateral section, cranial left and caudal right, yellow lines outline neural crest cell streams.

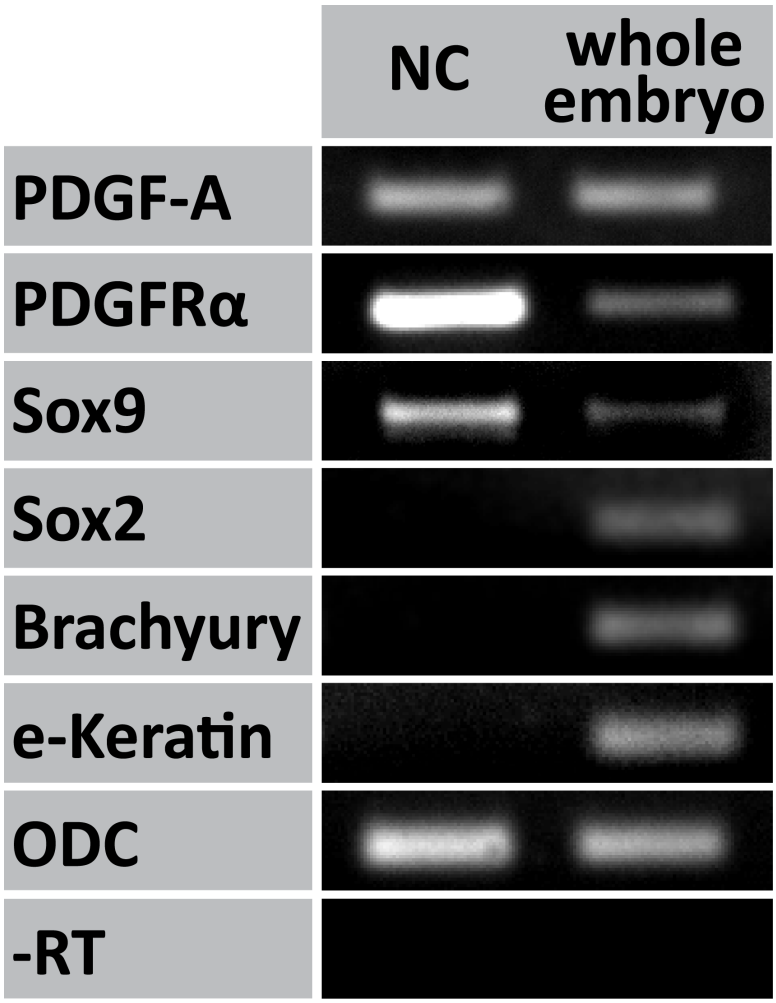

Figure 3-2 RT-PCR of microdissected neural crest cells for PDGF-A and PDGFRα

RT-PCR analysis of PDGF-A and PDGFRα expression in stage 18 neural crest cell tissue and control whole embryo, Sox9 neural crest marker, Sox2 neural plate marker, Brachyury mesoderm marker, e-Keratin epidermis marker, ODC lane loading control., -RT lane DNA contamination control .

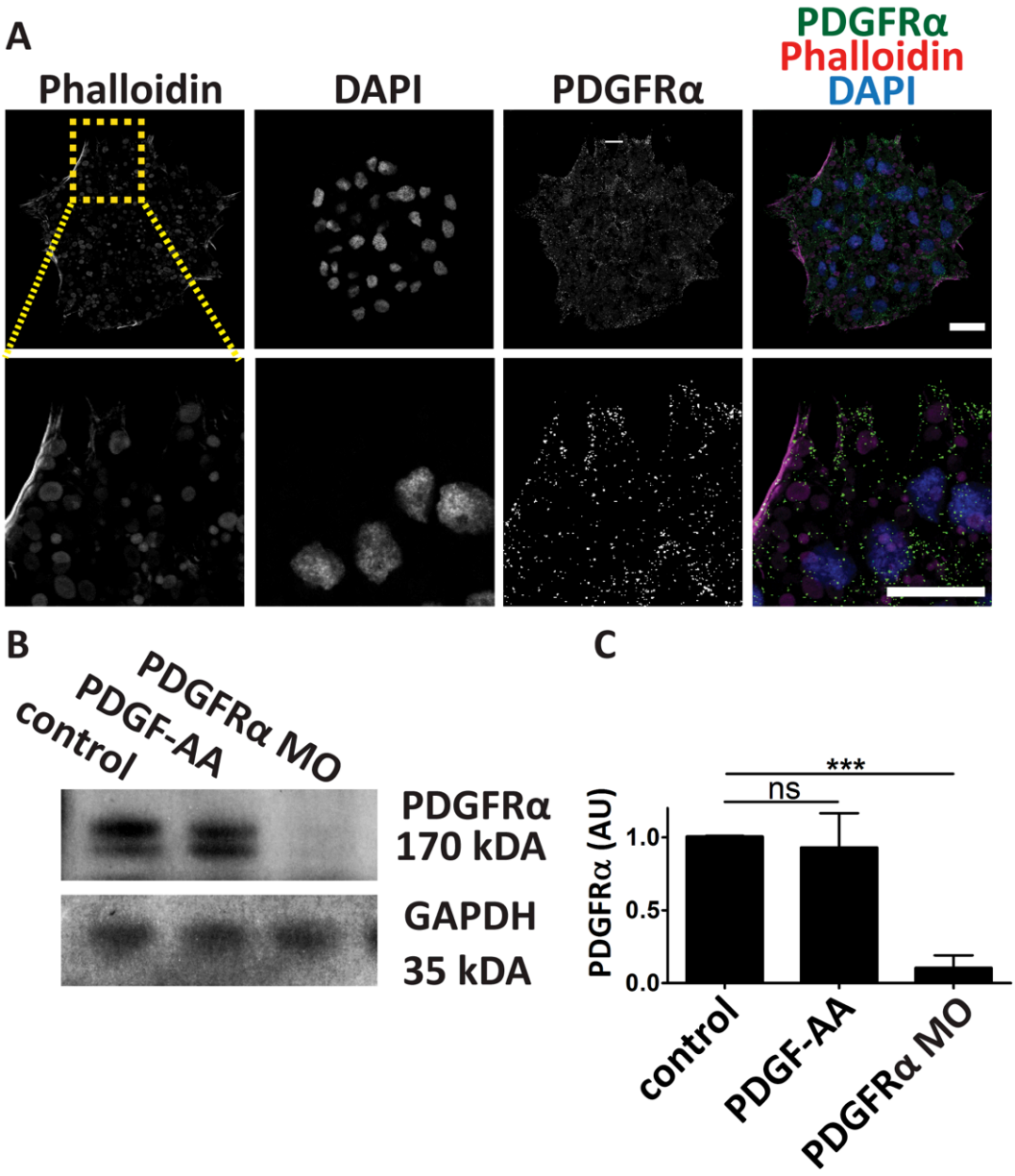

Figure 3-3 PDGFRα is expressed in neural crest cells

(A) Immunostaining of neural crest cell explants against PDGFRα (green), Phalloidin (red), DAPI (blue). Scale bars as indicated. Yellow box indicates zoom in. **(B)** Western blot analysis of PDGFRα protein using neural crest cell explants lysates of control, PDGF-AA treated (50ng mL^{-1} for 60min) or PDGFRα MO injected neural crest cells. **(C)** Band intensity normalized to loading control, bar graph shows mean and s.d., statistical analysis used one-way ANOVA followed by Student Newman-

Keuls test, data from three independent experiments. Control versus PDGF-A n=3, ^{ns}P=0.874; control versus PDGFRα n=3, $^{***}P$= 0.0006; AU= arbitrary units.

3.1.2 PDGF-A/PDGFRα signalling is required for neural crest cell migration

In section 3.1.1 I established that both the receptor (PDGFRα) and the ligand (PDGF-A) are expressed in neural crest cells. To address whether inhibition of either has an effect on neural crest cell migration *in vivo* I perturbed the signalling pathway using three different treatments: First, a previously published ATG site antisense Morpholino against PDGF-A (PDGF-A MO, Nagel et al., 2004). Second, a new designed Morpholino against PDGFRα (PDGFRα MO, see section 3.1.1). Third, mRNA of a dominant negative form of the PDGFRα, PDGFRαw37, which has a mutated glutamate residue converted to a lysine. This mutation prevents autophosphorylation of the Tyrosine 37 (W37) and prevents autophosphorylation of the receptor (Ataliotis et al., 1995). Both Morpholinos and dominant negative mRNA were injected at the late 8-cell stage into two dorsal blastomeres, in order to target neural crest cell tissue on one side of embryo and to minimise secondary effects on other tissues. The effect on neural crest cell migration was analysed by *in situ* hybridization against the neural crest cell marker *Twist* at stage 25. To evaluate the effect on neural crest cell migration, the length of the 2nd hyoid stream was compared between the un-injected and injected side of the embryo. All three different treatments, PDGFRα MO, PDGFRα MO and PDGFRαw37 mRNA, showed a significant inhibition of neural crest cell migration *in vivo* (Figure 3-4 A, B and C).

PDGFRα expression has been reported to be a downstream target of early neural crest cell progenitor transcription factors Pax3 and Zic1 (Bae et al., 2013). Therefore I addressed whether the impairment of neural crest cell migration by depletion of PDGFRα signalling could be due to an effect in neural crest cell migration and not neural crest cell induction. To investigate this I performed *in situ* hybridisation of the neural crest cell induction marker *Slug* on unilateral injected embryos with PDGF-A MO, PDGFRα MO and PDGFRαw37 mRNA. Importantly, the same level of reduction of PDGFRα or PDGF-A which affected neural crest cell migration, did not affect the neural crest cell specification marker slug (Figure 3-5 A, B). This suggests a specific mechanism of PDGF signalling during migration without affecting neural crest cell induction.

The use of antisense Morpholinos has been recently criticised due to its possibility of off-target effects (Kok et al., 2015; Schulte-Merker and Stainier, 2014). To verify the specificity of both receptor and ligand anti-sense Morpholinos I co-injected mouse mRNA, which had at least 5 mismatches to the *Xenopus laevis* target sequence (see methods section 2.2.5), together with the Morpholino at 8-cell stage. Subsequently the effect on neural crest cell migration was analysed, as before, by *in situ* hybridisation against neural crest cell marker *Twist at stage 25.* For both Morpholinos (PDGF-A MO and PDGFRα MO) co-injection of mouse mRNA rescued neural crest cell migration back to wild type levels (Figure 3-6 A-D). Taken together, these data show that specific inhibition of PDGF-A and PDGFRα impairs neural crest cell migration*,* suggesting a requirement of PDGF-A/PDGFRα signalling during neural crest cell migration *in vivo*.

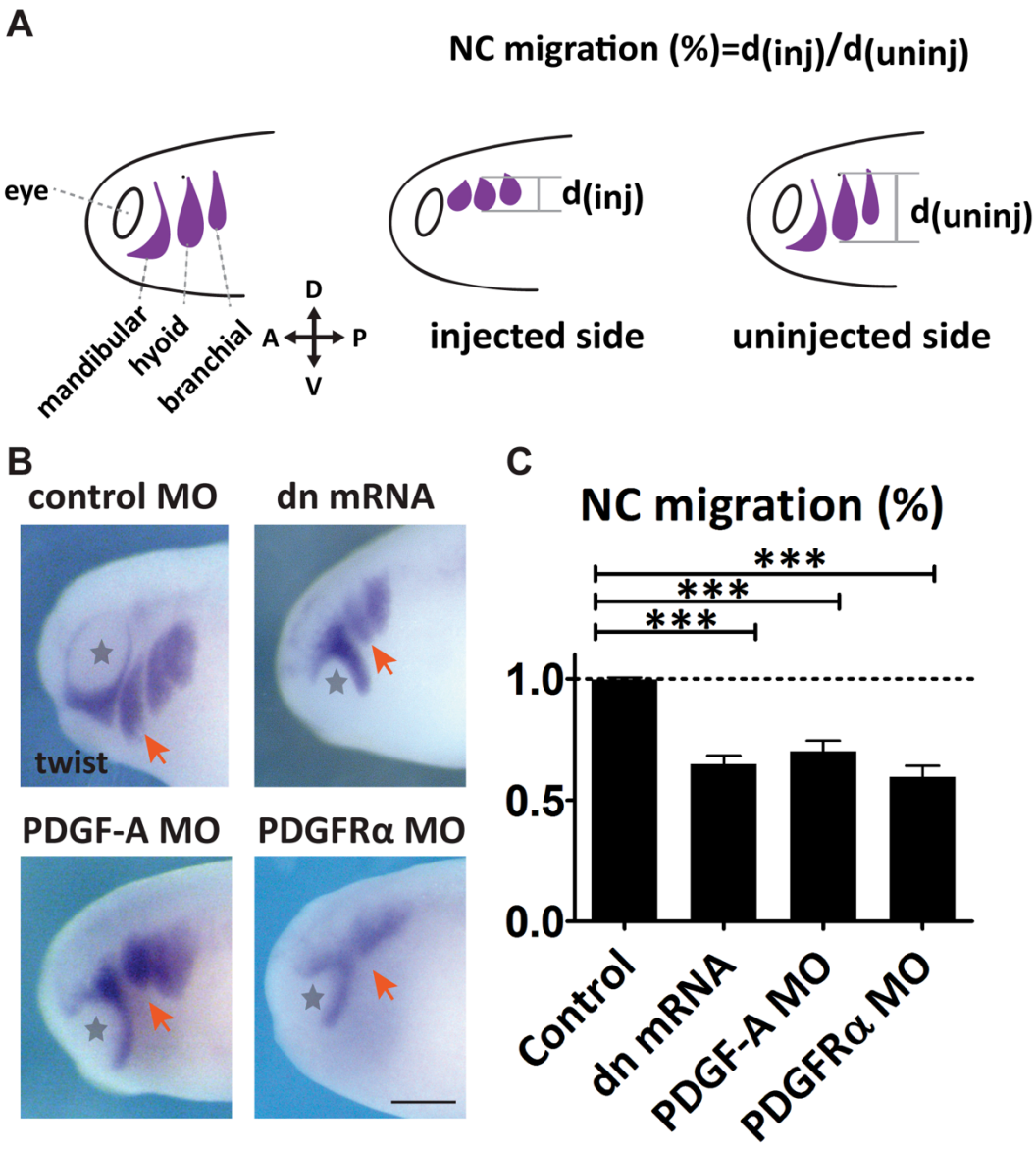

Figure 3-4 PDGF-A/PDGFRα inhibition impairs collective neural crest cell migration *in vivo*.

(A) Schematic whole mount *Twist in situ* hybridisation of *Xenopus laevis embryo* stage 25; anterior (A) to the left, posterior (P) to the right, dorsal (D) up and ventral (V) down. The three neural crest cell streams, 1st mandibular, 2nd hyoid and 3rd brachial are shown. **(B)** *Whole* mount *in situ* hybridisation of *Twist* neural crest cell migration marker, scale bar 1 mm. Red arrow indicates 2nd, (hyoid) neural crest cell stream, grey asterisk indicates eye. **(C)** Analysis of neural crest cell migration (%) for control n=30, dominant negative (dn) mRNA (PDGFRαw37) n=51, PDGF-A MO n=47, PDGFRα MO n=28 embryos, from three independent experiments. Control versus

dominant negative mRNA $^{***}P<0.0001$; Control versus PDGF-A MO $^{***}P<0.0001$; control versus PDGFRα MO $^{***}P<0.0001$. Bar graph for neural crest cell migration shows distance of 2nd (hyoid) neural crest cell stream migration of injected side normalized to uninjected control side. Bar graph indicates mean and s.e.m., statistical analysis using one-way ANOVA with a Dunnett's multiple a comparisons post-test.

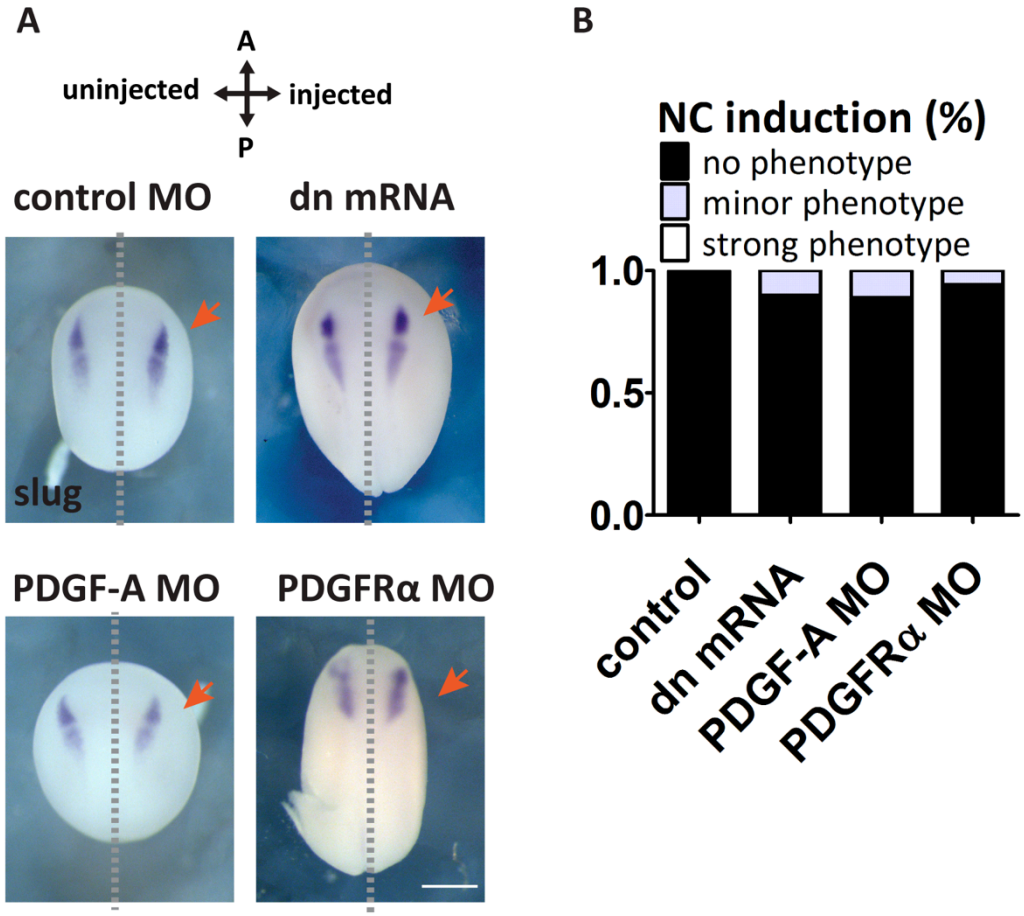

Figure 3-5 PDGF-A/PDGFRα inhibition might not affect neural crest cell induction

(A) *In situ* hybridization of *Slug* neural crest cell induction marker, dorsal view, anterior (A) to the top and posterior (P) to the bottom, uninjected side to the left and injected side to the right. Red arrow indicates side of injection, scale bar 500 µm. **(B)** Neural crest cell induction phenotype analysis. Strong phenotype= *Slug* neural crest marker not or only faintly visible on injected side compared to control side. Mild phenotype= lower *Slug* neural crest marker compared to control side. Control MO n= 15, dominant negative (dn) mRNA n=15, PDGF-A MO n=15, PDGFRα MO n=15.

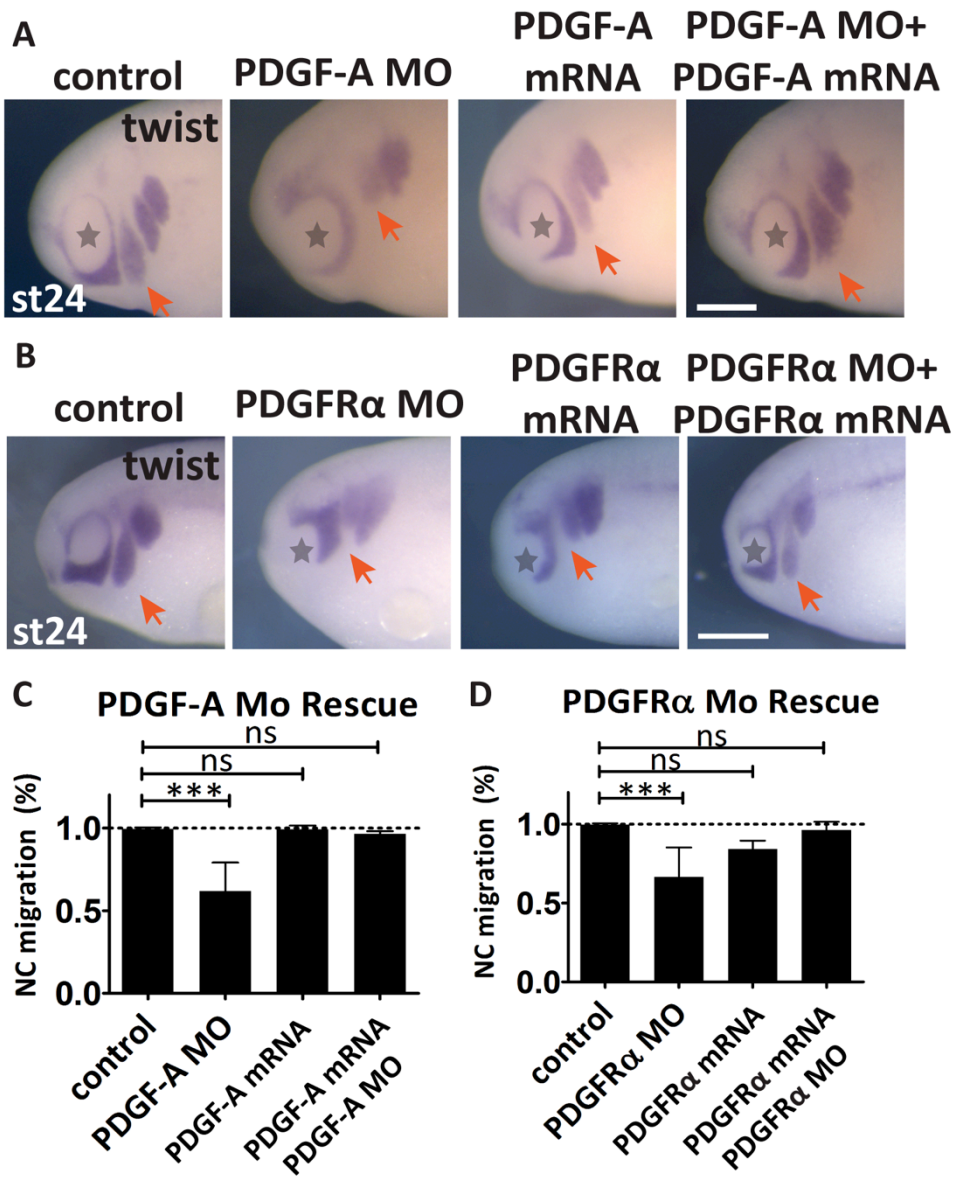

Figure 3-6 PDGF-A and PDGFRα Morpholino rescue.

(A, B) Whole mount *in situ* hybridization against *Twist* neural crest cell migration marker. Red arrow indicates 2nd (hyoid) neural crest cell stream, grey asterisk indicates eye, scale bar 1 mm. **(A, C)** PDGF-A MO *in vivo* rescue with control n=20, PDGFRα MO n=36, mouse PDGFRα mRNA n=22, PDGFRα MO and mouse PDGFRα mRNA n=41 embryos. Control versus PDGF-A MO $^{***}P$>0.0001, control versus PDGF-A mRNA ^{ns}P=0.9995, control versus PDGF-A MO and PDGF-A mRNA ^{ns}P=0.7303. **(B, D)** PDGFRα MO *in vivo* rescue with control n=30, PDGF-A MO n=24, mouse PDGF-A mRNA=28, PDGF-A MO and mouse PDGF-A mRNA n=27. Control versus PDGFRα MO

$^{***}P$<0.0001; control versus PDGFRα mRNA ^{ns}P=0.1919; control versus PDGFRα MO and PDGFRα mRNA ^{ns}P=0.9557. All Bar graphs for neural crest cell migration show distance of 2nd (hyoid) neural crest cell stream migration on injected side normalized to uninjected control side. All bar graphs indicates mean and s.e.m., statistical analysis using one-way ANOVA with a Dunnett's multiple comparisons post-test.

3.1.3 PDGF-A/PDGFRα signalling controls neural crest cell dispersion *in vitro*

In section 3.1.2 I showed that PDGF-A/PDGFRα inhibition impairs neural crest cell migration *in vivo*. Following this the next question I addressed was, what are the cellular activities controlled by PDGF during neural crest cell migration?

To investigate how inhibition of PDGF signalling could negatively impact on neural crest cell migration I analysed the following possible cellular behaviours in *in vitro* assays:

- cell motility
- chemotaxis
- cell dispersion.

Due to the cohesive properties of *Xenopus laevis* neural crest cells, it is possible to dissect the cranial neural crest cells before they start migration and culture them *in vitro* (Alfandari et al., 2010). PDGF signalling has been shown to be essential for cell motility during embryonic development in many different model organisms including the mouse, frog, zebrafish, and sea urchin (Andrae et al., 2008b) . Hence, I first addressed whether neural crest cell migration impairment is due to possible changes in neural crest cell motility.

For this, nuclear labelled neural crest cells were dissociated, plated on fibronectin coated dishes and single cell migration was monitored using time-lapse microscopy. Cell tracking and analysis of cell motility parameters did not reveal any difference in cell speed between PDGFRα MO injected and control neural crest cells (Figure 3-7 A, B). However, analysis of cell directionality, a measurement of how directional a cell migrates, revealed inhibition od directionality in PDGFRα MO injected cells. This shows that inhibition of PDGFRα does not affect cell motility of single cells, but their directional movement and suggests that inhibition of collective cell migration by PDGFRα depletion might not be due to an effect on neural crest cell motility.

It is known that directional migration of neural crest cells is controlled by chemotaxis towards the chemokine SDF-1 (Belmadani, 2005; Olesnicky Killian et al., 2009; Theveneau et al., 2010). I investigated whether the loss of neural crest cell migration after inhibition of PDGFRα is caused by a defect of chemotaxis towards the chemokine SDF-1. PDGFRα MO injected explants were plated in close proximity to SDF-1 protein-coated beads and their migratory behaviour was analysed by time-lapse microscopy. Cell tracking analysis of chemotaxing clusters revealed no difference in the migration towards the SDF-1 source between the PDGFRα depleted explants and the control cells (Figure 3-8 A, B; Movie 1). This indicates that the effect of PDGF-A/PDGFRα depletion on neural crest cell migration is not a consequence of disturbed SDF-1 chemotaxis.

Another possibility for the impaired migration of the neural crest cells could be defects during EMT. To assess the potential influence of PDGF signalling during EMT, the behaviour during neural crest cell dispersion was used as an EMT read-out. Fluorescently labelled neural crest cell clusters were monitored by time-lapse microscopy and dispersion was quantified using Delaunay triangulation of the cell nuclei (Carmona-Fontaine et al., 2011; Nawrocki Raby et al., 2001). Inhibition of either PDGF-AA or PDGFRα signalling by Morpholino injection reduced neural crest cell dispersion dramatically. Thus, confirming our previous observation that both PDGFRα MO and PDGF-AA are co-expressed by neural crest cells and functionally active in these cells (Figure 3-9 C,E and G; Movie 2). Moreover, addition of the ligand PDGF-AA to the culture media further increased cell dispersion of wild type neural crest cells (Figure 3-9 A, B and G; Movie2). Concentration for dispersion of PDGFRα MO, PDGF-A MO and PDGF-AA protein was determined by titration experiments (Figure 3-10 A, B and C). Following these experiments 8 ng of PDGFRα MO, 16ng PDGF-A MO and 50 ng mL^{-1} PDGF-AA protein where used. To test whether inhibition of PDGF-A MO and PDGFRα MO is specific, PDGF-AA protein was added to the Morpholino injected neural crest cell explants. The addition of PDGF-AA protein was only able to partially rescue the inhibition of PDGF-A MO dispersion, but not PDGFRα MO treated cells (Figure 3-9 D, F and G). Thus showing again the specificity and effectivity of the pathway inhibition using the PDGF-A and PDGFRα

Morpholinos. Taken together, I show that PDGF-A/PDGFRα signalling inhibition does not affect neural crest cell motility, nor chemotaxis towards SDF-1, but regulates neural crest cell dispersion.

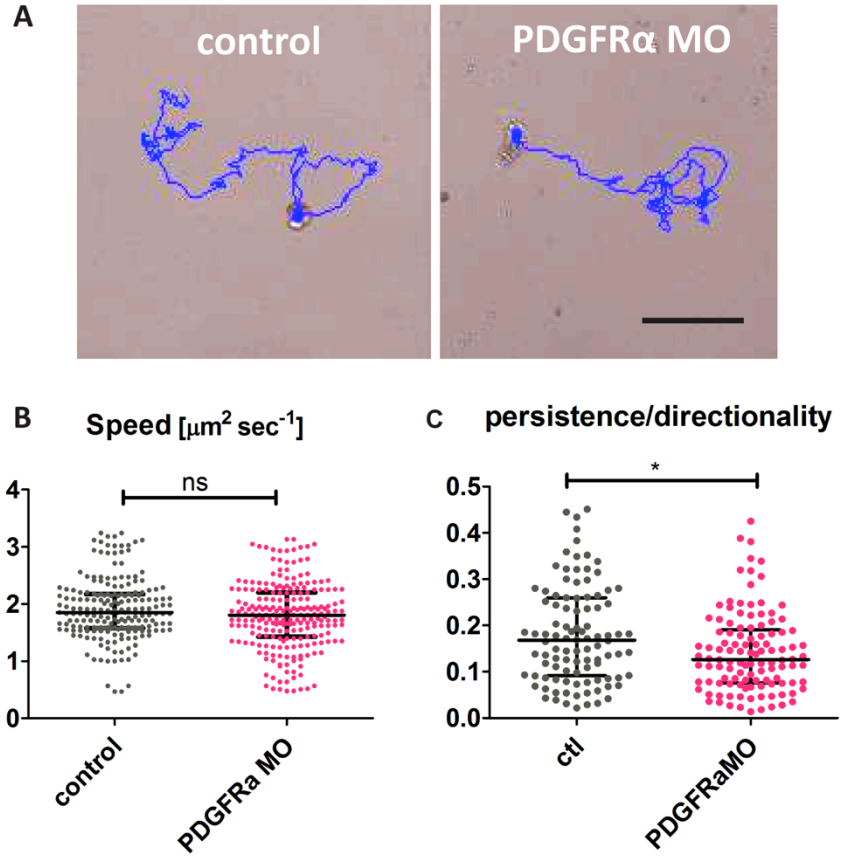

Figure 3-7 PDGFRα does not affect single cell motility.

(A) Images showing tracks of nuclear (nuc) RFP injected cells over 30min, scale bar 50μm. **(B)** Analysis of neural crest cell motility (Speed (μm seconds^{-1})) in control and PDGFRα MO injected single cells, control n=202, PDGFRα MO=228 cells from three independent experiments, scatter blot median and interquartile range, statistical analysis using Mann-Whitney's test; control versus PDGFRα MO ^{ns}P=0.1069; **(C)** Analysis of neural crest cell persistence/directionality in control and PDGFRα MO injected single cells, control n=100, PDGFRα MO=114 cells from three independent experiments, scatter blot median and interquartile range, statistical analysis using Mann-Whitney's test; control versus PDGFRα MO $^{*}P=0.00091$.

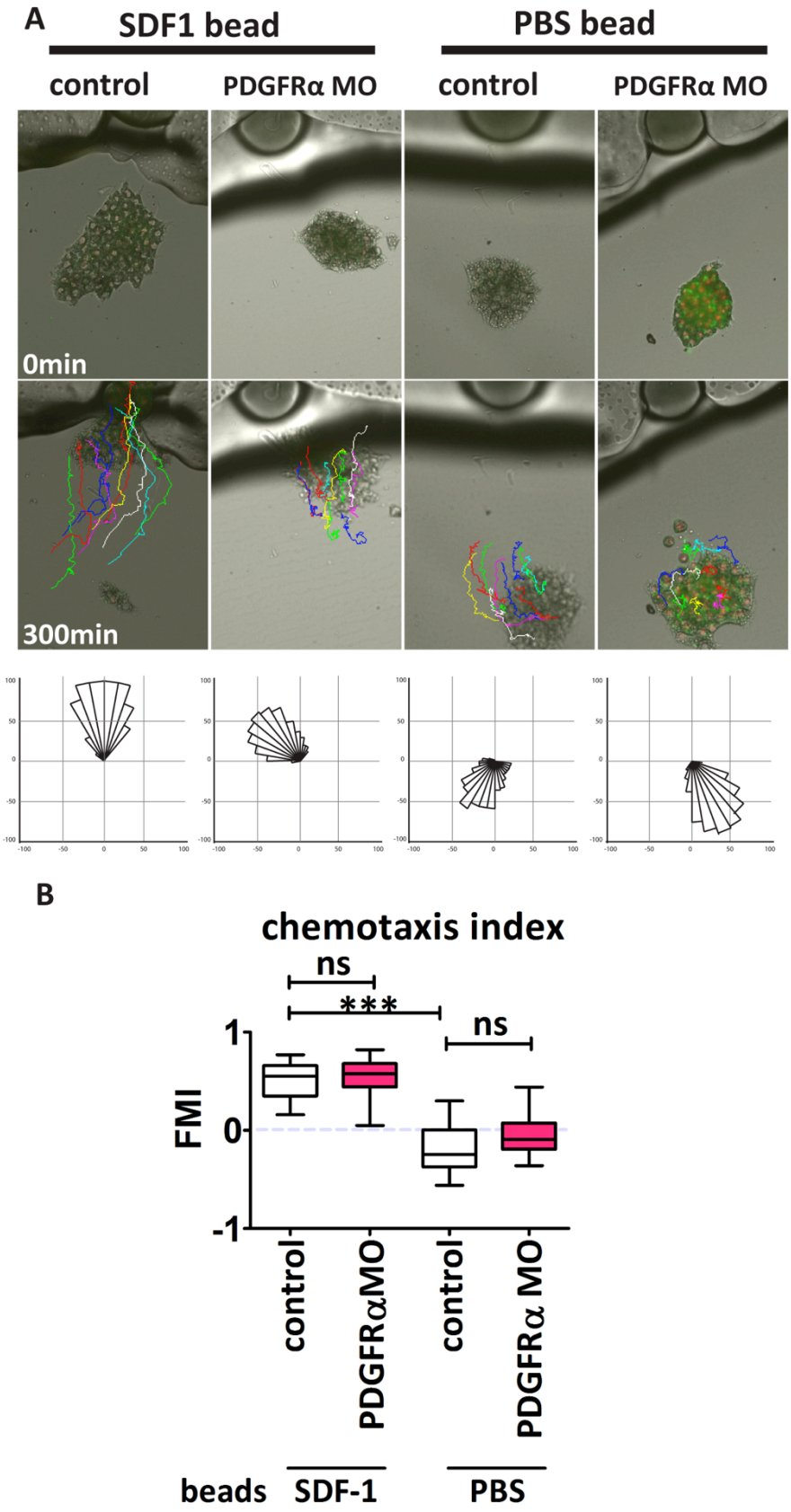

Figure 3-8 PDGFRα signalling is not required for SDF-1 chemotaxis.

(A) Representative images of chemotaxing clusters at t=0min and t=300min, scale bar 100µm. **(B)** Chemotaxis assay analysis showing Forward migration index (FMI) with SDF1 bead (control n=47, PDGFRα MO n=50) and PBS control beads (control n=50, PDGFRα MO n=50); box and whisker: box and median are ± 25^{th}/75^{th}percentile, whiskers are min. and max., statistical analysis using ANOVA with a Dunnett's multiple comparisons post-test; control (SDF-1 bead) versus PDGFRα MO (SDF-1 bead) ^{ns}P=0.9995; control (SDF-1 bead) versus control (PBS bead) $^{***}P$<0.0001; control (PBS bead) versus PDGFRα MO (PBS bead) ^{ns}P=0.3975.

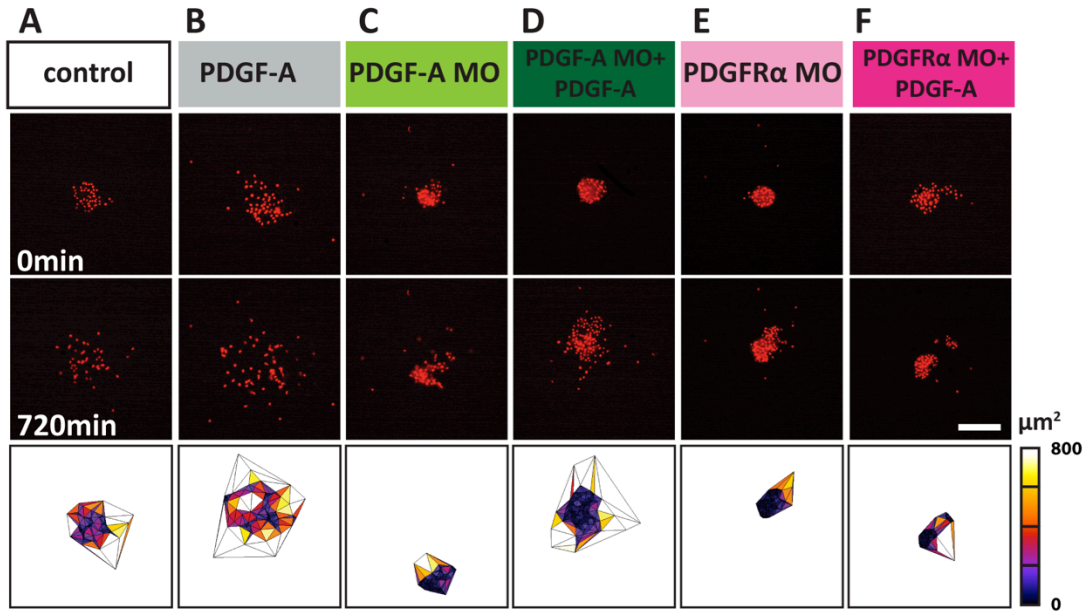

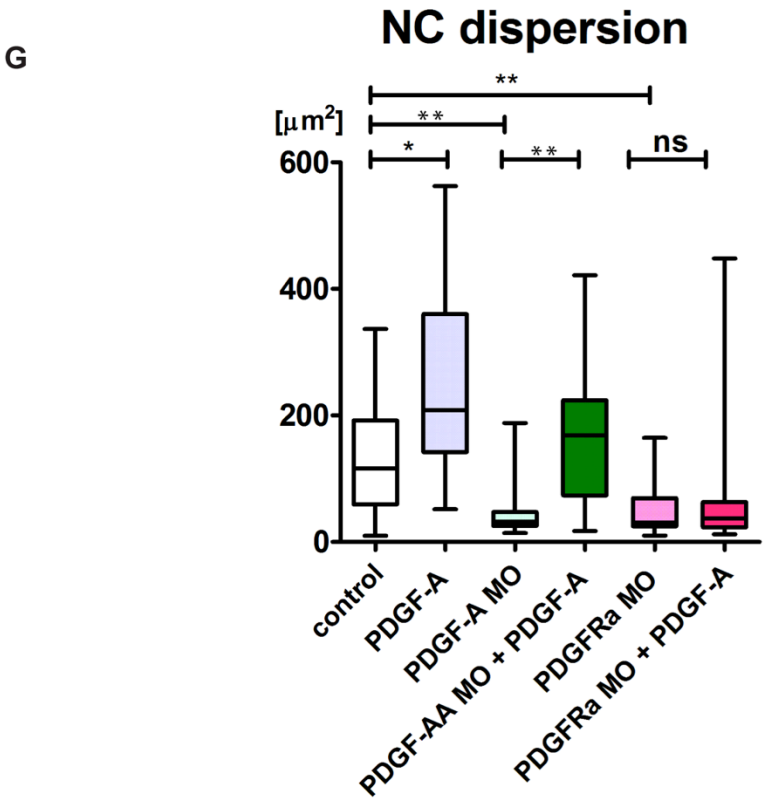

Figure 3-9 PDGF-A/PDGFRα required for neural crest cell dispersion.

(A-F) PDGF signalling dispersion with nuclear RFP mRNA (nucRFP) explants, example images of movies at t=0min and t=720min, scale bar 100µm and Delaunay triangulation examples at t=720min. **(G)** Average Delaunay triangulation area (μm^2) of control=43, PDGF-AA protein (50ng mL^{-1}) n=31, PDGF-A MO n=18, PDGF-AA MO&PDGF-A protein n=13, PDGFRα MO n=30, PDGFRα MO&PDGF-AA protein n=29 explant clusters from at least three independent experiments. Box and whisker: box and median are ± $25^{th}/75^{th}$percentile, whiskers are min. and max., statistical analysis using Kruskal-Wallis Anova with Dunnett's multiple comparisons post-test; control versus PDGF-A protein $^{***}P$<0.0001; control versus PDGF-A MO $^{*}P$=0.0217; control versus PDGFRα MO $^{**}P$=0.0052; PDGF-A MO versus PDGF-A MO&PDGF-A protein $^{**}P$=0.0059; PDGFRα MO versus PDGFRα MO&PDGF-A protein ^{ns}P=0.9956.

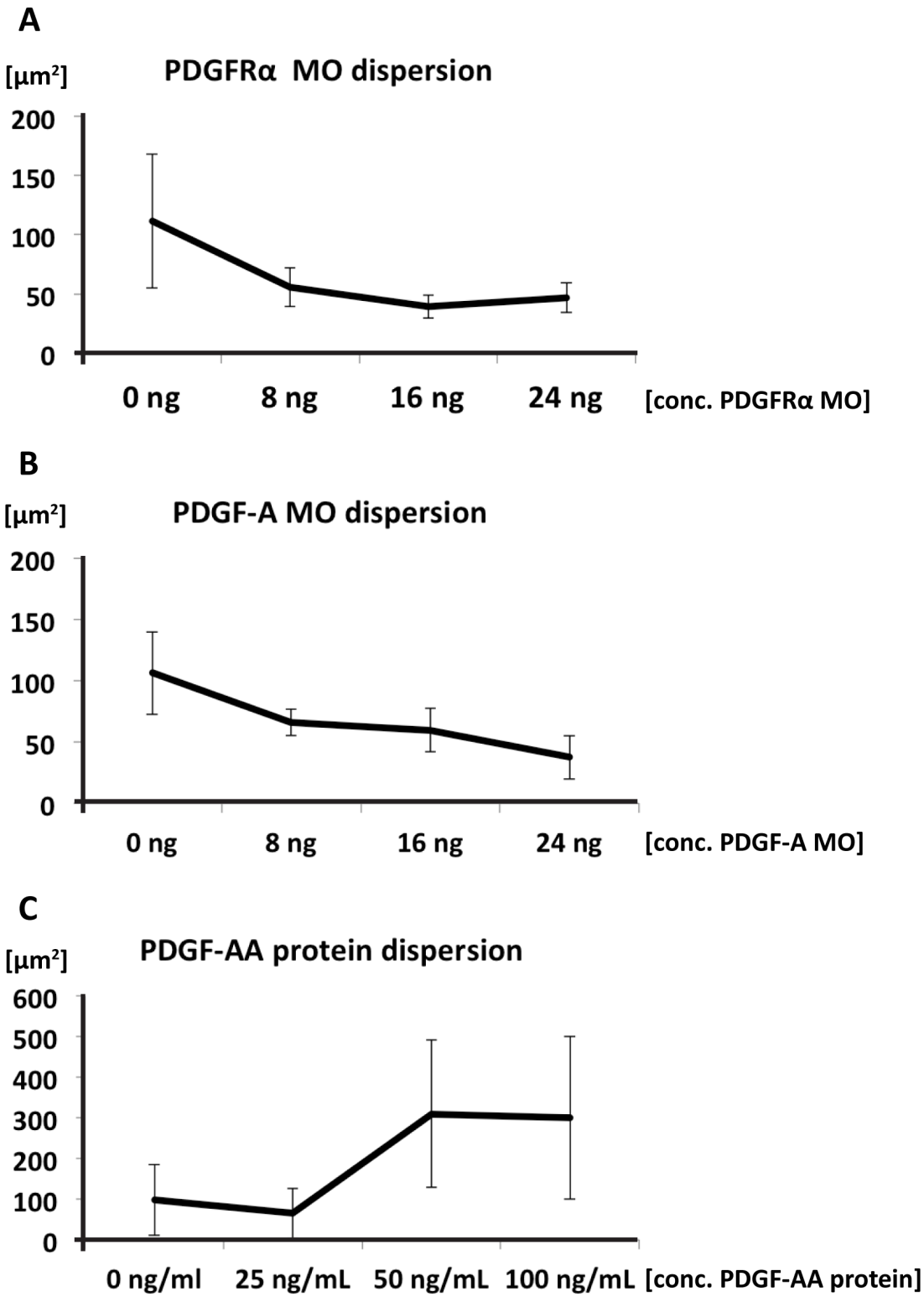

Figure 3-10 PDGFRα MO, PDGF-A MO and PDGF-AA protein dispersion titration

(A) PDGFRα MO titration (0 ng, 8 ng, 16 ng and 24 ng) analysed by delauney triangulation [μm^2] at 720 min. **(B)** PDGF-A MO titration (0 ng, 8 ng, 16 ng and 24 ng) analysed by delauney triangulation [μm^2] at 720 min. **(C)** PDGF-AA protein

titration (0 ng mL^{-1}, 25 ng mL^{-1}, 50 ng mL^{-1} and 100 ng mL^{-1}) analysed by delauney triangulation [μm^2] at 720 min.

3.2 PDGF-A/PDGFRα controls N-cadherin dependent contact inhibition of locomotion

3.2.1 PDGF-A/PDGFRα controls cell-cell adhesion via N-Cadherin regulation

In the section 3.1.3 I established that PDGF-A/PDGFRα signalling is controlling dispersion, an EMT property, *in vitro*. One of the hallmarks of EMT transition is the change in cell-cell adhesion from epithelial to mesenchymal character (Thiery et al., 2009). Specifically a switch from E-cadherin to N-cadherin is linked to EMT (Thiery et al., 2009) and has also been has been recently connected to neural crest cell EMT (Scarpa et al., 2015). Therefore, I investigated whether PDGF signalling inhibition is affecting cell-cell adhesion. To address this I made use of a previously published cell-cell sorting assay (Carmona-Fontaine et al., 2011; Moore et al., 2013; Scarpa et al., 2015). The cell sorting assay provides a readout of differences in cell-cell adhesion properties between two cell populations. Differently micro-dissected and labelled neural crest cells populations were dissociated, mixed and allowed to reaggregate in an agarose coated dish over night. The read out is given with the mixing capabilities of both populations. If the cell-cell adhesion properties between the two groups are the similar, the cell populations stay mixed, if they are different cell groups sort out into two distinct populations in the aggregate (Figure 3-11 A). After mixing PDGFRα MO injected neural crest cells with control neural crest cells we observed that re-aggregated cell populations grouped themselves into two distinct populations (Figure 3-11 B), in contrast to the control cells, which stayed mixed (Figure 3-11 B). This experiment might suggest a role of PDGFRα signalling in cell-cell adhesion.

As mentioned above one of the key families involved in cell-cell adhesion is the cadherin protein family (Thiery et al., 2009) and it has been recently shown that a switch from E- to N-cadherin is essential for neural crest cell EMT (Scarpa et al., 2015). Therefore I first investigated the impact of PDGFRα signalling on N-Cadherin and E-Cadherin levels in neural crest cells by western blot. Neural crest cell explants were micro-dissected and immunoblotted against N-cadherin and E-cadherin. Surprisingly, we observed a reduction of N-Cadherin protein levels in PDGFRα MO

injected neural crest cells, but no significant change in E-Cadherin levels (Figure 3-12 A, B). To verify the effect of PDGFRα depletion on N- and E-cadherin levels, I performed immunofluorescence staining in PDGFRα depleted neural crest cells. Immunofluorescence against N-cadherin or E-cadherin were imaged by confocal microscopy and analysed by measuring grey value intensity levels over the cell-cell border. Consistent with my previous data, I observed a specific decrease in fluorescently labelled N-cadherin (Figure 3-13 A, B), but not E-cadherin (Figure 3-14 A, B) after PDGFRa MO injection. Interestingly, N-cadherin levels were similarly diminished after PDGF-A MO treatment (Figure 3-13 A, B). Furthermore overexpression of the PDGF-A ligand, led to an increase in N-cadherin levels (Figure 3-13 A, B).

Taken together, the data in this chapter lead to the suggestion that PDGFRα signalling might control neural crest cell migration, at least *in vitro*, by a change in cell-cell adhesion. Further I show that the change in cell-cell adhesion could be due to a downregulation of N-cadherin levels in PDGFRa MO explants.

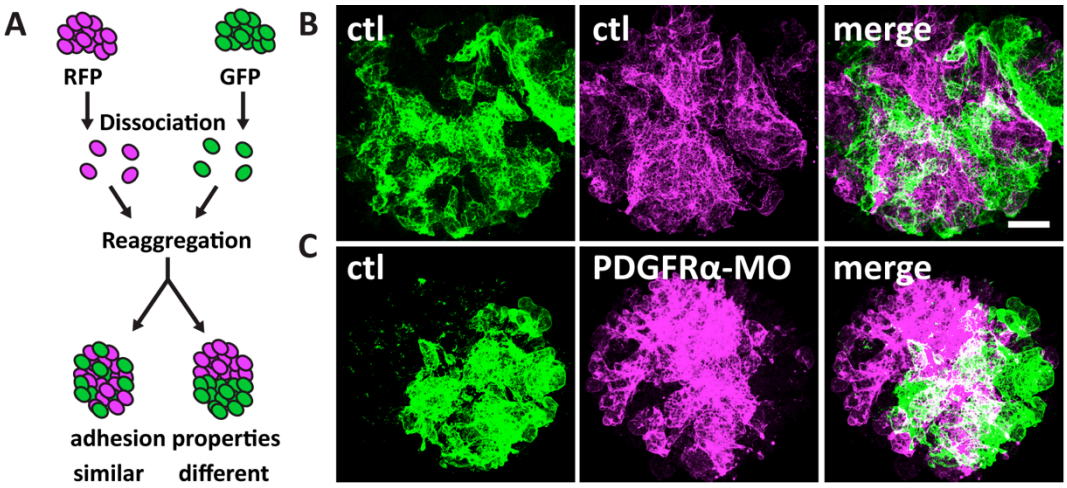

Figure 3-11 Cell-Cell Sorting assay: PDGFRα MO in neural crest cells show adhesion differences

(A) Schematic representation of cell-cell sorting assay adapted from Carmona-Fontaine et al., 2011 **(B,C)** Example confocal projections of differentially labelled control **(B)** and PDGFRα injected MO **(C)** neural crest cell aggregates. Example of two independent experiments, scale bar 50µm.

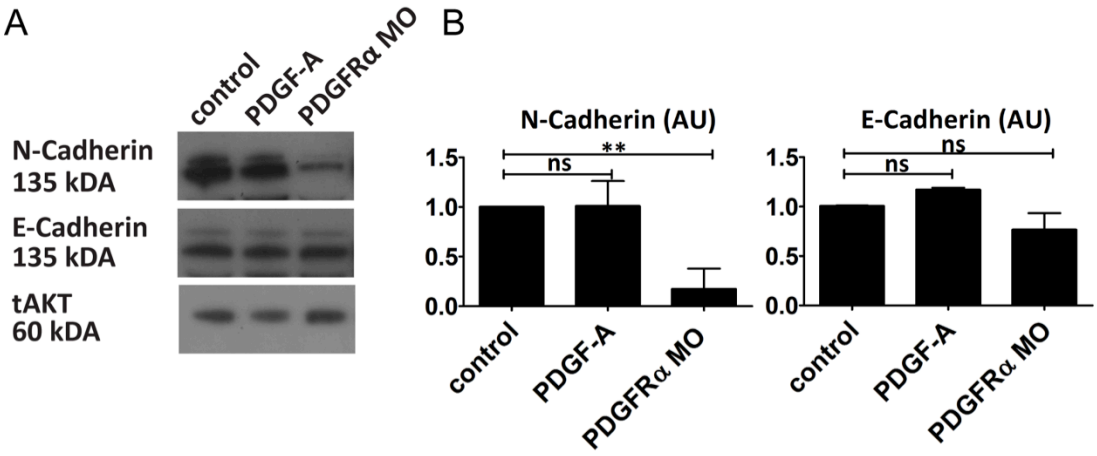

Figure 3-12 PDGFRα depletion affects N-cadherin level by western blot

(A) Immunoblot against N-cadherin and E-cadherin protein from of control, PDGF-AA protein (50ng mL-1 for 60min) and PDGFRα MO injected neural crest cell explant lysates **(B)** Band intensity normalized to loading control, bar graph shows mean and s.d., statistical analysis used one-way ANOVA followed by Student Newman-Keuls test, data from three independent experiments. N-cadherin: Control versus PDGF-A protein ^{ns}P=0.9985; control versus PDGFRα MO $^{**}P$=0.0040; E-cadherin: control versus PDGF-A protein ^{ns}P=0.1721; control versus PDGFR α MO ^{ns}P=0.0537; AU= arbitrary units.

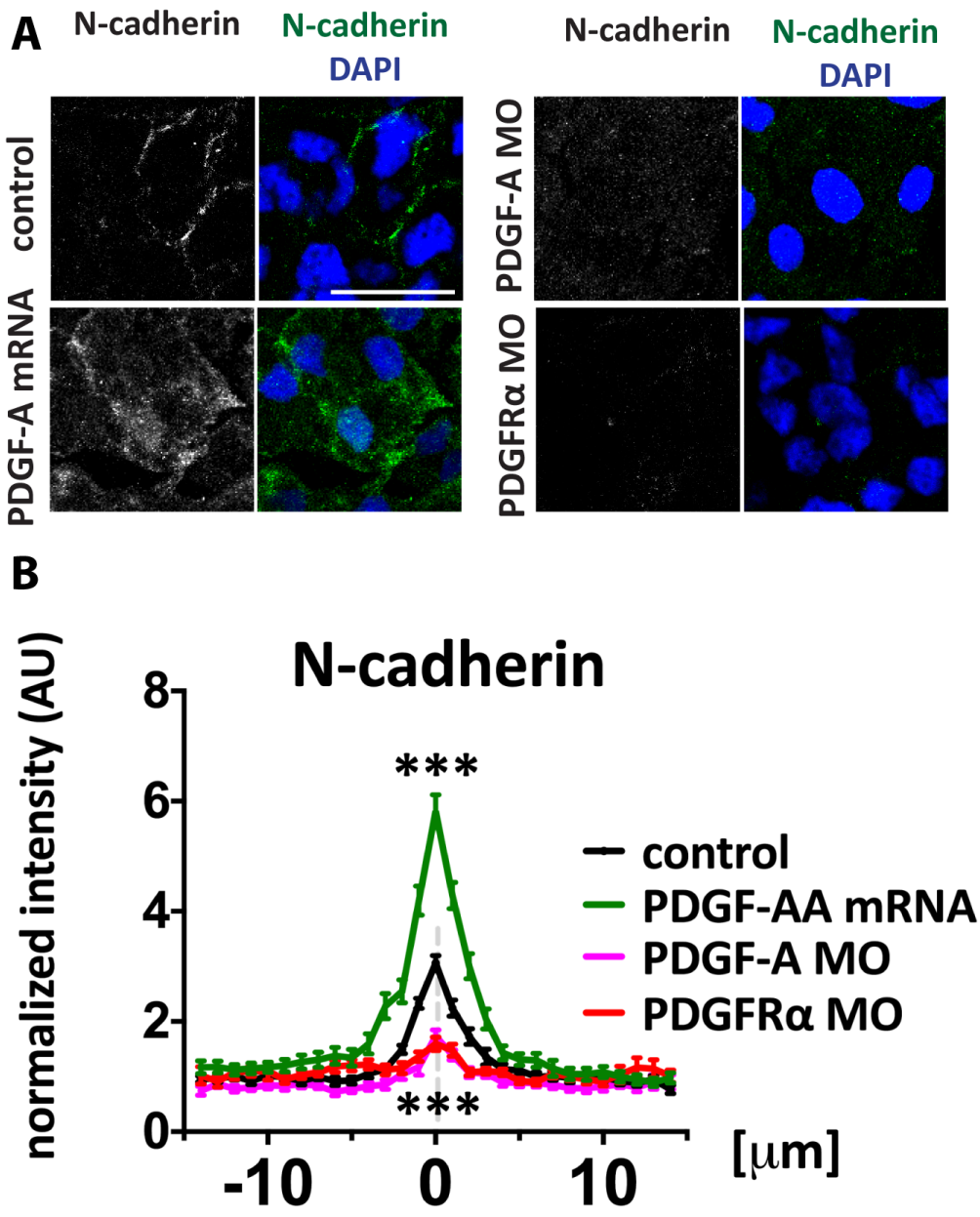

Figure 3-13 Immunostaining: PDGFRα signalling regulates N-cadherin level

(A,C) Immunostaining against N-cadherin (A, green), DAPI (blue) of control, PDGF-AA protein treated (50ng mL^{-1} for 180min), PDGF-A MO and PDGFRα MO injected neural crest cells. Scale bar 20 μM. **(B,D)** Analysis of pixel intensity across cell-cell contact (0 μm), normalized to average cell background level. Data points represent mean with s.e.m., statistical analysis using one-way ANOVA with a Dunnett's multiple comparisons post-test. Control n=118, PDGFRα MO n=61, PDGF-A MO n=50, PDGF-AA mRNA n=50; control versus PDGFRα MO $^{***}P<0.0001$; control versus

PDGF-A MO $^{***}P<0.0001$; control versus PDGF-AA mRNA $^{***}P<0.0001$. AU= arbitrary units.

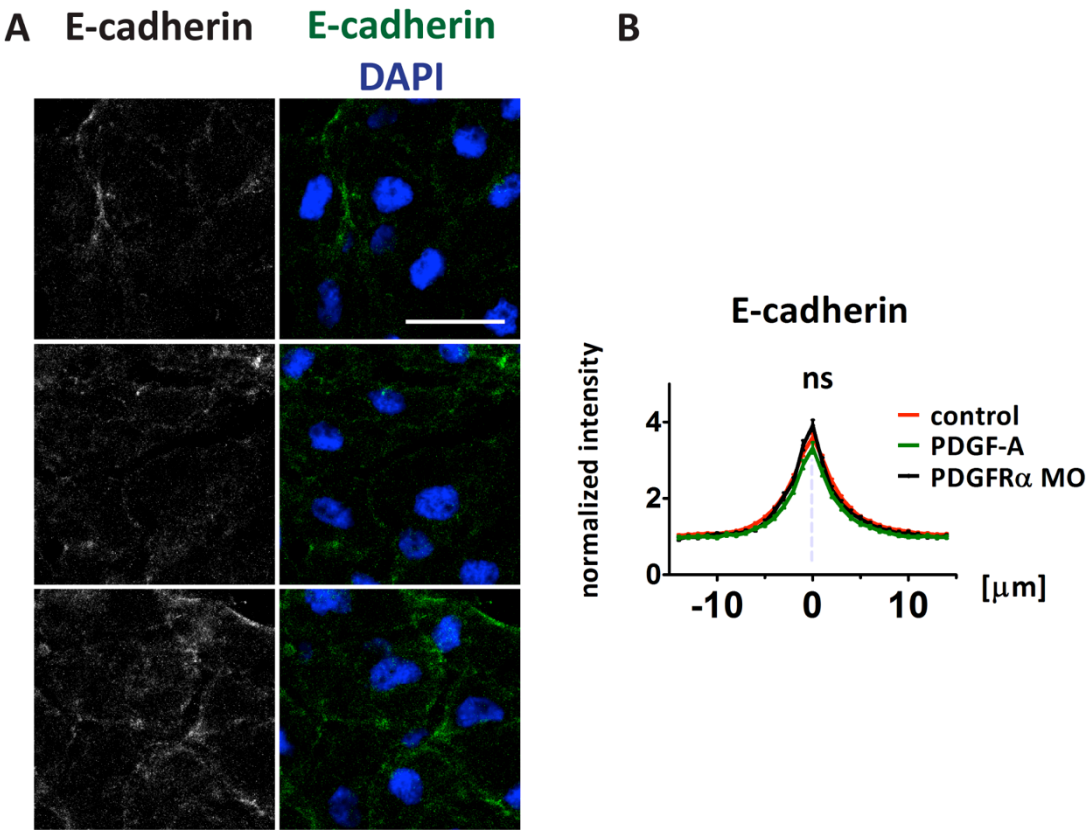

Figure 3-14 Immunostaining E-cadherin: PDGFRα signalling perturbation does not affect E-cadherin level

Immunostaining against E-cadherin (A, green), DAPI (blue) of control, PDGF-AA protein treated (50ng mL^{-1} for 180min), PDGF-A MO and PDGFRα MO injected neural crest cells. Scale bar 20 µm. **(B,D)** Analysis of pixel intensity across cell-cell contact (0 µm), normalized to average cell background level. Data points represent mean with s.e.m., statistical analysis using one-way ANOVA with a Dunnett's multiple comparisons post-test. E-cadherin: control n=445, PDGFRα MO n=137, PDGF-AA protein n=256. ^{ns}P>0.05, AU= arbitrary units.

3.2.2 N-cadherin dependent CIL is regulated by PDGF-A/PDGFRα signalling

So far, I found that inhibition of PDGF-AA/PDGFRα changes cell-cell adhesion and specifically decreases the levels of N-cadherin protein at the cell-cell contact (section 3.2.1). The next question asked was: How can this decrease in N-cadherin be related to reduced cell dispersion? Blocking N-cadherin leads to a loss of CIL behaviour in neural crest cells (Theveneau et al., 2010). Hence, I hypothesized that the decreased dispersion in PDGFRα MO explants (Fig.3 E, F) could be due to a N-cadherin dependent loss of CIL. It is well established that a cell cluster undergoing CIL will disperse (Davis et al., 2015; Scarpa et al., 2015; Stramer and Mayor, 2016; Villar-Cerviño et al., 2013), conversely the depletion of CIL behaviour causes an inhibition of dispersion, as observed in PDGF-A MO and PDGFRα MO explants (Figure 3-9; Movie 2).

To further investigate whether CIL is impaired in a PDGFRα depletion background I used two different assays to test for a change in CIL; first a single cell based collision assay (or 2D kinematic assay) and second an explant invasion assay (Carmona-Fontaine et al., 2008b; Moore et al., 2013; Scarpa et al., 2015).

First, when two cells undergoing CIL collide they remain briefly in contact before they move away from each other. However, if CIL is impaired the two colliding cells remain in contact for longer time. We measured the time that pairs of colliding cells remain together as an outcome of CIL (Stramer and Mayor, 2016, Figure 3.13 B). PDGFRα depleted and control dissociated single cells were plated on fibronectin coated dishes and their behaviour was monitored using time-lapse microscopy. Our results show that cells expressing the PDGFRα MO remain in contact much longer compared to control cells, indicating impairment in the CIL response (Figure 3-15 A).

Second, PDGFRα depletion was analysed by its capability to invade. When two cell-explants that exhibit CIL are confronted, they do not overlap; on the other hand an overlapping between adjacent explants is an indication of CIL deficiency (Stramer and Mayor, 2016). Two neural crest cell explants fluorescently labelled with two distinct tracers were cultured at a short distance and their behaviour analysed by

time-lapse microscopy. The overlapping area between them was analysed as readout of CIL deficiency (Figure 3-16 A). This assay showed that while control explants did not overlap, PDGFRα deficient explants showed a clear overlapping (Figure 3-16 B, C). This indicates a striking reduction in CIL response.

In order to undergo CIL and move away from each other cells must be able to change their polarity upon cell contact. This change in contact-dependent polarity has been linked to N-cadherin dependent cell adhesion (Scarpa et al., 2015; Theveneau et al., 2010). To assess whether inhibition of PDGFRα changes polarity in neural crest cells we measured the protrusion area as readout in Morpholino injected explants. We found a reduced protrusion size in PDGFRα MO injected explants (Figure 3-17), suggesting a change in polarity. Taken together, this further supports the hypothesis that PDGFRα MO depletion impairs CIL in neural crest cell migration.

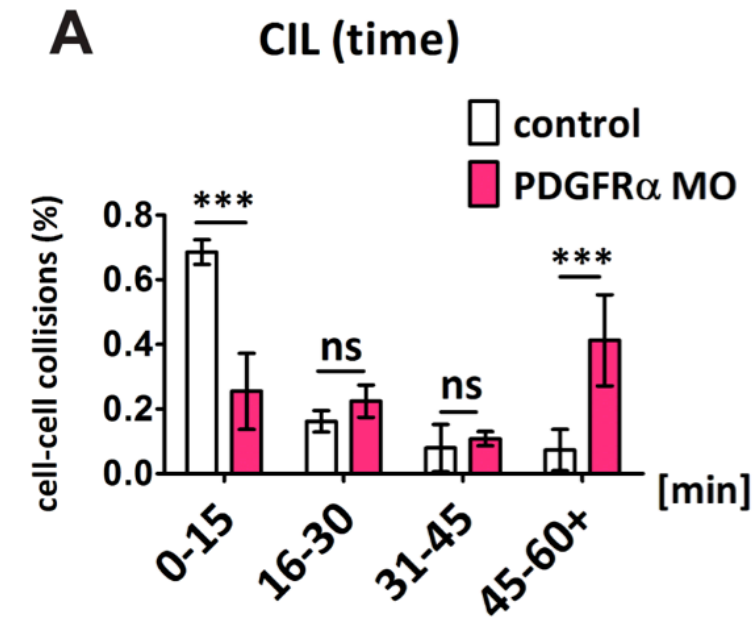

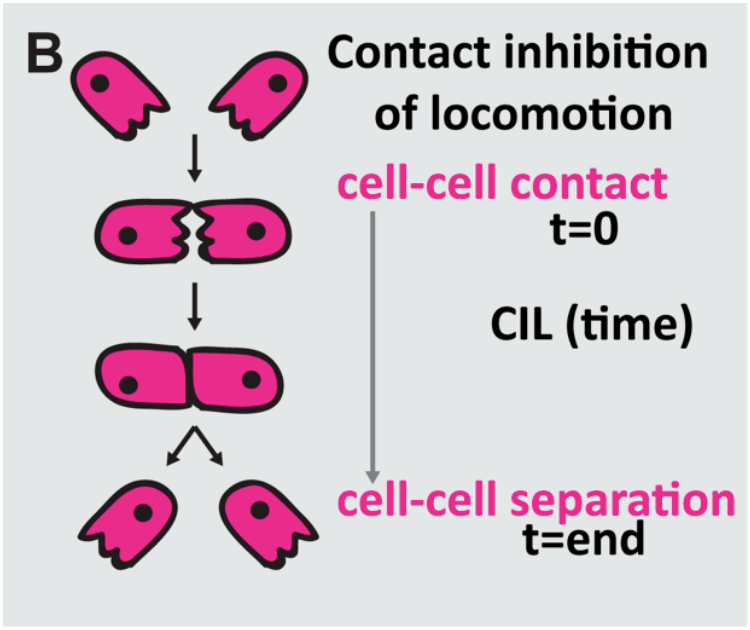

Figure 3-15 PDGFRα required for contact inhibition of locomotion

(A,B) Single cell collision assay representing CIL time between first contact and separation, also considered as the stability of the contact. PDGFRα MO explants have impaired CIL, control-control CIL events n=58 and PDGFRα MO-PDGFRα MO events n=63, bar graph shows mean and s.d., from three independent experiments, statistical analysis by two-way ANOVA followed by Bonferroni post-tests; 0-15 min data bin control versus PDGFRα MO $^{***}P<0.0001$; 16-30 min data bin control versus

PDGFRα MO ^{ns}P=0.9999; 31-45 min data bin control versus PDGFRα MO ^{ns}P=0.9999; 45-60 min data bin control versus PDGFRα MO $^{***}P$=0.0003.

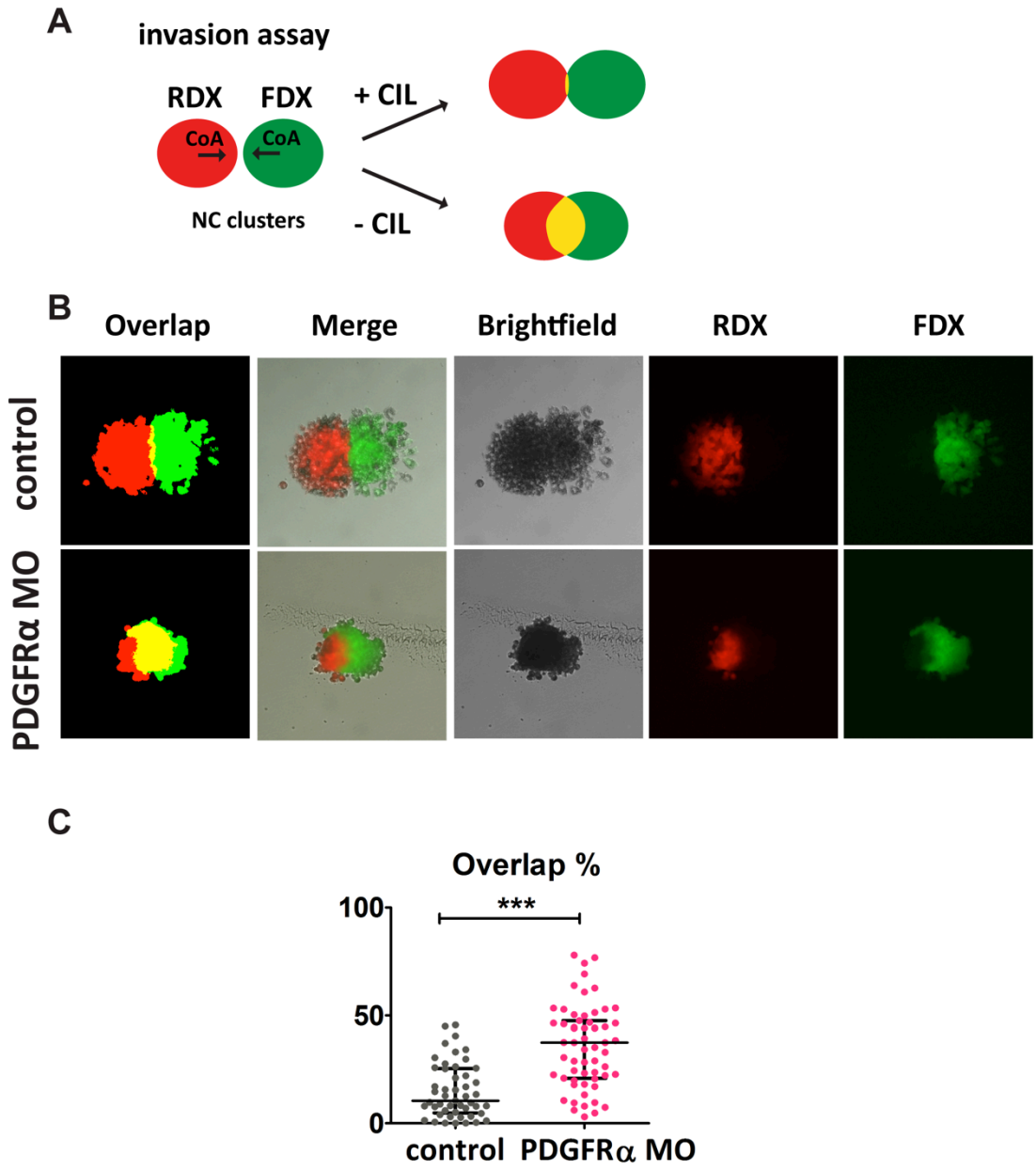

Figure 3-16 PDGFRα depleted neural crest cells are able to invade each other

(A) Schematic representation of invasion assay. RDX (rhodamine-dextran) and FDX (fluorescein-dextran) where used as tracers. CoA (co-attraction) attracts two neural crest cluster. There is little to none to very little overlap between two neural crest clusters with wild type CIL behaviour, if there is diminished CIL neural crest cell clusters overlap. **(B)** Thresholded, brightfield and fluorescent images of explant invasion assay, scale bar 100µm. **(C)** Overlap percentage between two neural crest cell explants of control-control explants n=52, PDGFRα-PDGFRα MO explants n=59, from three independent experiments. Scatter blot represents median with

interquartile range, statistical analysis used Mann-Whitney's test; control versus PDGFRα $^{***}P<0.0001$.

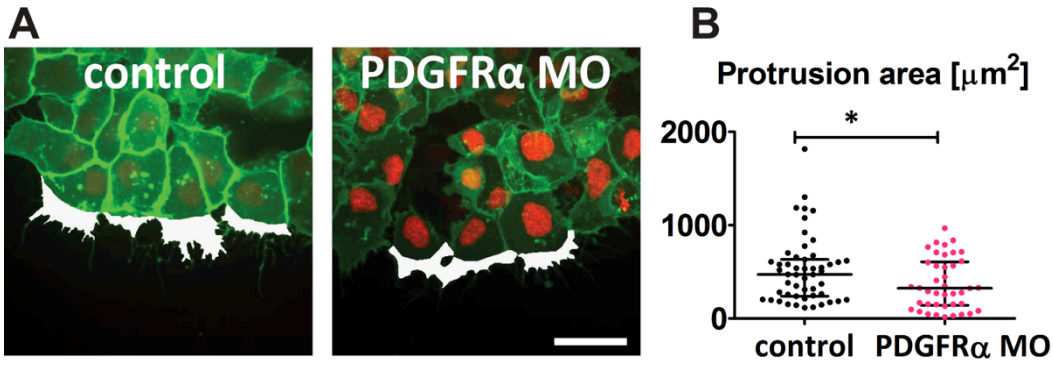

Figure 3-17 PDGFRα depletion affects protrusion formation

(A) Free edge protrusion area (defined as the regions devoid of vitelline platelets; labelled in white) confocal projections, scale bar 30 μM. **(B)** Protrusion area analysis (μm^2) of control n=51, PDGF-AA (50ng mL^{-1}) n=34, PDGFRα MO n=41 cells, scatter blot represents median with interquartile range, statistical analysis by unpaired t-test with Welch's corrections; control versus PDGFRα MO $^{*}P$=0.0281.

3.3 PI3K/AKT signalling downstream of PDGFRα during neural crest cell migration

3.3.1 PDGF-A/Rα controls neural crest cell migration via PI3K/AKT pathway

In the previous sections (3.1 and 3.2) I describe that PDGF-A/PDGFRα is required for neural crest cell migration *in vivo.* Further, I have shown that PDGFRα depletion leads to impairment of dispersion *in vitro* and that this inhibition could be due to reduction of N-cadherin dependent CIL.

Next I tried to elucidate the possible downstream signalling pathway/s, which could mediate this response. It is known that PDGF can activate several signalling pathways, such as PI3K, MAPK, PKC, JAK-STAT, and Src (Demoulin and Essaghir, 2014). Studies in mouse and zebrafish during craniofacial neural crest cell migration, showed PI3K signalling as the main downstream effector of PDGF signalling (Klinghoffer et al., 2001; Vasudevan et al., 2015). To test the contribution of PI3K as a downstream component of PDGFRα signalling I made use of the AKT pleckstrin homology (ph) domain biosensor ph-AKT-GFP (Montero et al., 2003). Activation of PI3K results in the addition of a phosphate molecule to phosphoinositides, generating phosphatidylinositol 3,4,5-trisphosphate (PIP3). The PH domain has a high and specific affinity for PIP3 and therefore ph-AKT-GFP translocates to the plasma membrane upon binding PIP3. Thus, a GFP intensity change from the cytosolic to membrane bound form is used as a read-out of PI3K pathway activation. The ph-AKT-sensor was exogenously expressed, by mRNA injection and PI3K/AKT activity was monitored the by high-time resolution microscopy in micro-dissected neural crest cells.

Strikingly, the treatment of PH-AKT-GFP expressing cells with PDGF-AA protein induced a clear increase in the membrane GFP intensity, compared to untreated neural crest cells (Figure 3-18 A-D; Movie 3). As a positive control I co-injected ph-AKT-GFP mRNA with a dominate active from of PI3K kinase (PI3K-p110-CAAX) mRNA, which resulted in a strong membrane GFP response without PDGF-AA protein addition (Figure 3-19 A, C). This suggests that PI3K/AKT signalling acts

downstream of the PDGF-A ligand. To verify that the observed response acts via the receptor PDGFRα, I treated ph-AKT-GFP and PDGFRα Morpholino injected cells with PDGF-AA protein, which led to no membrane localization (Figure 3-19 B, C).

To further examine the role of PI3K/AKT signalling I tested for endogenous pathway activation by western blot against phosphorylated AKT (pAKT). Treatment with PDGF-AA protein led to an increase in AKT phosphorylation in neural crest cells, whereas PDGFRα MO led to a slight, but not significant, decrease in pAKT levels (Figure 3-20 A, B). This, so far, suggests an involvement of PI3K/AKT signalling downstream of PDGF-A/PDGFRα signalling. But the question remains whether PI3K/AKT signalling is involved in PDGF-A/PDGFRα mediated neural crest cell migration?

To interfere with PI3K/AKT signalling *in vivo* and *in vitro* I used small pharmacological molecule inhibitors against PDGFR (AG1296), PI3K (LY294002) and AKT (MK2206) (Figure 3-21 A). As a control for the specificity in targeting the PI3K/AKT pathway, I also included treatment of the unrelated MAPK/ERK signalling pathway by use of the MEK inhibitor (UO126).

Treatment of PDGFR, PI3K and AKT inhibitors *in vivo* led to inhibition of neural crest cell migration (Figure 3-21 B, C) supporting our earlier findings. No significant effect of MAPK inhibition on neural crest cell migration was detected (Figure 3-21 B, C). This indicates a role for PI3K/AKT signalling in neural crest cell migration *in vivo* supporting our earlier findings with the ph-AKT-GFP inhibitor.

To investigate a possible effect on CIL I investigated the effect of PI3K/AKT pharmacological inhibition on neural crest cell explants dispersion, which is considered as an assay for CIL (Stramer and Mayor, 2016). PI3K (LY294002) and AKT (MK-2206) inhibitor treatment alone led to an inhibition of neural crest cell dispersion (Figure 3-22 Fig. 7 B, C and I: black bars). Surprisingly, also treatment with the MAPK inhibitor showed a reduction in neural crest cell dispersion despite showing no effect neural crest cell migration *in vivo* (Figure 3-22 D, I: black bars).

As some of these inhibitors could also affect other pathways present in the neural crest cells, different to the one activated by PDGF-AA, I continued to use the inhibitors after treating the neural crest cell clusters with PDGF-AA protein. As previously shown, treatment of neural crest cell with PDGF-AA leads to cell dispersion (Figure 3-9 A, B). However, this dispersion was dramatically impaired when PDGF-AA treated cells were co-incubated with PI3K and AKT inhibitors, but not with the MAPK inhibitor (Figure 3-22 F-H and I: grey bars). These results show that PDGF-AA promotes cell dispersion in a PI3K/AKT manner, but independent on MAPK, which is consistent with the effect of the inhibitors of these pathways on neural crest cell migration *in vivo*. To verify the efficacy of the inhibitors at the used concentration I performed Immunoblotting for pAKT on inhibitor treated embryos. This confirmed a decrease after PDGFR inhibitor treatment (Figure 3-23 A, D), similar to inhibitor treatment of PI3K and AKT (Figure 3-23 C, E and F).

Taken together, both the analysis of the ph-AKT-GFP biosensor and dissection of the downstream pathway with pharmacological inhibitors strongly suggest that PDGF-A/PDGFRα controls neural crest cell migration and dispersion via the PI3K/AKT signalling pathway.

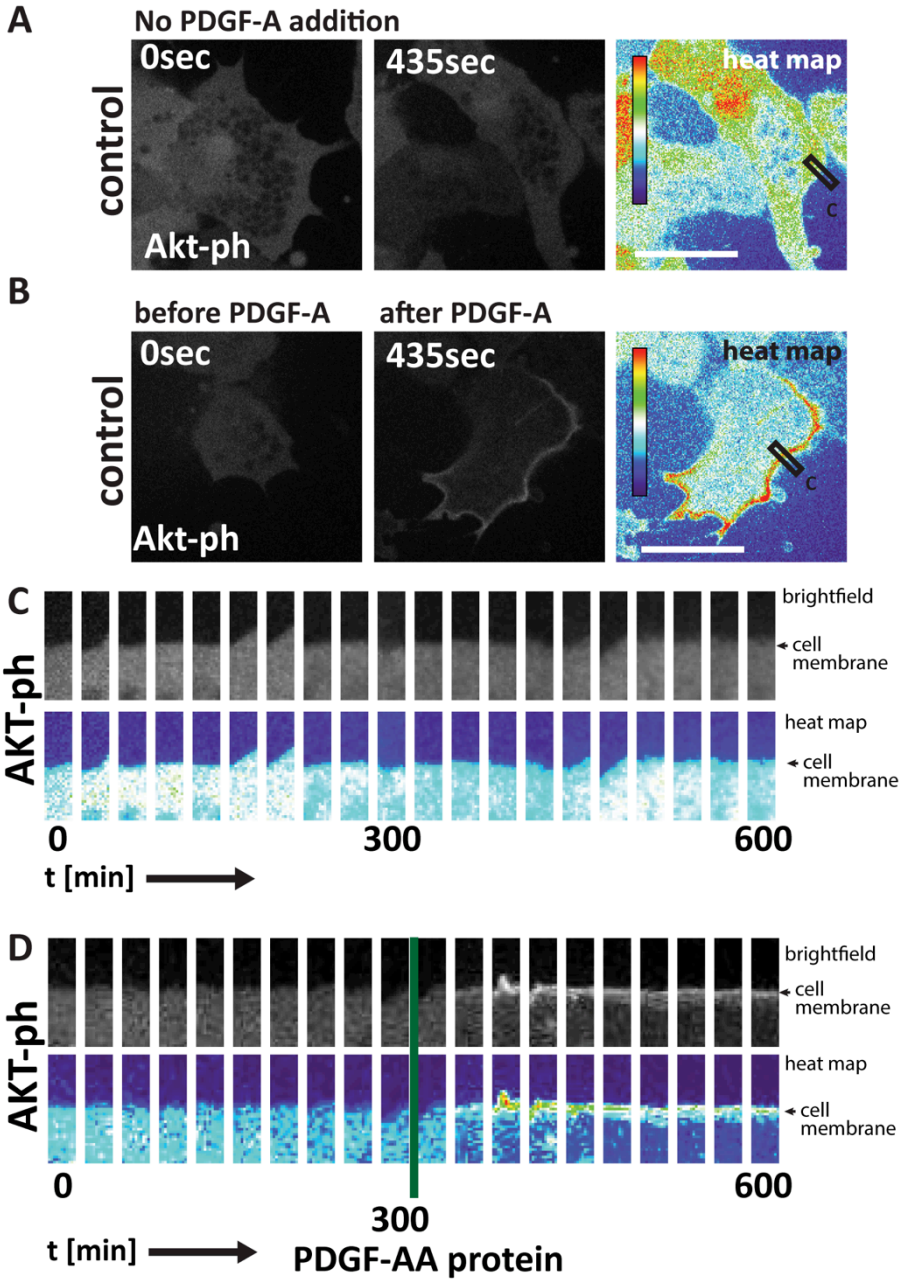
A
No PDGF-A addition
0sec
435sec
heat map
control
Akt-ph
C
B
before PDGF-A
after PDGF-A
0sec
435sec
heat map
control
Akt-ph
C
C
AKT-ph
brightfield
cell membrane
heat map
cell membrane
0
300
600
t [min]
D
AKT-ph
brightfield
cell membrane
heat map
cell membrane
0
600
300
t [min]
PDGF-AA protein

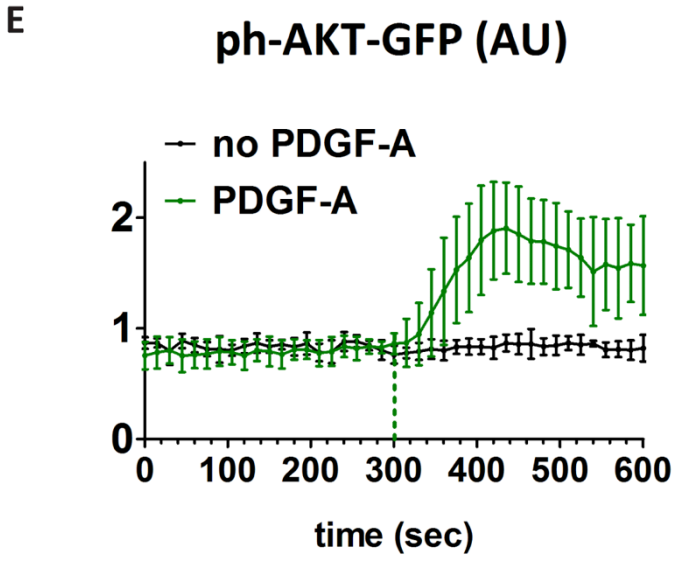
E
ph-AKT-GFP (AU)
no PDGF-A
PDGF-A
2
1
0
0
100
200
300
400
500
600
time (sec)

Figure 3-18 PDGF-AA addition leads to ph-AKT translocation to the plasma membrane

(A-C) Confocal projections of *Ph-AKT-GFP* mRNA injected neural crest cell images from t=0sec and t=425sec movies. Scale bar 20 µM. **(A,D)** Time course (10min) of stills at cell membrane, displaying membrane localization after PDGF-AA addition 50ng mL^{-1} and **(A,C)** No PDGF-AA protein addition control. **(B,D)** PDGF-AA protein 50ng mL^{-1} addition at 300sec after start. Heat map images depict pixel count, with red high pixel count and blue with low pixel count. **(E)** Analysis of ph-AKT-GFP pixel intensity at membrane normalized to cytoplasmic ph-AKT-GFP level over time (seconds). PDGF-AA protein addition control n=12, no PDGF-AA addition control n=7 cells, from three independent experiments, line graph represents mean and s.d., AU= arbitrary units.

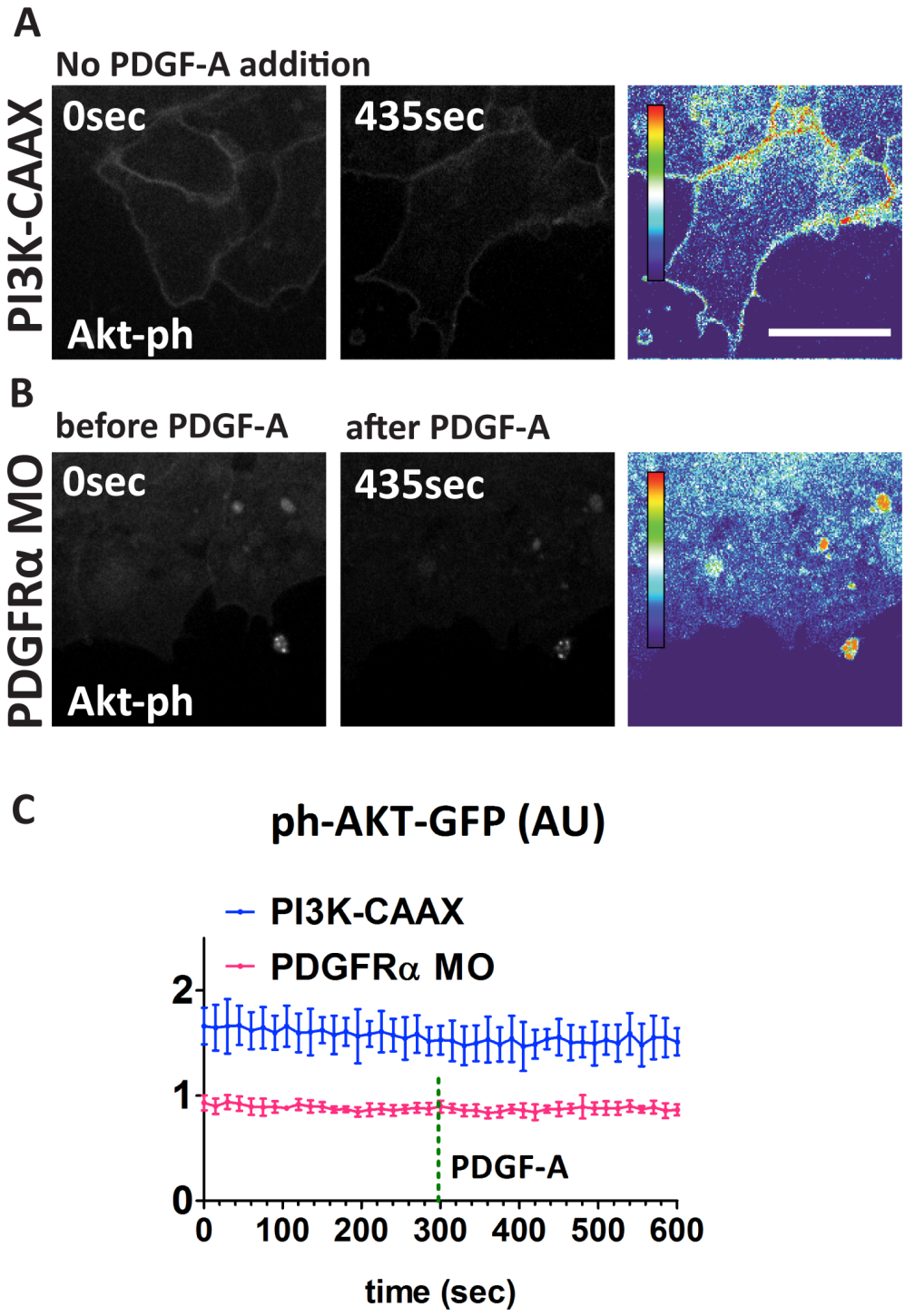

Figure 3-19 dominant active PI3K and PDGFRα inhibition and ph-AKT translocalisation

(A, B) Confocal projections of *Ph-AKT-GFP* mRNA injected neural crest cell images from t=0sec and t=425sec movies with PDGF-AA protein 50 ng mL^{-1} addition at 300sec after start. Scale bar 20 µM. **(A)** Additional PI3K-CAAX mRNA injected neural crest cells (lower panel). **(B)** Additional PDGFRα MO injected neural crest cells

treated. **(C)** Analysis of ph-AKT-GFP pixel intensity at membrane normalized to cytoplasmic ph-AKT-GFP level over time (seconds). PDGFRα MO n=11, PI3K-CAAX n=10 cells, from three independent experiments, line represents mean and error bars are s.d., AU= arbitrary units.

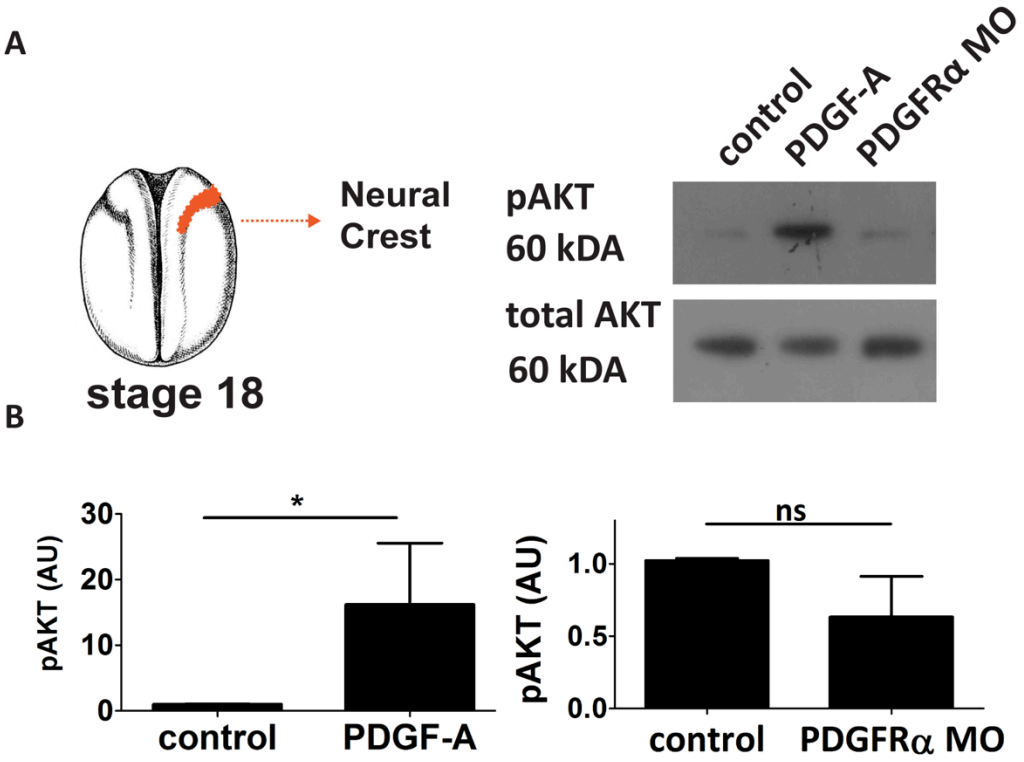

Figure 3-20 PDGFRα depletion decreased phosphorylated AKT in neural crest cells

(A) Western blot analysis of pAKT (Ser437) using neural crest cells explants lysates control, PDGF-AA protein (50 ng mL^{-1} for 60 min) or injected with PDGFRα MO. Dissection scheme adapted from Nieuwkoop et al., 1994. **(B)** Band intensity normalized to total AKT control, bar graph shows mean and s.d., statistical analysis by one-way ANOVA followed by Student Newman-Keuls test, from three independent experiments; control versus PDGF-A protein $^{*}P$=0.0318; control versus PDGFRα Mo ^{ns}P=0.9957.

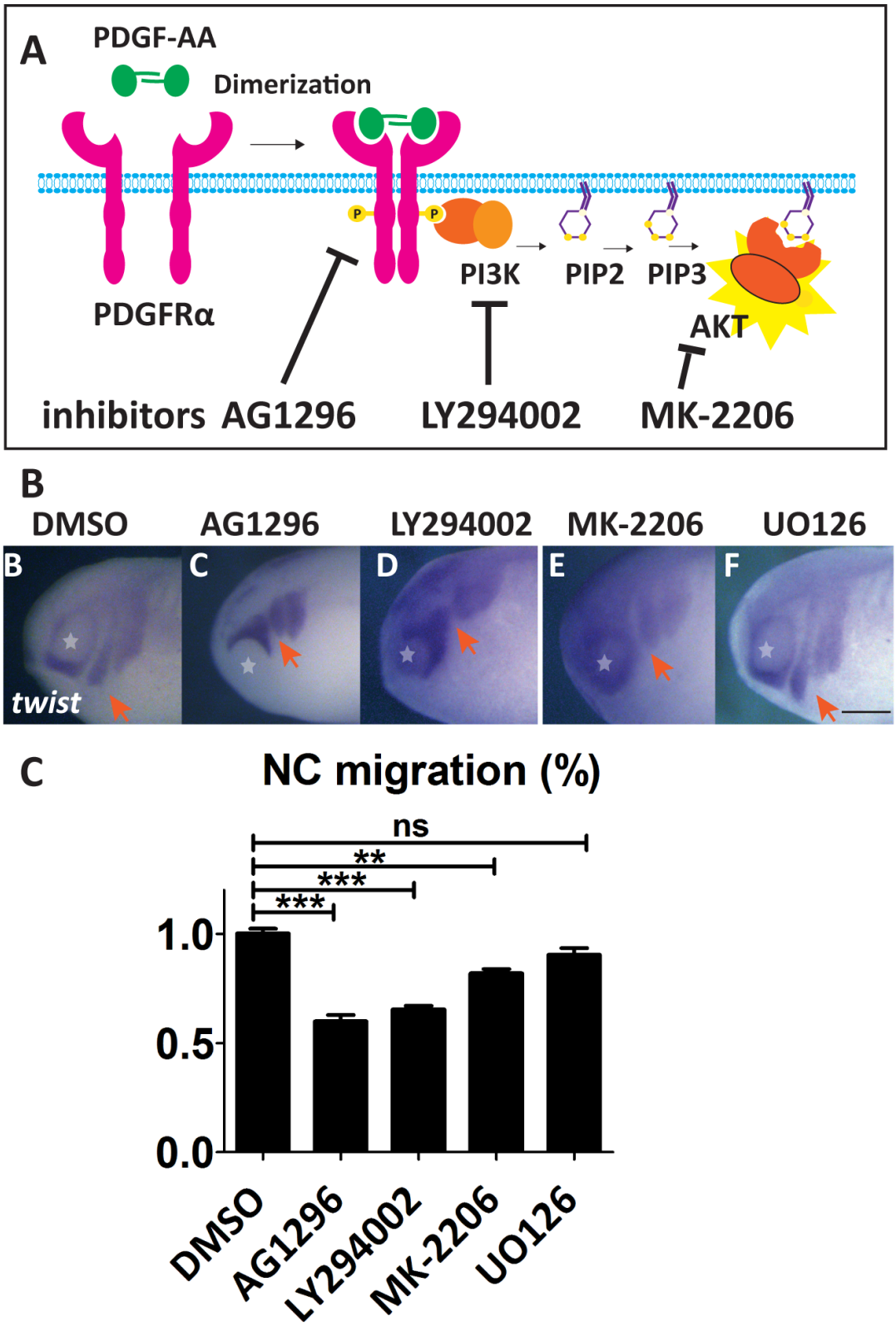

Figure 3-21 PI3K and AKT pharmacological inhibition impairs neural crest cell migration *in vivo*

(A) Scheme illustrating PDGF-PI3K-AKT signalling axis. Signalling is activated upon PDGF ligand/PDGF receptor binding, inducing receptor dimerization and subsequent autophosphorylation. PI3K gets activated, leading to the phosphorylation of phosphoinositol (PI) residues in the plasma membrane, converting PIP2 to PIP3. Downstream effector kinase AKT binds (with its pleckstrin homology (ph) domain) to PIP3 residues and gets activated. **(B)** *In situ* of inhibitor treated embryos stage 14 to stage 24. DMSO control, AG1296 (20 µM), LY294002 (40 µM), MK-2206 (100 µM), UO126 (100 µM), scale bar 100 µm. **(C)** neural crest cell migration normalised to control average of each experiment. DMSO control n=256, AG1296 n=101, LY294002 n=40, MK-2206 n=106, UO126 n=68 embryos, from three independent experiments. Scale bar 1 mm. Bar graph indicates mean and sem., statistical analysis by one-way ANOVA followed by Dunnett's post-test; DMSO control versus AG1296 $^{***}P<0.0001$; DMSO control versus LY294002 $^{***}P<0.0001$; DMSO control versus MK-2206 $^{**}P=0023$; DMSO control versus UO126 $^{ns}P=0.999$.

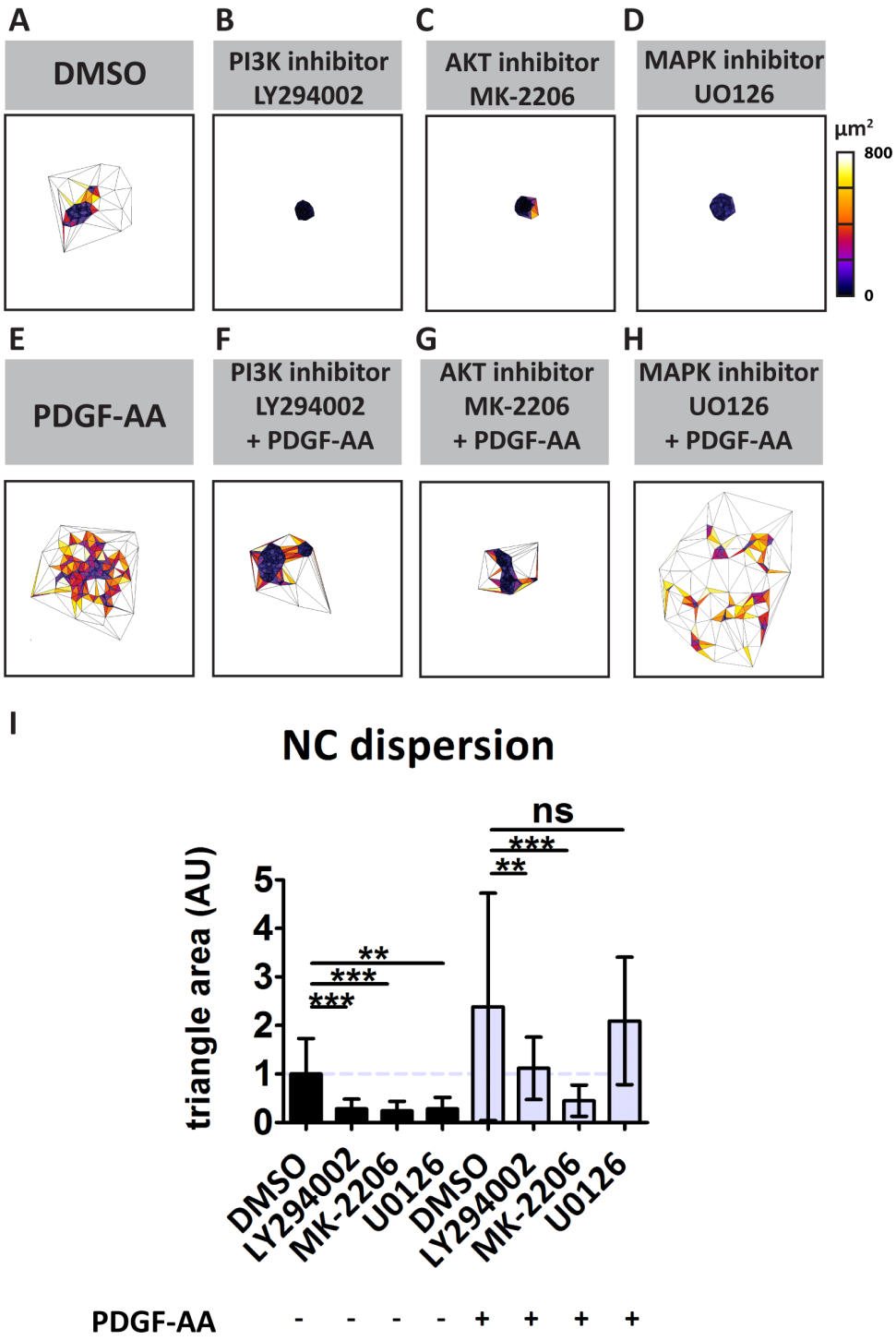

Figure 3-22 neural crest cell dispersion and small molecule inhibition of PI3K/AKT signalling

(A-H) Delaunay triangulation examples of small molecule inhibitor treated explants and their effect on PDGF-AA (50 ng mL^{-1}) induced dispersion, t=720 min. (I) Average triangulation area normalized to control of each experiment, control n=92, control and PDGF-AA protein n=55, LY294002 5 µM n=21, MK-2206 5 µM n=16, UO126 25 µM n=14, LY294002 5 µM and PDGF-AA n=25, MK-2206 5 µM and PDGF-AA protein n=35, UO126 25 µM and PDGF-AA n=19 explants, PDGF-AA concentration used for all conditions 50 ng mL^{-1}. Bar graphs indicate mean and s.d., statistical analysis by one-way ANOVA followed by Dunnett's post-test; DMSO control versus LY294002 $^{***}P$<0.0001; DMSO control versus MK-2206 $^{***}P$=0.0002; DMSO control versus UO126 $^{***}P$=0.0001; DMSO control versus LY294002 and PDGF-AA protein $^{**}P$=0.0015; DMSO control versus MK-2206 and PDGF-AA protein $^{***}P$<0.0001; DMSO control versus UO126 and PDGF-AA protein ^{ns}P<0.9999.

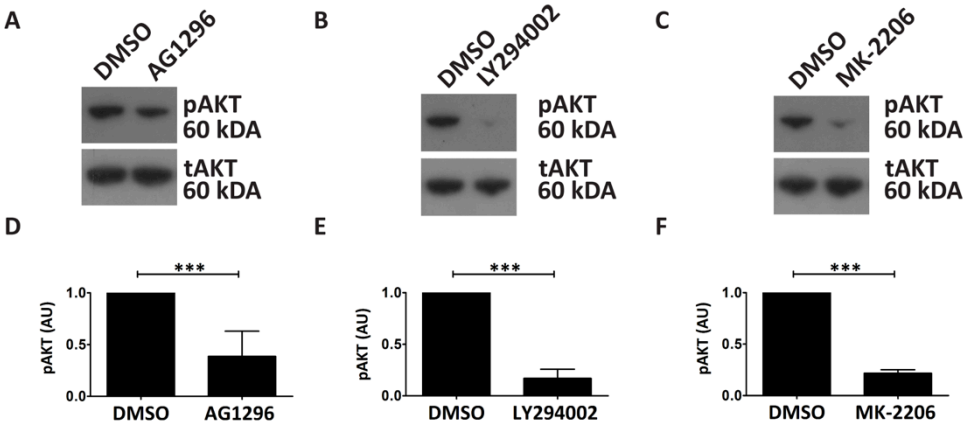

Figure 3-23 pharmacological inhibition leads to reduction of phosphorylated AKT by western blot

(A-C) Western blot against pAKT using lysates of whole embryos treated with small molecule inhibitors stage 14 to stage 24. (A) AG1296 (20 µM), (B) LY294002 (40 µM) and (C) MK-2206 (100 µM) showed decrease of AKT activation upon inhibitor treatment. (D-E) Band intensity of pAKT normalized to total AKT control, bar graph indicates mean and s.d. of three independent experiments, statistical analysis by one-way ANOVA followed by Student Newman-Keuls test; DMSO control versus AG1296 $^{***}P<0.0001$; DMSO control versus LY294002 $^{***}P<0.0001$; DMSO control versus MK-2206 $^{***}P<0.0001$. AU= arbitrary units.

3.3.2 N-cadherin dependent CIL is regulated via PI3K/AKT signalling downstream of PDGF-A/PDGFRα signalling

It is well established that a cell cluster undergoing CIL will disperse (Davis et al., 2015; Scarpa et al., 2015; Stramer and Mayor, 2016; Villar-Cerviño et al., 2013), conversely the depletion of CIL behaviour causes an inhibition of dispersion, as observed in PDGF-A/ PDGFRα MO explants (Figure 3-9, Movie 4). To assess whether this observed inhibition of dispersion is due to a lack of N-cadherin, I co-injected N-cadherin mRNA together with the PDGFRα MO. Strikingly, co-injection of PDGFRα MO/N-cadherin mRNA rescued the dispersion inhibition phenotype of PDGFRα Mo explants (Figure 3-24 A-E, Movie 4). This suggests that PDGF-A/PDGFRα signalling controls N-cadherin dependent CIL in neural crest cells.

Finally, I investigated whether the N-cadherin regulation, that I have shown is controlled by PDGF-A/PDGFRα (Figure 3-12 and Figure 3-13), is also PI3K/AKT dependent. For this embryos were treated with either a PDGF receptor inhibitor or a PI3K inhibitor from stage 14 to stage 24 and N-cadherin levels were analysed by western blot. Similar to the inhibition with the PDGFRa MO (Figure 3-12), pharmacological inhibition of the PDGF receptor by AG1296 led also to a decrease of N-cadherin protein levels. In line with our previous observation, inhibition of PI3K kinase signalling also decreased N-cadherin protein levels (Figure 3-25 A, B).

In conclusion, these results suggest that the tissue-intrinsic PDGF-A/PDGFRα-PI3K-AKT signalling pathway controls N-cadherin levels, which are essential for CIL and hence collective neural crest cell migration.

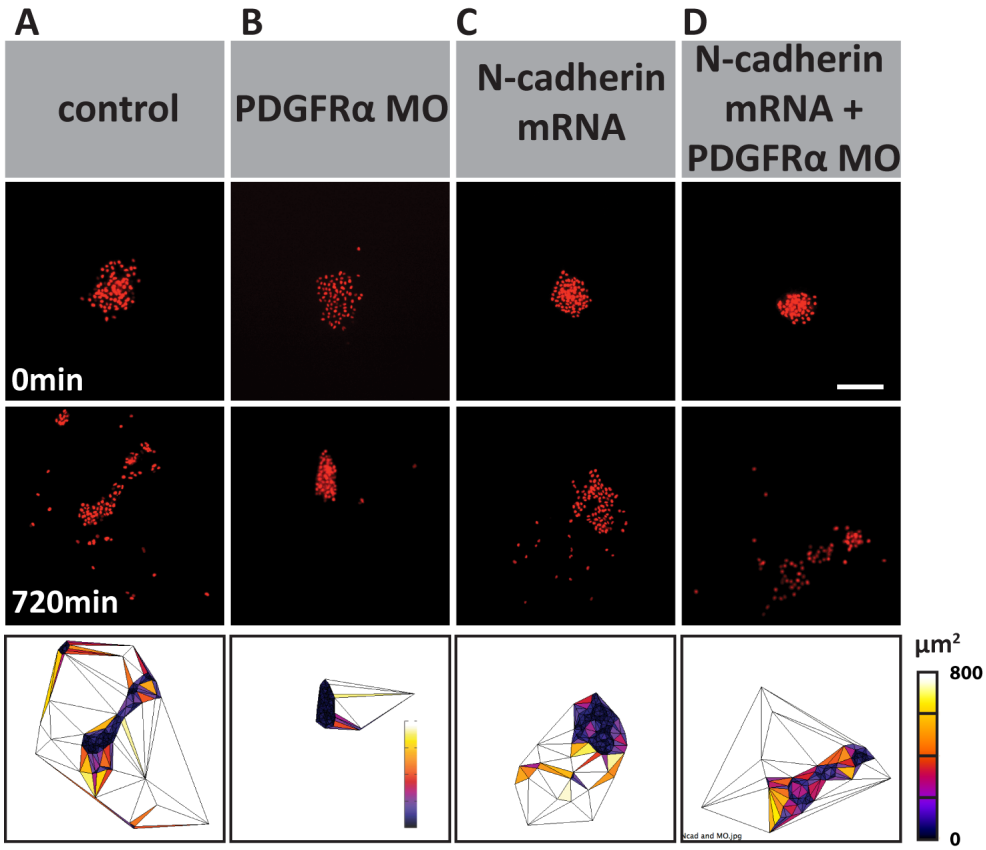

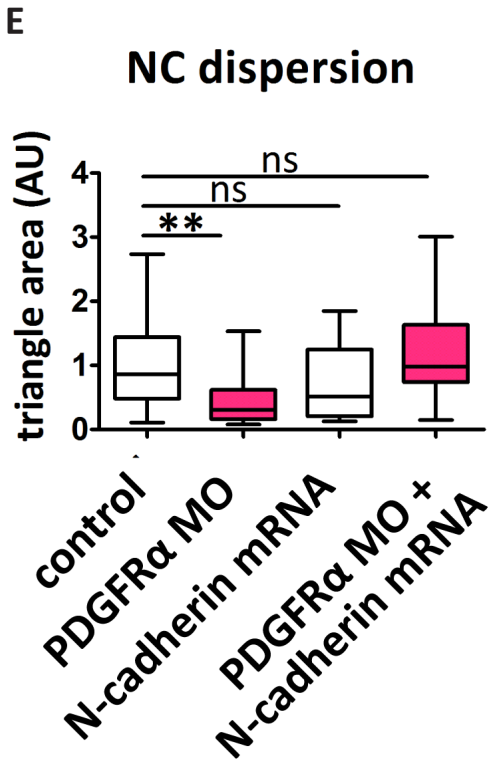

Figure 3-24 N-cadherin mRNA co-injection rescues PDGFRα dispersion inhibition

(A-D) N-cadherin mRNA and PDGFRα MO dispersion stills of *nuclear RFP* mRNA at t=0 min and t=720 min and Delaunay triangulation at t=720 min. (E) Average triangulation area at 720 min normalized to control average of each experiment, control n=41, PDGFRα MO n=19, *N-cadherin-GFP* mRNA n=23, *N-cadherin-GFP* mRNA and PDGFRα MO n=23 explants, scale bar 100 μm. Box and whisker: box and median are ± 25th/75thpercentile, whiskers are min. and max., statistical analysis by one-way ANOVA followed by Dunnett's post-test; control versus PDGFRa MO $^{**}P$=0.0041; control versus N-cadherin mRNA ^{ns}P=0.1603; control versus PDGFRa MO ^{ns}P=0.4041. AU= arbitrary units.

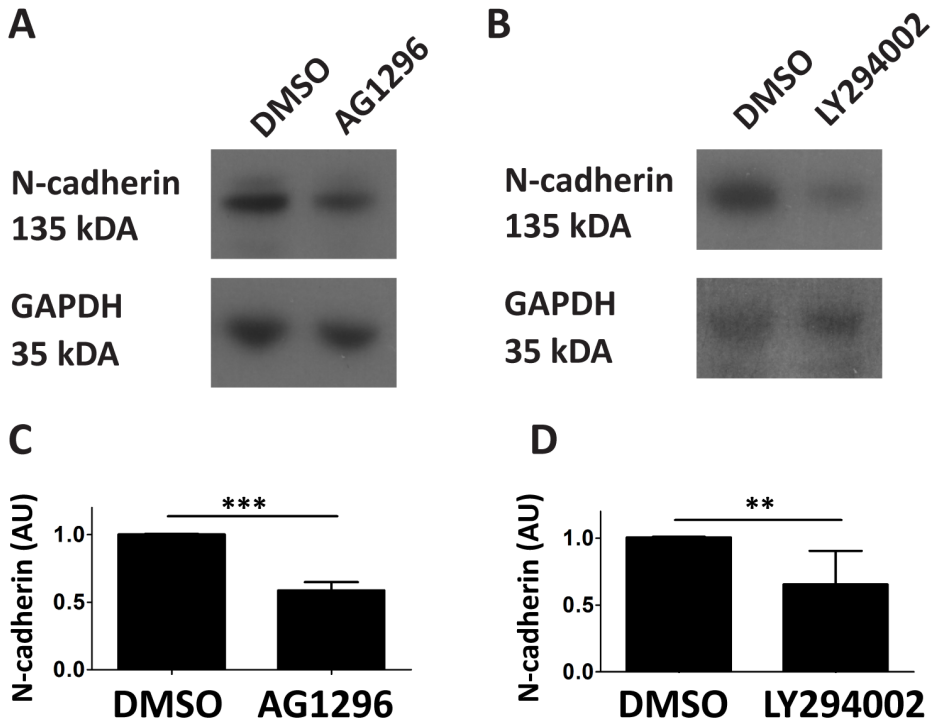

Figure 3-25 PI3K inhibition decreases N-cadherin protein level

(A,B) Western blot for N-cadherin using lysates of whole embryos treated with small molecule inhibitors AG1296 (20 µM) LY294002 (40 µM) showed decrease of N-cadherin level upon PDGFR (AG1296) and PI3K (LY294002) inhibitor treatment. (B) Band intensity of N-cadherin normalized to loading control, bar graph indicate mean and s.d. of at least three independent experiments, statistical analysis by one-way ANOVA followed by Student Newman-Keuls test; control DMSO versus AG1296 $^{**}P$=0.0093; control versus LY294002 $^{*}P$=0.002 ; AU= arbitrary units.

Chapter 4 Discussion

4.1 Model overview

In this thesis I investigate the role of PDGF signalling during collective cranial neural crest migration in *Xenopus lavis*. I show that PDGFRα and its ligand PDGF-A are expressed in pre-migratory and migrating cranial neural crest cells. Inhibition of either PDGF-A or PDGFRα impairs neural crest migration *in vivo* and dispersion of neural crest clusters *in vitro*. I find that this deficiency in migration and dispersion is caused by the impairment of N-cadherin dependent CIL. CIL is a fundamental property of collective neural crest cell migration which has been shown to be acquired in neural crest cells during EMT by a switch to N-cadherin (Scarpa et al., 2015). Moreover I find PI3K/AKT as a downstream effector of the PDGFRα cellular response.

This body of work supports the following novel model for PDGF signalling during cranial neural crest migration in *Xenopus laevis*. PDGFRα and its corresponding ligand are expressed on neural crest cells. This leads to the autocrine or at least tissue-autonomous regulation of CIL during neural crest EMT by PDGF signalling. This CIL response is controlled by PDGF signalling via regulation of N-cadherin levels in a PI3K/AKT signalling pathway dependent way. This proposed model shows PDGF signalling as a essential effector for the acquirement of CIL capability during *Xenopus laevis* neural crest EMT.

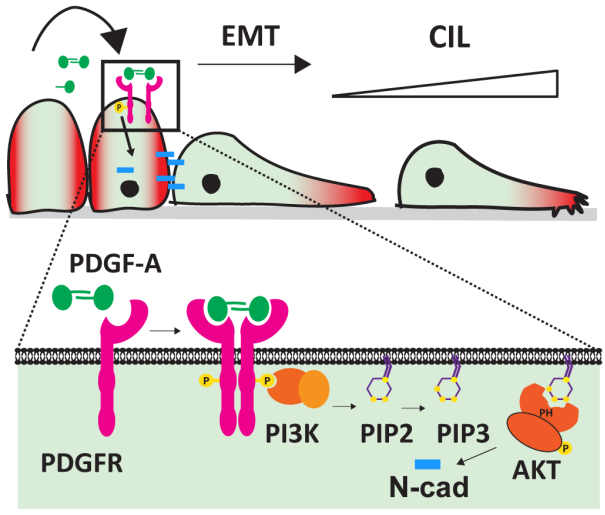

Figure 4-1 Model Overview

Schematic representation of PDGF signalling model in *Xenopus laevis* neural crest cell migration. Red indicates polarity change from a more epithelial static polarity to a front-rear polarity during EMT. Square shows zoom in.

4.2 PDGF-A/PDGFRα signalling is required for neural crest migration in *Xenopus laevis*

Many different signalling pathways have been reported to be required for neural crest migration. Here, I give the first report of the role PDGF during neural crest migration in *Xenopus laevis.* I show, that the PDGF-A ligand and PDGFRα receptor are both expressed in pre-migratory and migrating neural crest. Consistent with my data, expression of PDGFRα has been reported to be neural crest cell specific in mouse, zebrafish and *Xenopus*, previously (Ho et al., 1994; Liu et al., 2002b; Orr-Urtreger and Lonai, 1992). However, different to our finding that PDGF-A is expressed in Xenopus cranial neural crest cells, the expression PDGF-A in other animal models has so far been attributed only to the neural crest cell surrounding tissues in later cranial neural crest cell migratory stages and in trunk neural crest cells (Ho et al., 1994; Liu et al., 2002a; Orr-Urtreger and Lonai, 1992). In support, of PDGF-A being produced by the neural crest cells, I show that depletion of PDGF-A in the neural crest by a Morpholino inhibited neural crest cell dispersion *in vitro*, in a condition where the only possible source of PDGF are the neural crest cells themselves.

So far, analysis of PDGF-A expression in *Xenopus* has only been performed using low resolution radioactive *in situ* hybridization that can be easily confused with background signal (Ho et al., 1994). Here I employed higher resolution colorimetric *in situ*. Further I confirmed my results, concerning the co-expression of PDGFRα and PDGF-A by RT-PCR, a much more sensitive technique than *in situ* hybridization. My

data suggest revisiting the studies of PDGF-A expression during early cephalic neural crest cell migration in other model organisms. However, it is also possible that the PDGF-A/PDGFRα has a divergent role in cranial neural crest cell migration to other model organism than *Xenopus laevis*. Nevertheless, I show a novel way of tissue-autonomous PDGF-A/PDGFRα signalling during neural crest cell migration. Future experiments have to clarify whether the ligand works in an autocrine or paracrine manner on neural crest cells. However the expression in neural crest cells itself and the nature of the long-from PDGF-A isoform, with its ECM binding motif, suggests at least in part autocrine fashion of signalling activation. So far this is the first report of a autocrine or tissue-autonomous role of PDGF signalling, apart from malignant cancers (Heldin, 2012). Interestingly, autocrine PDGF/PDGFR loop has been implicated in EMT maintenance and the metastatic potential of mammary cancer cells (Jechlinger et al., 2006b). This autocrine PDGF/PDGFR loop is established as a consequence of TGF-β–induced metastasis which is well known to induce EMT in epithelial cells and invasiveness of metastasizing cancers (Jechlinger et al., 2006b; Thiery and Sleeman, 2006). Neural crest cell EMT and cancer metastasis have been reported to use similar signalling pathways and molecular machinery to reach their migratory capacity (Theveneau and Mayor, 2012). Consequently TGF-β signalling might be one of the responsible triggers to start the PDGF/PDGFR autocrine loop. However it is more likely that a set of different signalling pathways, for example WNT and BMP, are needed to start the PDGF/PDGFR autocrine or tissue-autonomous loop in neural crest cells.

Various interactions between different ligands (PDGF-AA, PDGF-AB, PDGF-BB, PDGF-CC, PDGF-DD) and receptors (PDGFRα/Rα, PDGFRβ/Rβ, PDGFRα/Rβ) have been described *in vitro*, but only the depletion PDGF-A and PDGF-C, upstream of PDGFRα signalling, have been shown to be functionally important during mouse embryonic development (Boström et al., 1996; Ding et al., 2004; Soriano, 1997). I cannot rule out a potential role of PDGF-C in Xenopus neural crest cell migration, nonetheless a PDGF-C ligand has so far not been described for *Xenopus laevis* development. Likewise PDGFRβ expression has yet to be determined during *Xenopus* laevis development. PDGFRα and PDGFRβ can form a heterodimer which

has been shown to be functionally active during neural crest cell migration in mouse embryos (Klinghoffer et al., 2002; Richarte et al., 2007). Future investigations have to look at the potential role of PDGFRβ and the PDGFRα/PDGFRβ heterodimer during neural crest cell migration in Xenopus CIL. Especially the expression of the PDGFRα/PDGFRβ heterodimer, its ligand binding capacity *in vivo* and whether the downstream signalling diverges in general or in a spatial or temporal way, from PDGFRα/PDGFRα homodimer would be an interesting field of study for the future.

Not only the receptor has been shown to form heterodimers, also the heterodimeric ligand PDGF-AB has been reported to activate both PDGFRα and PDGFRb receptor dimers *in vitro* (Heldin et al., 1979). Furthermore, future research has to investigate the potential role of heterodimeric PDGF ligands during neural crest migration in different model organisms *in vivo*. However the PDGF-B ligand is not expressed in neural crest tissue in *Xenopus laevis*, but only in some regions of the neighbouring neural plate (Giannetti et al., 2016). So the PDGF-AB heterodimer might not have a role in *Xenopus* neural crest migration *in vivo, but in the developing central nervous system*.

In line with my data, mouse and zebrafish PDGFRα knock-down studies have shown defects in cranial and cardiac neural crest cell derived tissues (Eberhart et al., 2008; Soriano, 1997; Tallquist et al., 2003). In this study I focused on the onset of neural crest cell migration, however it would be very informative to investigate the effect of PDGF-A and PDGFRα depletion on cranial neural crest cell derived tissues in *Xenopus*. In mouse, extensive studies have shown that conditional knock down of PDGFRα signalling using the Wnt1-Cre driver line (Tallquist et al., 2003) leads to a subset of the phenotypes observed in the PDGFRα mutant embryo (Grüneberg and Truslove, 1960; Robbins et al., 1999; Schatteman et al., 1992), including facial clefting, haemorrhaging in the midline, defects in the heart outflow tract and thymus malformations (Tallquist et al., 2003). The fact that only a subset of phenotypes was observed could have been caused by the Wnt1-Cre line which has been recently found to have ectopic activation of Wnt signalling (Lewis et al., 2013). Also the Wnt1 driver might not be perfect choice for a conditional knock down of

PDGFRα, as the expression of Wnt1 is not limited to the neural crest territories in the embryo and the onset of expression might be to late to affect early neural crest cell developmental defects (Barriga et al., 2015; McMahon et al., 1992).

I showed that loss-of-function of both PDGF-A and the receptor PDGFRα inhibits neural crest cell migration *in vivo* using Morpholinos against PDGF-A and PDGFRα, a dominant negative form of the PDGFRα and pharmacological inhibition of PDGFR phosphorylation, AG1296. During neural crest specification PDGFRα expression has been reported to be a downstream target of early neural crest cell progenitor transcription factors Pax3 and Zic1 (Bae et al., 2013). Neural crest cell specification was not affected using the Morpholinos and the dominant negative form of PDGFRα, excluding that the inhibition of neural crest cell migration is due to a defect in neural crest cell specification. The use of antisense Morpholinos has been recently highly debated due to its possibility off-target effects and the availability of the CRISPR/Cas9 system (Kok et al., 2015; Schulte-Merker and Stainier, 2014). To verify the use of Morpholinos in this study I performed rescue experiments. Thus, proving the specificity of both Morpholinos. Nevertheless, the CRISPR/CAS9 system has not been well established in *Xenopus laevis* yet, and its possible superiority to the Morpholino system needs to be carefully validated.

Analysis of PDGFRα signalling in zebrafish and mouse did show a wide variety of malformations in cranial and cardiac neural crest cell derivatives (Eberhart et al., 2008; Soriano, 1997; Tallquist et al., 2003). However, other studies suggested that only this subset of cranial and cardiac neural crest tissues is affected by PDGFRα depletion and that neural or pigment derivatives develop normally (Morrison-Graham et al., 1992; Schatteman et al., 1992; Wehrle-Haller et al., 1996). This might indicate that PDGFRα is only expressed or functions in a subset of mouse neural crest cells. The same might be true for Xenopus laevis neural crest cells and future studies have to examine the cranial neural crest cell derivatives affected by a depletion of PDGFRα signalling. Here, especially the use of an inducible knock-down system, as for example photo-convertible Morpholinos, would allow to distinguish between early developmental and neural crest migratory roles, as well as it would

ensure that the affected cranial neural crest derivatives are due to a migratory role of PDGF signalling and not an early adverse effect of development.

Further to the *in vivo* migration studies, I show that the cellular behaviour, at least *in vitro,* is controlled by the PDGFRα induced neural crest cell dispersion. Additional PDGFRα depletion showed that the signalling has no effect on single cell motility or chemotaxis towards SDF-1. Consistent with my observations, PDGFRα conditional knockdown using the Wnt1-Cre line in mice, have shown defects in neural crest explant outgrowth *in vitro* (He and Soriano, 2013). However, the same study also showed that PDGFRα controls chemotaxis towards PDGF-A of neural crest derivatives *in vitro* (He and Soriano, 2013). Further exogenous PDGF-A source has been shown to attract mouse cranial neural crest cells *in vivo* (Kawakami et al., 2011). Although, it has not yet been fully established if PDGFRα signalling can act as a chemotactic signal during mouse neural crest cell migration.

One of the criteria, which need to be fulfilled to categorise a chemical signal as chemotaxing agent, is that the target tissue needs to express and secrete the chemotaxing signal and the responding cell has to express an appropriate receptor. Consequently, with its tissue-autonomous expression PDGF-A/PDGFRα in neural crest cells, it is unlikely that PDGF-A works as a chemotaxing signal during cranial neural crest cell migration in *Xenopus*. However, it might be classified as a chemokinetic signal or PDGF-A signalling might have a dual function during neural crest migration. Future studies need to look into the possibility of PDGF signalling as a chemotaxing signal during cranial neural crest cell migration in *Xenopus laevis*.

4.3 PDGF-A/PDGFRα and N-cadherin dependent Contact inhibition of locomotion

Neural crest cells are known to undergo EMT-like dispersion *in vitro* (Kuriyama et al., 2014) due to a switch of cell-cell adhesion molecules, from E-cadherin to N-cadherin (Scarpa et al., 2015). In line with this data, I demonstrate that PDGFRα signalling controls neural crest cell-cell adhesion by regulating N-cadherin levels.

Importantly, we were able to partially rescue the inhibition of dispersion by overexpression of N-cadherin mRNA. This strongly suggests that PDGFRα signalling works upstream of N-cadherin levels. N-cadherin has been shown to be required for CIL and a cell adhesion complex formed by N-cadherin, p120, a-catenin, and b-catenin is transiently assembled upon cell-cell interactions in cranial neural crest cells (Kuriyama et al., 2014; Theveneau et al., 2010). Inhibition of N-cadherin leads to loss of contact dependent polarity (Theveneau et al., 2010). Thus neural crest cell dispersion *in vitro* and neural crest cell migration *in* vivo have been shown to be affected by a loss of N-cadherin (Theveneau et al., 2010). However the mechanism of N-cadherin dependent contact polarity and how PDGFRα signalling controls the level of N-cadherin still needs to be addressed in detail. For the latter, several possibilities are probable- PDGFRa could control N-cadherin levels directly or indirectly by regulation of its transcription, translation, posttranscriptional modification or by modifying its turnover.

More recently the acquisition of CIL behaviour has been linked to EMT and a switch to N-cadherin in Xenopus cranial neural crest cell migration (Scarpa et al., 2015). Scarpa et al. showed that pre-migratory neural crest cells predominantly express E-cadherin and no N-cadherin and that migrating neural crest cells that went through EMT, express E-cadherin and no N-cadherin. By comparing these pre-migratory and migratory neural crest cells, they showed that this switch from E- to N-cadherin during EMT is essential for acquisition of CIL behaviour (Scarpa et al., 2015). In context with these findings, I demonstrate that PDGFRα MO injected neural crest cells were not able to undergo efficient CIL, in single cell collision and explant invasion assays, supporting the hypothesis that PDGFRα is regulating CIL.

However the mechanism how PDGFRα signalling is regulating the N-cadherin dependent CIL remains to be investigated. One possibility could be via RAC1 pathway. N-cadherin expression in *Xenopus neural crest cells* promotes polarisation of RAC1 activity towards the leading edge during CIL and N-cadherin depleted cells display a reduction in protrusion size (Theveneau et al., 2010). As expected, due to their reduction in N-cadherin, PDGFRα MO injected neural crest cell explants

displayed a decrease in protrusion area, indicating a loss in polarity. Thus, PDGFRα signalling could be an important polarisation cue during neural crest cell migration. A recent study found that N-cadherin promotes activation of PDGF dependent PI3K and Rac localization at the free edge. This is thought to work via integrin inhibition at the side of cell-cell contact by N-cadherin bound p120, while integrin-PI3K-Rac activation is supported at the free edge (Ouyang et al., 2013). This result is in line with my observation, that loss of PDGF-A/PDGFRα signalling leads to a downregulation of N-cadherin in a PI3K dependent manner, and this eventually leads to a loss of cell polarity. The GTPase Rac and its regulation of cellular polarity has been shown to be essential for neural crest cell collective migration (Moore et al., 2013; Scarpa et al., 2015; Theveneau et al., 2010). Thus Rac might be downstream of the PDGFRα-PI3K-N-cadherin response. Future studies might in more detail look into the connection between Rac1 and PDGFRα signalling. Consistent with the presented data, PDGF signalling has been shown to control N-cadherin expression in the migration of mesoderm cells during chick gastrulation (Yang et al., 2008). However CIL has not been investigated in this study. Taken together my observations suggest that PDGFRα signalling controls EMT in a CIL dependent manner by regulation of N-cadherin levels.

As stated before, mouse studies reported that conditional PDGFRα KO in the neural crest, using Wnt1-Cre1 driver, showed palatogenesis defects, linked to delayed migration of neural crest in the frontal-nasal prominence (He and Soriano, 2013; Tallquist et al., 2003). This delayed migration in mouse could be consistent with the observed phenotype of CIL reduction in PDGFRα depleted neural crest cells. Isolation of PDGFRα KO mouse neural crest cells and *in vitro* analysis of their migratory behaviour could help to elucidate if the same CIL behaviour as in *Xenopus laevis* can be observed.

Interestingly, neural crest cell EMT and migration do have very similar characteristic with malignant cancer invasion (Theveneau and Mayor, 2012). In line with this, PDGF signalling has been implicated in EMT during cancer invasion (Eckert et al., 2011; Jechlinger et al., 2006a; Thiery and Sleeman, 2006). Hyper-activation of the

PDGF signalling pathway have been shown to increase invasive properties of cancer cells and kinase inhibitors have been approved for clinical use (Heldin, 2012; Wu et al., 2013). For example, PDGFRα and PDGFRb expression has been shown to be specifically upregulated in human late stage mammary tumours (Jechlinger et al., 2006a). And autocrine PDGF/PDGFR signalling has been linked to increased EMT and invasive potential of mouse oncogenic mammary cells (Jechlinger et al., 2006a).

Interestingly, Abercrombie already hypothesised in 1962, that homotypic CIL response between cancer cells would increase invasive behaviour. So far this interaction has not been studied in detail. However it is intriguing to hypothesise that an increase in CIL response, maybe through the activation of a PDGF-A/PDGFRα autocrine loop, could play a role during metastatic cancer invasion. Thus the presented data might be useful to develop future studies into PDGF signalling related malignancies.

4.4 PDGF-A/PDGFRα and PI3K/AKT signalling

Using a biosensor and pharmacological inhibition, I was able to link the PDGFRα signalling to the PI3K/AKT downstream pathway. PI3K signalling downstream of PDGFRα appears to be a conserved mechanism in development. In mouse depletion of the PI3K binding domain in PDGFRα has been shown to mimic phenotypes in craniofacial development of the complete knock-down (Klinghoffer et al., 2002). Also the increase of PI3K signalling in zebrafish is able to rescues craniofacial development in a PDGFRα knock down background (McCarthy et al., 2016). Albeit these studies focus on the late, frontonasal migration of cranial neural crest cells, the PI3K/AKT signalling appears to be conserved for neural crest development. Nonetheless, it is noteworthy that crosstalk between the PI3K/AKT and FGF signalling pathway have been reported to converge on ERK signalling in neural crest cell derivatives (Vasudevan et al., 2015). However, I did not observe any effect on neural crest migration *in vivo* by pharmacological inhibition of the ERK/MAPK signalling pathway in *Xenopus* embryos. Additional to the PI3K/ATK signalling pathway, I cannot exclude that the PDGFRα signalling response might work through

another downstream signalling effector such as JNK, PKC and Rac signalling pathways.

Spatial PI3K activation in the leading edge of chemotaxing cells has been shown to be a crucial intracellular guidance cue in cell culture assays and *Dictyostelium* (Cain and Ridley, 2009; Merlot and Firtel, 2003; Yamaguchi et al., 2015). Contrary to this, I did not detect high levels of ph-AKT-GFP localisation without PDGF-A protein addition at the free edge. This is most likely due to low levels of PDGF-A protein and a more sensitive sensor might reveal intracellular spatial differences in PI3K localisation.

I was able to control the CIL dependent dispersion process in neural crest cells by modulating PDGF-A/PDGFRα signalling. Depletion of PDGF-A/PDGFRα signalling inhibited dispersion. Most importantly the inhibition of dispersion by PDGFRα depletion could be rescued by co-injection with N-cadherin. This proves N-cadherin as a downstream target of the PDGFRα cellular response. Further analysis by immunoblotting showed that pharmacological inhibition of the PDGFR/PI3K/AKT axis indeed leads to a downregulation of N-cadherin. This demonstrates N-Cadherin as a regulator of CIL controlled by PI3K/AKT signalling. A remaining question for further studies will be the link between AKT and N-cadherin regulation. However, in a recent study the protein p53, which is know for its tumorigenic role, was reported as a downstream effector of AKT activation through PDGFRα signalling in craniofacial neural crest development in mouse (Fantauzzo and Soriano, 2014). Interestingly p53 has also has been linked to EMT and the regulation of cadherin expressions (Chang et al., 2011).

4.5 PDGF-A/PDGFRα signalling in the context of other modes of NC migration

Here I show that the regulation of N-cadherin during neural crest migration is PDGF-A/PDGFRα dependent and that loss of N-cadherin by depletion of PDGFRα signalling leads to an inhibition of neural crest migration. My data suggests that inhibition of neural crest migration by PDGFRα depletion is due to a N-cadherin dependent

impairment of CIL. As described in chapter 1.1.3 Neural crest migration collective migration of the neural crest cell stream is controlled by several different mechanisms, namely restriction into different streams, cell-substrate interactions, chemotaxis, CoA and CIL. But how does PDGF signalling fit with the other modes of neural crest cell migration? In this chapter I will discuss PDGF signalling in the context of other modes of NC migration and its possible implications into future research.

Permissive spaces have been thought to support the splitting of the neural crest cell population into their defined streams. In *Xenopus laevis*, especially fibronectin has been shown to have a permissive role during neural crest migration (Perris and Perissinotto, 2000). Interestingly, PDGF-AA binds directly to fibronectin and heparan sulphate proteoglycans (HSPGs) and which are required PDGF-AA-guided mesendoderm movement in *Xenopus* embryos (Smith et al., 2009). Thus PDGF-AA together with fibronectin could play a dual role- in which fibronectin is the permissive agent allowing neural crest cell migration and PDGF-AA bound to fibronectin exercises CIL in order to polarise and channel the stream towards its target, preventing the cells to invade the neighbouring tissue. Thus PDGF-AA would work as one of the reported non-permissive ligands (Eph and semaphorin) expressed in the neural crest surrounding tissue, which restrict ectopic neural crest cell migration.

As discussed in chapter 4.2 PDGF-A/PDGFRα signalling is required for neural crest migration in *Xenopus laevis*. PDGFRα has been reported to controls chemotaxis towards PDGF-A of mouse neural crest derivatives *in vitro* (He and Soriano, 2013) and exogenous PDGF-A source has been shown to attract mouse cranial neural crest cells *in vivo* (Kawakami et al., 2011). However, it has not yet been fully established if PDGFRα signalling can act as a chemotactic signal during mouse neural crest cell migration. In the case of *Xenopus laevis* PDGF-AA has not been reported to be a chemotactic signal during neural crest cell migration. My data suggest that this is not the case during onset of neural crest cell migration, as the ligand it self is expressed by neural crest cells. This however does not exclude the

possibility of PDGF signalling working as a chemotaxing signal during later stages of neural crest cell migration, which would give PDGF-A signalling a dual role during neural crest migration. To investigate this chemotaxis assays towards a PDGF-AA source could with pre-migratory (stage 14) and migratory (stage 19) neural crest cells could be performed.

Cell substrate adhesion, chemotaxis and CoA modes provide ways that support neural crest cell migration. However they need CIL mode to convene appropriate polarity to the migrating neural crest cells. CIL seems to play a dual role in neural crest cell migration. CIL between neural crest cells is thought to promote their collective directional migration by inhibition of protrusions at the cell-cell contact in the cluster and promoting the formation of protrusions forming at the free, leading edge (Mayor and Carmona-Fontaine, 2010). In Xenopus neural crest cell protrusive activity so far has been shown to be repressed by inhibition of small GTPase RAC1 in a N-cadherin and WNT-PCP signalling dependent way (Carmona-Fontaine et al., 2008b; Moore et al., 2013; Theveneau et al., 2010). Here, I show that the N-cadherin required for CIL levels might regulate by PDGFRα signalling. Thus suggesting that PDGF signalling directly regulates inhibition of RAC1 at the cell-cell contact thus leading to polarization of the neural crest cell stream. Additionally it is likely that the WNT/PCP and PDGF signalling converge at least in the regulation of RAC1.

4.6 Concluding Remarks

In conclusion, the results presented in this thesis show that PDGFRα signalling is required for neural crest cell migration. Both the ligand and the receptor are expressed by neural crest cells, where they act in an autocrine loop to control N-cadherin dependent CIL during the early stages of neural crest cell migration. While this work has resolved many questions regarding the nature of PDGF signalling in *Xenopus laevis* neural crest, many questions continue to be unanswered such as the exact mechanism N-cadherin regulation via the PDGF-A/PDGFRα-PI3K-AKT axis, how N-cadherin itself is regulating subcellular polarisation and thus polarisation of the

collective neural crest and whether PDGF signalling is involved in other modes of neural crest cell migration as chemotaxis or co-attraction during later stages. PDGF signalling occurs in many different developmental and adult cellular processes. The novel mechanism proposed in this thesis, by which PDGF signalling controls CIL, presents a new and exiting role of the signalling pathway, not only due to the nature of the dual expression of the ligand and receptor in the target tissue, but also to the PDGF pathways and CILs role in development and cancer metastasis

References

Abercrombie, M. (1967). Contact inhibition: the phenomenon and its biological implications. *Natl. Cancer Inst. Monogr.* **26**, 249–277.

Abercrombie, M. (1970). Control mechanisms in cancer. *Eur. J. Cancer* **6**, 7–13.

Abercrombie, M. (1978). Contact inhibition and malignancy. *Nature* **281**, 259–262.

Abercrombie, M. and Ambrose, E. (1958). Interference microscope studies of cell contacts in tissue culture. *Exp. Cell Res.* **15**, 332–345.

Abercrombie, M. and Dunn, G. A. (1975). Adhesions of fibroblasts to substratum during contact inhibition observed by interference reflection microscopy. *Exp. Cell Res.* **92**, 57–62.

Abercrombie, M. and Heaysman, J. E. M. (1954). Invasiveness of Sarcoma Cells. *Nature* **174**, 697–698.

Adams, R. H., Diella, F., Hennig, S., Helmbacher, F., Deutsch, U. and Klein, R. (2001). The cytoplasmic domain of the ligand EphrinB2 is required for vascular morphogenesis but not cranial neural crest migration. *Cell* **104**, 57–69.

Ahlstrom, J. D. and Erickson, C. a (2009). The neural crest epithelial-mesenchymal transition in 4D: a “tail” of multiple non-obligatory cellular mechanisms. *Development* **136**, 1801–12.

Alexopoulou, A. N., Multhaupt, H. A. B. and Couchman, J. R. (2007). Syndecans in wound healing, inflammation and vascular biology. *Int. J. Biochem. Cell Biol.* **39**, 505–528.

Alfandari, D., Cousin, H., Gaultier, A., Hoffstrom, B. G. and DeSimone, D. W. (2003). Integrin α5β1 supports the migration of Xenopus cranial neural crest

on fibronectin. *Dev. Biol.* **260**, 449–464.

Alfandari, D., Cousin, H. and Marsden, M. (2010). Mechanism of Xenopus cranial neural crest cell migration. *Cell Adh. Migr.* **4**, 553–560.

Amano, H., Ikeda, W., Kawano, S., Kajita, M., Tamaru, Y., Inoue, N., Minami, Y., Yamada, A. and Takai, Y. (2008). Interaction and localization of Necl-5 and PDGF receptor ?? at the leading edges of moving NIH3T3 cells: Implications for directional cell movement. *Genes to Cells* **13**, 269–284.

Andrae, J., Gallini, R. and Betsholtz, C. (2008a). Role of platelet-derived growth factors in physiology and medicine. 1276–1312.

Andrae, J., Gallini, R. and Betsholtz, C. (2008b). Role of platelet-derived growth factors in physiology and medicine. *Genes Dev.* **22**, 1276–312.

Anear, E. and Parish, R. W. (2012). The effects of modifying RhoA and Rac1 activities on heterotypic contact inhibition of locomotion. *FEBS Lett.* **586**, 1330–1335.

Astin, J. W., Batson, J., Kadir, S., Charlet, J., Persad, R. A., Gillatt, D., Oxley, J. D. and Nobes, C. D. (2010). Competition amongst Eph receptors regulates contact inhibition of locomotion and invasiveness in prostate cancer cells. *Nat Cell Biol* **12**, 1194–1204.

Ataliotis, P., Symes, K., Chou, M. M., Ho, L. and Mercola, M. (1995). PDGF signalling is required for gastrulation of Xenopus laevis. *Development* **121**, 3099–110.

Bae, C.-J., Park, B.-Y., Lee, Y.-H., Tobias, J. W., Hong, C.-S. and Saint-Jeannet, J.-P. (2013). Identification of Pax3 and Zic1 targets in the developing neural crest. *Dev. Biol.* 1–11.

Ball, S. G., Shuttleworth, C. A. and Kielty, C. M. (2007). Vascular endothelial growth factor can signal through platelet-derived growth factor receptors. *J. Cell Biol.* **177**, 489–500.

Barembaum, M. and Bronner-fraser, M. (2005). Early steps in neural crest specification. **16**, 642–646.

Barriga, E. H. and Mayor, R. (2015). *Embryonic cell-cell adhesion: A key player in collective neural crest migration*. 1st ed. Elsevier Inc.

Barriga, E. H., Maxwell, P. H., Reyes, A. E. and Mayor, R. (2013). The hypoxia factor Hif-1α controls neural crest chemotaxis and epithelial to mesenchymal transition. *J. Cell Biol.* **201**, 759–76.

Barriga, E. H., Trainor, P. a, Bronner, M. and Mayor, R. (2015). Animal models for studying neural crest development: is the mouse different? *Development* **142**, 1555–60.

Batson, J., Astin, J. W. and Nobes, C. D. (2013). Regulation of contact inhibition of locomotion by Eph-ephrin signalling. *J. Microsc.* **251**, 232–241.

Batson, J., Maccarthy-Morrogh, L., Archer, A., Tanton, H. and Nobes, C. D. (2014). EphA receptors regulate prostate cancer cell dissemination through Vav2-RhoA mediated cell-cell repulsion. *Biol. Open* **3**, 453–62.

Bazenet, C. E. and Kazlauskas, A. (1994). The PDGF receptor alpha subunit activates p21ras and triggers DNA synthesis without interacting with rasGAP. *Oncogene* **9**, 517–525.

Becker, S. F. S., Mayor, R. and Kashef, J. (2013). Cadherin-11 mediates contact inhibition of locomotion during Xenopus neural crest cell migration. *PLoS One* **8**, 1–9.

Belmadani, A. (2005). The Chemokine Stromal Cell-Derived Factor-1 Regulates the Migration of Sensory Neuron Progenitors. *J. Neurosci.* **25**, 3995–4003.

Bergsten, E., Uutela, M., Li, X., Pietras, K., Ostman, A., Heldin, C.-H., Alitalo, K. and Eriksson, U. (2001). PDGF-D is a specific, protease-activated ligand for the PDGF [beta]-receptor. *Nat Cell Biol* **3**, 512–516.

Berndt, J. D., Clay, M. R., Langenberg, T. and Halloran, M. C. (2008). Rho-kinase and myosin II affect dynamic neural crest cell behaviors during epithelial to mesenchymal transition in vivo. *Dev. Biol.* **324**, 236–44.

Bershadsky, A. D., Vaisberg, E. A. and Vasiliev, J. M. (1991). Pseudopodial activity at the active edge of migrating fibroblast is decreased after drug-induced microtubule depolymerization. *Cell Motil. Cytoskeleton* **19**, 152–158.

Borges, E., Jan, Y. and Ruoslahti, E. (2000). Platelet-derived growth factor receptor beta and vascular endothelial growth factor receptor 2 bind to the beta 3 integrin through its extracellular domain. *J. Biol. Chem.* **275**, 39867–39873.

Bos, J., Rehmann, H. and Wittinghofer, A. (2007). GEFs and GAPs : Critical Elements in the Control of Small G Proteins. *Cell* 865–877.

Boström, H., Willetts, K., Pekny, M., Levéen, P., Lindahl, P., Hedstrand, H., Pekna, M., Hellström, M., Gebre-Medhin, S., Schalling, M., et al. (1996). PDGF-A signaling is a critical event in lung alveolar myofibroblast development and alveogenesis. *Cell* **85**, 863–873.

Boucaut, J. C., Darribere, T., Poole, T. J., Aoyama, H., Yamada, K. M. and Thiery, J. P. (1984). Biologically active synthetic peptides as probes of embryonic development: A competitive peptide inhibitor of fibronectin function inhibits gastrulation in amphibian embryos and neural cell migration in avian embryos. *J. Cell Biol.* **99**, 1822–1830.

Brachmann, S. M., Yballe, C. M., Innocenti, M., Deane, J. A., Fruman, D. A., Thomas, S. M. and Cantley, L. C. (2005). Role of Phosphoinositide 3-Kinase Regulatory Isoforms in Development and Actin Rearrangement. *Mol. Cell. Biol.* **25**, 2593–2606.

Bracke, M. E., Depypere, H., Labit, C., Van Marck, V., Vennekens, K., Vermeulen, S. J., Maelfait, I., Philippe, J., Serreyn, R. and Mareel, M. M. (1997). Functional downregulation of the E-cadherin/catenin complex leads to loss of contact inhibition of motility and of mitochondrial activity, but not of growth in confluent epithelial cell cultures. *Eur. J. Cell Biol.* **74**, 342–349.

Bronner, M. E. and LeDouarin, N. M. (2012). Development and evolution of the neural crest: an overview. *Dev. Biol.* **366**, 2–9.

Bronner-Fraser, M. (1986). An antibody to a receptor for fibronectin and laminin perturbs cranial neural crest development in vivo. *Dev. Biol.* **117**, 528–536.

Bronner-Fraser, M., Wolf, J. J. and Murray, B. A. (1992). Effects of antibodies against N-cadherin and N-CAM on the cranial neural crest and neural tube. *Dev. Biol.* **153**, 291–301.

Brunet, A., Bonni, A., Zigmond, M. J., Lin, M. Z., Juo, P., Hu, L. S., Anderson, M. J., Arden, K. C., Blenis, J. and Greenberg, M. E. (1999). Akt Promotes Cell Survival by Phosphorylating and Inhibiting a Forkhead Transcription Factor. *Cell* **96**, 857–868.

Buchanan, F. G., Elliot, C. M., Gibbs, M. and Exton, J. H. (2000). Translocation of the Rac1 guanine nucleotide exchange factor Tiam1 induced by platelet-derived growth factor and lysophosphatidic acid. *J. Biol. Chem.* **275**, 9742–9748.

Burstyn-Cohen, T., Stanleigh, J., Sela-Donenfeld, D. and Kalcheim, C. (2004). Canonical Wnt activity regulates trunk neural crest delamination linking

BMP/noggin signaling with G1/S transition. *Development* **131**, 5327–39.

Bustos, R. I., Forget, M. A., Settleman, J. E. and Hansen, S. H. (2008). Coordination of Rho and Rac GTPase Function via p190B RhoGAP. *Curr. Biol.* **18**, 1606–1611.

Cai, D. and Montell, D. J. (2012). Diverse and dynamic sources and sinks in gradient formation and directed migration. **100**, 130–134.

Cain, R. J. and Ridley, A. J. (2009). Phosphoinositide 3-kinases in cell migration. *Biol. Cell* **101**, 13–29.

Cantemir, V., Cai, D. H., Reedy, M. V. and Brauer, P. R. (2004). Tissue Inhibitor of Metalloproteinase-2 (TIMP-2) expression during cardiac neural crest cell migration and its role in ProMMP-2 activation. *Dev. Dyn.* **231**, 709–719.

Carl, T. F., Dufton, C., Hanken, J. and Klymkowsky, M. W. (1999). Inhibition of neural crest migration in Xenopus using antisense slug RNA. *Dev. Biol.* **213**, 101–115.

Carmona-Fontaine, C., Matthews, H. and Mayor, R. (2008a). Directional cell migration in vivo: Wnt at the crest. *Cell Adh. Migr.* **2**, 240–242.

Carmona-Fontaine, C., Matthews, H. K., Kuriyama, S., Moreno, M., Dunn, G. a, Parsons, M., Stern, C. D. and Mayor, R. (2008b). Contact inhibition of locomotion in vivo controls neural crest directional migration. *Nature* **456**, 957–61.

Carmona-Fontaine, C., Theveneau, E., Tzekou, A., Tada, M., Woods, M., Page, K. M., Parsons, M., Lambris, J. D. and Mayor, R. (2011). Complement fragment C3a controls mutual cell attraction during collective cell migration. *Dev. Cell* **21**, 1026–37.

Cebra-Thomas, J. A., Terrell, A., Branyan, K., Shah, S., Rice, R., Gyi, L., Yin, M., Hu,

Y., Mangat, G., Simonet, J., et al. (2013). Late-emigrating trunk neural crest cells in turtle embryos generate an osteogenic ectomesenchyme in the plastron. *Dev. Dyn.* **242**, 1223–1235.

Chalpe, A. J., Prasad, M., Henke, A. J. and Paulson, A. F. (2010). Regulation of cadherin expression in the chicken neural crest by the Wnt/??-catenin signaling pathway. *Cell Adhes. Migr.* **4**, 431–438.

Chang, C.-J., Chao, C.-H., Xia, W., Yang, J.-Y., Xiong, Y., Li, C.-W., Yu, W.-H., Rehman, S. K., Hsu, J. L., Lee, H.-H., et al. (2011). p53 regulates epithelial-mesenchymal transition and stem cell properties through modulating miRNAs. *Nat Cell Biol* **13**, 317–323.

Charrasse, S., Meriane, M., Comunale, F., Blangy, A. and Gauthier-Rouvière, C. (2002). N-cadherin-dependent cell-cell contact regulates Rho GTPases and β-catenin localization in mouse C2C12 myoblasts. *J. Cell Biol.* **158**, 953–965.

Chen, W. and Obrink, B. (1991). Cell-cell contacts mediated by E-cadherin (uvomorulin) restrict invasive behavior of L-cells. *J. Cell Biol.* **114**, 319–327.

Cheung, M. and Briscoe, J. (2003). Neural crest development is regulated by the transcription factor Sox9. *Development* **130**, 5681–5693.

Cheung, M., Chaboissier, M. C., Mynett, A., Hirst, E., Schedl, A. and Briscoe, J. (2005). The transcriptional control of trunk neural crest induction, survival, and delamination. *Dev. Cell* **8**, 179–192.

Cho, H., Mu, J., Kim, J. K., Thorvaldsen, J. L., Chu, Q., Crenshaw, E. B., Kaestner, K. H., Bartolomei, M. S., Shulman, G. I. and Birnbaum, M. J. (2001). Insulin Resistance and a Diabetes Mellitus-Like Syndrome in Mice Lacking the Protein Kinase Akt2 (PKBβ). *Science (80-.).* **292**, 1728 LP-1731.

Chrzanowska-Wodnicka, M. and Burridge, K. (1996). Rho-stimulated Contractiliry

Drives the Formation of Stress Fibers and Focal Adhesions. *J. Cell Biol.* **133**, 1403–1415.

Clay, M. R. and Halloran, M. C. (2010). Control of neural crest cell behavior and migration: Insights from live imaging. *Cell Adh. Migr.* **4**, 586–94.

Clay, M. R. and Halloran, M. C. (2013). Rho activation is apically restricted by Arhgap1 in neural crest cells and drives epithelial-to-mesenchymal transition. *Development* **140**, 3198–209.

Clay, M. R. and Halloran, M. C. (2014). Cadherin 6 promotes neural crest cell detachment via F-actin regulation and influences active Rho distribution during epithelial-to-mesenchymal transition. *Development* **141**, 2506–15.

Comber, K., Huelsmann, S., Evans, I., Sánchez-Sánchez, B., Chalmers, a, Reuter, R., Wood, W. and Martín-Bermudo, M. (2013). A dual role for the βPS integrin myospheroid in mediating Drosophila embryonic macrophage migration. *J. Cell Sci.* **126**, 3475–84.

Copp, A. J., Greene, N. D. E. and Murdoch, J. N. (2003). The genetic basis of mammalian neurulation. *Nat. Rev. Genet.* **4**, 784–93.

Dady, A., Blavet, C. and Duband, J. L. (2012). Timing and kinetics of E- to N-cadherin switch during neurulation in the avian embryo. *Dev. Dyn.* **241**, 1333–1349.

Damm, E. W. and Winklbauer, R. (2011). PDGF-A controls mesoderm cell orientation and radial intercalation during Xenopus gastrulation. *Development* **138**, 565–75.

Datta, S. R., Dudek, H., Xu, T., Masters, S., Haian, F., Gotoh, Y. and Greenberg, M. E. (1997). Akt phosphorylation of BAD couples survival signals to the cell-intrinsic death machinery. *Cell* **91**, 231–241.

Davis, M. A., Ireton, R. C. and Reynolds, A. B. (2003). A core function for p120-catenin in cadherin turnover. *J. Cell Biol.* **163**, 525–534.

Davis, J. R., Huang, C.-Y., Zanet, J., Harrison, S., Rosten, E., Cox, S., Soong, D. Y., Dunn, G. a and Stramer, B. M. (2012). Emergence of embryonic pattern through contact inhibition of locomotion. *Development* **139**, 4555–60.

Davis, J. R., Luchici, A., Mosis, F., Thackery, J., Salazar, J. A., Mao, Y., Dunn, G. A., Betz, T., Miodownik, M. and Stramer, B. M. (2015). Inter-cellular forces orchestrate contact inhibition of locomotion. *Cell* **161**, 361–373.

Davy, A., Aubin, J. and Soriano, P. (2004). Ephrin-B1 forward and reverse signaling are required during mouse development. *Genes Dev.* **18**, 572–583.

De Calisto, J., Araya, C., Marchant, L., Riaz, C. F. and Mayor, R. (2005). Essential role of non-canonical Wnt signalling in neural crest migration. *Development* **132**, 2587–97.

Delannet, M., Martin, F., Bossy, B., Cheresh, D. A., Reichardt, L. F. and Duband, J. L. (1994). Specific roles of the alpha V beta 1, alpha V beta 3 and alpha V beta 5 integrins in avian neural crest cell adhesion and migration on vitronectin. *Development* **120**, 2687–2702.

Demoulin, J.-B. and Essaghir, A. (2014). PDGF receptor signaling networks in normal and cancer cells. *Cytokine Growth Factor Rev.* **25**, 273–83.

Desai, R. A., Gopal, S. B., Chen, S. and Chen, C. S. (2013). Contact inhibition of locomotion probabilities drive solitary versus collective cell migration. *J. R. Soc. Interface* **10**, 20130717–20130717.

Ding, H., Wu, X., Kim, I., Tam, P. P., Koh, G. Y. and Nagy, a (2000). The mouse Pdgfc gene: dynamic expression in embryonic tissues during organogenesis. *Mech. Dev.* **96**, 209–13.

Ding, H., Wu, X., Boström, H., Kim, I., Wong, N., Tsoi, B., O'Rourke, M., Koh, G. Y., Soriano, P., Betsholtz, C., et al. (2004). A specific requirement for PDGF-C in palate formation and PDGFR-alpha signaling. *Nat. Genet.* **36**, 1111–1116.

Dottori, M., Gross, M. K., Labosky, P. and Goulding, M. (2001). The winged-helix transcription factor Foxd3 suppresses interneuron differentiation and promotes neural crest cell fate. *Development* **128**, 4127–4138.

Duband, J. L. (2010). Diversity in the molecular and cellular strategies of epithelium-to- mesenchyme transitions: Insights from the neural crest. *Cell Adhes. Migr.* **4**, 458–482.

Duband, J. L. and Thiery, J. P. (1982). Distribution of fibronectin in the early phase of avian cephalic neural crest cell migration. *Dev. Biol.* **93**, 308–323.

Duband, J. L., Dady, A. and Fleury, V. (2015). *Resolving time and space constraints during neural crest formation and delamination*. 1st ed. Elsevier Inc.

Duchek, P. and Rørth, P. (2001). Guidance of cell migration by EGF receptor signaling during Drosophila oogenesis. *Science* **291**, 131–3.

Duchek, P., Somogyi, K., Jekely, G., Beccari, S. and Rorth, P. (2001). Guidance of cell migration by the Drosophila PDGF/VEGF receptor. *Cell* **107**, 17–26.

Dufour, S., Duband, J. L., Humphries, M. J., Obara, M., Yamada, K. M. and Thiery, J. P. (1988). Attachment, spreading and locomotion of avian neural crest cells are mediated by multiple adhesion sites on fibronectin molecules. *EMBO J.* **7**, 2661–71.

Dumortier, J. G., Martin, S., Meyer, D., Rosa, F. M. and David, N. B. (2012). Collective mesendoderm migration relies on an intrinsic directionality signal transmitted through cell contacts. *Proc. Natl. Acad. Sci.* **109**, 16945–16950.

Dupin, I., Camand, E. and Etienne-Manneville, S. (2009). Classical cadherins control nucleus and centrosome position and cell polarity. *J. Cell Biol.* **185**, 779–786.

Duttlinger, R., Manova, K., Berrozpe, G., Chu, T. Y., DeLeon, V., Timokhina, I., Chaganti, R. S., Zelenetz, a D., Bachvarova, R. F. and Besmer, P. (1995). The Wsh and Ph mutations affect the c-kit expression profile: c-kit misexpression in embryogenesis impairs melanogenesis in Wsh and Ph mutant mice. *Proc. Natl. Acad. Sci. U. S. A.* **92**, 3754–8.

Eberhart, J. K., He, X., Swartz, M. E., Yan, Y.-L., Song, H., Boling, T. C., Kunerth, A. K., Walker, M. B., Kimmel, C. B. and Postlethwait, J. H. (2008). MicroRNA Mirn140 modulates Pdgf signaling during palatogenesis. *Nat. Genet.* **40**, 290–8.

Eckert, M. A., Lwin, T. M., Chang, A. T., Kim, J., Danis, E., Ohno-Machado, L. and Yang, J. (2011). Twist1-Induced Invadopodia Formation Promotes Tumor Metastasis. *Cancer Cell* **19**, 372–386.

Eickholt, B. J., Mackenzie, S. L., Graham, A., Walsh, F. S. and Doherty, P. (1999). Evidence for collapsin-1 functioning in the control of neural crest migration in both trunk and hindbrain regions. *Development* **126**, 2181–2189.

Epperlein, H. H., Halfter, W. and Tucker, R. P. (1988). The distribution of fibronectin and tenascin along migratory pathways of the neural crest in the trunk of amphibian embryos. *Development* **103**, 743–56.

Fan, Q., Cheng, C., Knight, Z. A., Haas-kogan, D., Stokoe, D., James, C. D., Mccormick, F., Shokat, K. M. and Weiss, A. (2009). EGFR signals to mTOR through PKC and independently of Akt in Glioma. **2**,.

Fantauzzo, K. A. and Soriano, P. (2014). PI3K-mediated PDGFRα signaling regulates survival and proliferation in skeletal development through p53-dependent intracellular pathways. *Genes Dev.* **28**, 1005–1017.

Fantauzzo, K. A. and Soriano, P. (2015). *Receptor tyrosine kinase signaling: Regulating neural crest development one phosphate at a time*. 1st ed. Elsevier Inc.

Fredriksson, L., Li, H., Fieber, C., Li, X. and Eriksson, U. (2004). Tissue plasminogen activator is a potent activator of PDGF-CC. *EMBO J.* **23**, 3793–3802.

Friedl, P. and Gilmour, D. (2009). Collective cell migration in morphogenesis, regeneration and cancer. *Nat. Rev. Mol. Cell Biol.* **10**, 445–457.

Fritz, R. D., Menshykau, D., Martin, K., Reimann, A., Pontelli, V. and Pertz, O. (2015). SrGAP2-Dependent Integration of Membrane Geometry and Slit-Robo-Repulsive Cues Regulates Fibroblast Contact Inhibition of Locomotion. *Dev. Cell* **35**, 78–92.

Fruttiger, M., Karlsson, L., Hall, a C., Abramsson, a, Calver, a R., Boström, H., Willetts, K., Bertold, C. H., Heath, J. K., Betsholtz, C., et al. (1999). Defective oligodendrocyte development and severe hypomyelination in PDGF-A knockout mice. *Development* **126**, 457–467.

Fulga, T. a and Rørth, P. (2002). Invasive cell migration is initiated by guided growth of long cellular extensions. *Nat. Cell Biol.* **4**, 715–9.

Gammill, L. S., Constanza, G. and Bronner-Fraser, M. (2007). Neuropilin 2/Semaphorin 3F Signaling is essential for cranial neural crest migration and trigeminal ganglion condensation. *J. Neurobiol.* **66**, 677–686.

Gans, C. and Northcutt, R. G. (1983). Neural Crest and the Origin of Vertebrates: A New Head. *Science (80-.).* **220**, 268 LP-273.

Geissler, E. N., McFarland, E. C. and Russell, E. S. (1981). Analysis of pleiotropism at the dominant white-spotting (W) locus of the house mouse: a description of ten new W alleles. *Genetics* **97**, 337–361.

Giannetti, K., Corsinovi, D., Rossino, C., Appolloni, I., Malatesta, P. and Ori, M. (2016). Platelet derived growth factor B gene expression in the Xenopus laevis developing central nervous system. *Int. J. Dev. Biol.* **60**, 175–179.

Giovannone, D., Reyes, M., Reyes, R., Correa, L., Martinez, D., Ra, H., Gomez, G., Kaiser, J., Ma, L., Stein, M. P., et al. (2012). Slits affect the timely migration of neural crest cells via robo receptor. *Dev. Dyn.* **241**, 1274–1288.

Glasgow, J. E. and Daniele, R. P. (1994). Role of microtubules in random cell migration: Stabilization of cell polarity. *Cell Motil. Cytoskeleton* **27**, 88–96.

Gloushankova, N. a, Krendel, M. F., Alieva, N. O., Bonder, E. M., Feder, H. H., Vasiliev, J. M. and Gelfand, I. M. (1998). Dynamics of contacts between lamellae of fibroblasts: essential role of the actin cytoskeleton. *Proc. Natl. Acad. Sci. U. S. A.* **95**, 4362–4367.

Goicoechea, S. M., Awadia, S. and Garcia-Mata, R. (2014). I'm coming to GEF you: Regulation of RhoGEFs during cell migration. *Cell Adhes. Migr.* **8**, 535–549.

Grassot, J., Gouy, M., Perrie, G. and Mouchiroud, G. (2006). Origin and Molecular Evolution of Receptor Tyrosine Kinases with Immunoglobulin-Like Domains. *Mol. Biol. Evol.* **23**, 1232–1241.

Grosheva, I., Shtutman, M., Elbaum, M. and Bershadsky, a D. (2001). p120 catenin affects cell motility via modulation of activity of Rho-family GTPases: a link between cell-cell contact formation and regulation of cell locomotion. *J. Cell Sci.* **114**, 695–707.

Groysman, M., Shoval, I. and Kalcheim, C. (2008). A negative modulatory role for rho and rho-associated kinase signaling in delamination of neural crest cells. *Neural Dev.* **3**, 27.

Grüneberg, H. and Truslove, G. M. (1960). Two closely linked genes in the mouse.

Genet. Res. **1**, 69–90.

Han, J., Luby-Phelps, K., Das, B., Shu, X., Xia, Y., Mosteller, R. D., Krishna, U. M., Falck, J. R., White, M. A. and Broek, D. (1998). Role of substrates and products of PI 3-kinase in regulating activation of Rac-related guanosine triphosphatases by Vav. *Science (80-.).* **279**, 558–560.

Hanada, M., Feng, J. and Hemmings, B. A. (2004). Structure, regulation and function of PKB/AKT - A major therapeutic target. *Biochim. Biophys. Acta - Proteins Proteomics* **1697**, 3–16.

Harris, A. (1973). Location of cellular adhesions to solid substrata. *Dev. Biol.* **35**, 97–114.

Haÿ, E., Nouraud, A. and Marie, P. J. (2009). N-cadherin negatively regulates osteoblast proliferation and survival by antagonizing Wnt, ERK and PI3K/Akt signalling. *PLoS One* **4**,.

He, F. and Soriano, P. (2013). A Critical Role for PDGFRα Signaling in Medial Nasal Process Development. *PLoS Genet.* **9**,.

Heaysman, J. E. and Pegrum, S. M. (1973). Early contacts between normal fibroblasts and mouse sarcoma cells. An ultrastructural study. *Exp. Cell Res.* **78**, 479–481.

Heeneman, S., Haendeler, J., Saito, Y., Ishida, M. and Berk, B. C. (2000). Angiotensin II induces transactivation of two different populations of the platelet-derived growth factor ?? receptor: Key role for the p66 adaptor protein Shc. *J. Biol. Chem.* **275**, 15926–15932.

Heldin, C.-H. (2004). Platelet-derived growth factor--an introduction. *Cytokine Growth Factor Rev.* **15**, 195–6.

Heldin, C.-H. (2012). Autocrine PDGF stimulation in malignancies. *Ups. J. Med. Sci.* **117**, 83–91.

Heldin, C.-H. and Lennartsson, J. (2013). Structural and functional properties of platelet-derived growth factor and stem cell factor receptors. *Cold Spring Harb. Perspect. Biol.* **5**, a009100.

Heldin, C. H. and Westermark, B. (1999). Mechanism of action and in vivo role of platelet-derived growth factor. *Physiol. Rev.* **79**, 1283–316.

Heldin, C. H., Westermark, B. and Wasteson, A. (1979). Platelet-derived growth factor: purification and partial characterization. *Proc. Natl. Acad. Sci. U. S. A.* **76**, 3722–6.

Heldin, C. H., Ostman, a and Rönnstrand, L. (1998). Signal transduction via platelet-derived growth factor receptors. *Biochim. Biophys. Acta* **1378**, F79-113.

Higuchi, M., Masuyama, N., Fukui, Y., Suzuki, A. and Gotoh, Y. (2001). Akt mediates Rac/Cdc42-regulated cell motility in growth factor-stimulated cells and in invasive PTEN knockout cells. *Curr. Biol.* **11**, 1958–1962.

Ho, L., Symes, K. and Yordán, C. (1994). Localization of PDGF A and PDGFRα mRNA in Xenopus embryos suggests signalling from neural ectoderm and pharyngeal endoderm to neural crest cells. *Mech. Dev.* **48**, 165–174.

Hoch, R. V and Soriano, P. (2003). Roles of PDGF in animal development. *Development* **130**, 4769–84.

Holmes, D. I. R. and Zachary, I. (2005). The vascular endothelial growth factor (VEGF) family: angiogenic factors in health and disease. *Genome Biol.* **6**, 209.

Hopwood, N. D., Pluck, A. and Gurdon, J. B. (1989). A Xenopus mRNA related to

Drosophila twist is expressed in response to induction in the mesoderm and the neural crest. *Cell* **59**, 893–903.

Huttenlocher, A., Lakonishok, M., Kinder, M., Wu, S., Truong, T., Knudsen, K. A. and Horwitz, A. F. (1998). Integrin and cadherin synergy regulates contact inhibition of migration and motile activity. *J. Cell Biol.* **141**, 515–526.

Itoh, R. E., Kurokawa, K., Ohba, Y., Yoshizaki, H., Mochizuki, N. and Matsuda, M. (2002). Activation of rac and cdc42 video imaged by fluorescent resonance energy transfer-based single-molecule probes in the membrane of living cells. *Mol. Cell. Biol.* **22**, 6582–6591.

Izzard, C. S. and Lochner, L. R. (1976). Cell-to-substrate contacts in living fibroblasts: an interference reflexion study with an evaluation of the technique. *J. Cell Sci.* **21**, 129–159.

Jackson, R. E. and Eickholt, B. J. (2009). Semaphorin signalling. *Curr. Biol.* **19**, 504–507.

Jechlinger, M., Sommer, A., Moriggl, R., Seither, P., Kraut, N., Capodiecci, P., Donovan, M., Cordon-Cardo, C., Beug, H. and Gr??nert, S. (2006a). Autocrine PDGFR signaling promotes mammary cancer metastasis. *J. Clin. Invest.* **116**, 1561–1570.

Jechlinger, M., Jechlinger, M., Sommer, A., Sommer, A., Moriggl, R., Moriggl, R., Seither, P., Seither, P., Kraut, N., Kraut, N., et al. (2006b). Autocrine PDGFR signalling promotes mammary cancer metastasis. *J. Clin. Invest.* **116**, 1–10.

Jeibmann, A., Halama, K., Witte, H. T., Kim, S. N., Eikmeier, K., Koos, B., Klämbt, C. and Paulus, W. (2015). Involvement of CD9 and PDGFR in migration is evolutionarily conserved from Drosophila glia to human glioma. *J. Neurooncol.* **124**, 373–383.

Jia, L., Cheng, L. and Raper, J. (2005). Slit/Robo signaling is necessary to confine early neural crest cells to the ventral migratory pathway in the trunk. *Dev. Biol.* **282**, 411–421.

Jiang, K., Zhong, B., Gilvary, D. L., Corliss, B. C., Hong-Geller, E., Wei, S. and Djeu, J. Y. (2000). Pivotal role of phosphoinositide-3 kinase in regulation of cytotoxicity in natural killer cells. *Nat Immunol* **1**, 419–425.

Joly, M., Kazlauskas, A., Fay, F. S. and Corvera, S. (1994). Disruption of PDGF Receptor Trafficking by Mutation of Its PI-3 Kinase Binding Sites Author (s): Marguerite Joly , Andrius Kazlauskas , Fredric S . Fay and Silvia Corvera Published by : American Association for the Advancement of Science Stable URL : ht. **263**, 684–687.

Kadir, S., Astin, J. W., Tahtamouni, L., Martin, P. and Nobes, C. D. (2011). Microtubule remodelling is required for the front-rear polarity switch during contact inhibition of locomotion. *J. Cell Sci.* **124**, 2642–2653.

Kai, M., Heisenberg, C. and Tada, M. (2008). Sphingosine-1-phosphate receptors regulate individual cell behaviours underlying the directed migration of prechordal plate progenitor cells during zebrafish gastrulation. **3051**, 3043–3051.

Kaltschmidt, B., Kaltschmidt, C. and Widera, D. (2012). Adult Craniofacial Stem Cells: Sources and Relation to the Neural Crest. *Stem Cell Rev. Reports* **8**, 658–671.

Kang, Y. and Massagué, J. (2004). Epithelial-mesenchymal transitions: Twist in development and metastasis. *Cell* **118**, 277–279.

Kasemeier-Kulesa, J. C., McLennan, R., Romine, M. H., Kulesa, P. M. and Lefcort, F. (2010). CXCR4 controls ventral migration of sympathetic precursor cells. *J. Neurosci. Off. J. Soc. Neurosci.* **30**, 13078–13088.

Kashef, J., Kohler, A., Kuriyama, S., Alfandari, D., Mayor, R. and Wedlich, D. (2009). Cadherin-11 regulates protrusive activity in Xenopus cranial neural crest cells upstream of Trio and the small GTPases. *Genes Dev.* 1393–1398.

Kawada, K., Upadhyay, G., Ferandon, S., Janarthanan, S., Hall, M., Vilardaga, J.-P. and Yajnik, V. (2009). Cell migration is regulated by platelet-derived growth factor receptor endocytosis. *Mol. Cell. Biol.* **29**, 4508–4518.

Kawakami, M., Umeda, M., Nakagata, N., Takeo, T. and Yamamura, K. (2011). Novel migrating mouse neural crest cell assay system utilizing P0-Cre/EGFP fluorescent time-lapse imaging. *BMC Dev. Biol.* **11**, 68.

Kay, R. R., Langride, P., Traynor, D. and Hoeller, O. (2008). Changing diresctions in the study of chemotaxis. *Nat. Rev. Mol. Cell Biol.* **9**, 455–463.

Kil, S. H., Krull, C. E., Cann, G., Clegg, D. and Bronner-Fraser, M. (1998). The α4Subunit of Integrin Is Important for Neural Crest Cell Migration. *Dev. Biol.* **202**, 29–42.

Klinghoffer, R. a, Mueting-Nelsen, P. F., Faerman, a, Shani, M. and Soriano, P. (2001). The two PDGF receptors maintain conserved signaling in vivo despite divergent embryological functions. *Mol. Cell* **7**, 343–54.

Klinghoffer, R. A., Hamilton, T. G., Hoch, R. and Soriano, P. (2002). An allelic series at the PDGFaR locus indicates unequal contributions of distinct signaling pathways during development. *Dev. Cell* **2**, 103–113.

Koestner, U., Shnitsar, I., Linnemannstöns, K., Hufton, A. L. and Borchers, A. (2008). Semaphorin and neuropilin expression during early morphogenesis of Xenopus laevis. *Dev. Dyn.* **237**, 3853–3863.

Kok, F. O., Shin, M., Ni, C. W., Gupta, A., Grosse, A. S., vanImpel, A., Kirchmaier, B. C., Peterson-Maduro, J., Kourkoulis, G., Male, I., et al. (2015). Reverse genetic

screening reveals poor correlation between morpholino-induced and mutant phenotypes in zebrafish. *Dev. Cell* **32**, 97–108.

Krause, M. and Gautreau, A. (2014). Steering cell migration: lamellipodium dynamics and the regulation of directional persistence. *Nat. Rev. Mol. Cell Biol.* **15**, 577–590.

Krull, C. E., Lansford, R., Gale, N. W., Collazo, A., Marcelle, C., Yancopoulos, G. D., Fraser, S. E. and Bronner-Fraser, M. (1997). Interactions of Eph-related receptors and ligands confer rostrocaudal pattern to trunk neural crest migration. *Curr. Biol.* **7**, 571–580.

Kundra, V., Escobedo, J. A., Kaziauskas, A., Kim, H. K., Rhee, S. G., Williams, L. T. and Zetter BR (1994). Regulation of chemotaxis by the platelet derived growth facto beta. *Nature* **367**, 532–8.

Kuriyama, S., Theveneau, E., Benedetto, A., Parsons, M., Tanaka, M., Charras, G., Kabla, A. and Mayor, R. (2014). In vivo collective cell migration requires an LPAR2-dependent increase in tissue fluidity. *J. Cell Biol.* **206**, 113–127.

Lallier, T., Deutzmann, R., Perris, R. and Bronner-Fraser, M. (1993). Neural crest cell interactions with laminin:Structural requirements and localization of the binding site of a1b1 integrin. *Dev. Biol.* 451–463.

Le Douarin and Kalcheim, C. (1999). *The Neural Crest*. 2nd ed. New York, NY: Cambridge University Press.

Learte, A. R., Forero, M. G. and Hidalgo, A. (2008). Gliatrophic and gliatropic roles of PVF/PVR signaling during axon guidance. *Glia* **56**, 164–176.

Lee, C., Zhang, F., Tang, Z., Liu, Y. and Li, X. (2016). PDGF-C: a new performer in the neurovascular interplay. *Trends Mol. Med.* **19**, 474–486.

Letourneau, P. C., Roche, F. K., Shattuck, T. A., Lemmon, V. and Takeichi, M. (1991). Interactions of Schwann cells with neurites and with other Schwann cells involve the calcium-dependent adhesion molecule, N-cadherin. *J. Neurobiol.* **22**, 707–720.

Levéen, P., Pekny, M., Gebre-Medhin, S., Swolin, B., Larsson, E. and Betsholtz, C. (1994). Mice deficient for PDGF B show renal, cardiovascular, and hematological abnormalities. *Genes Dev.* **8**, 1875–1887.

Lewis, A. E., Vasudevan, H. N., O'Neill, A. K., Soriano, P. and Bush, J. O. (2013). The widely used Wnt1-Cre transgene causes developmental phenotypes by ectopic activation of Wnt signaling. *Dev. Biol.* **379**, 229–234.

Li, X., Ponten, A., Aase, K., Karlsson, L., Abramsson, A., Uutela, M., Backstrom, G., Hellstrom, M., Bostrom, H., Li, H., et al. (2000). PDGF-C is a new protease-activated ligand for the PDGF [alpha]-receptor . *Nat Cell Biol* **2**, 302–309.

Liliental, J., Moon, S. Y., Lesche, R., Mamillapalli, R., Li, D., Zheng, Y., Sun, H. and Wu, H. (2000). Genetic deletion of the Pten tumor suppressor gene promotes cell motility by activation of Rac1 and Cdc42 GTPases. *Curr. Biol.* **10**, 401–404.

Lin, B., Yin, T., Wu, Y. I., Inoue, T. and Levchenko, A. (2015). Interplay between chemotaxis and contact inhibition of locomotion determines exploratory cell migration. *Nat. Commun.* **6**, 6619.

Lindahl, P., Johansson, B. R., Levéen, P. and Betsholtz, C. (1997). Pericyte Loss and Microaneurysm Formation in PDGF-B-Deficient Mice. *Science (80-.).* **277**, 242 LP-245.

Lindblom, P., Gerhardt, H., Liebner, S., Abramsson, A., Enge, M., Hellström, M., Bäckström, G., Fredriksson, S., Landegren, U., Nyström, H. C., et al. (2003). Endothelial PDGF-B retention is required for proper investment of pericytes in the microvessel wall. *Genes Dev.* **17**, 1835–1840.

Lisabeth, E. M., Falivelli, G. and Pasquale, E. B. (2013). Eph receptor signaling and ephrins. *Cold Spring Harb. Perspect. Biol.* **5**,.

Liu, J. P. and Jessell, T. M. (1998). A role for rhoB in the delamination of neural crest cells from the dorsal neural tube. *Development* **125**, 5055–5067.

Liu, L., Korzh, V., Balasubramaniyan, N., Ekker, M. and Ge, R. (2002a). Platelet-derived growth factor A (pdgf-a) expression during zebrafish embryonic development. *Dev. Genes Evol.* **212**, 298–301.

Liu, L., Chong, S.-W., Balasubramaniyan, N. V, Korzh, V. and Ge, R. (2002b). Platelet-derived growth factor receptor alpha (pdgfr-alpha) gene in zebrafish embryonic development. *Mech. Dev.* **116**, 227–30.

Lui, J. H., Nowakowski, T. J., Pollen, A. A., Javaherian, A., Kriegstein, A. R. and Oldham, M. C. (2014). Radial glia require PDGFD-PDGFR[bgr] signalling in human but not mouse neocortex. *Nature* **515**, 264–268.

Machacek, M., Hodgson, L., Welch, C., Elliott, H., Pertz, O., Nalbant, P., Abell, A., Johnson, G. L., Hahn, K. M. and Danuser, G. (2009). Coordination of Rho GTPase activities during cell protrusion. *Nature* **461**, 99–103.

Martin, K., Vilela, M., Jeon, N., Danuser, G. and Pertz, O. (2014). A Growth Factor-Induced, Spatially Organizing Cytoskeletal Module Enables Rapid and Persistent Fibroblast Migration. *Dev. Cell* **30**, 701–716.

Matthews, H. K., Marchant, L., Carmona-Fontaine, C., Kuriyama, S., Larraín, J., Holt, M. R., Parsons, M. and Mayor, R. (2008). Directional migration of neural crest cells in vivo is regulated by Syndecan-4/Rac1 and non-canonical Wnt signaling/RhoA. *Development* **135**, 1771–80.

Mayo, L. D. and Donner, D. B. (2001). A phosphatidylinositol 3-kinase/Akt pathway promotes translocation of Mdm2 from the cytoplasm to the nucleus. *Proc.*

Natl. Acad. Sci. U. S. A. **98**, 11598–11603.

Mayor, R. and Carmona-fontaine, C. (2010). Keeping in touch with contact inhibition of locomotion. **20**, 319–328.

Mayor, R. and Etienne-Manneville, S. (2016). The front and rear of collective cell migration. *Nat Rev Mol Cell Biol* **17**, 97–109.

Mayor, R. and Theveneau, E. (2014). The role of the non-canonical Wnt-planar cell polarity pathway in neural crest migration. *Biochem. J.* **457**, 19–26.

Mayor, R., Morgan, R. and Sargent, M. G. (1995). Induction of the prospective neural crest of Xenopus. **777**, 767–777.

Mayor, Roberto; Theveneau, E. (2013). The neural crest. *Development* **2251**, 2247–2251.

McCarthy, N., Liu, J. S., Richarte, A. M., Eskiocak, B., Lovely, C. Ben, Tallquist, M. D. and Eberhart, J. K. (2016). Pdgfra and Pdgfrb genetically interact during craniofacial development. *Dev. Dyn.* **245**, 641–652.

McDonald, J. A., Pinheiro, E. M., Kadlec, L., Schupbach, T. and Montell, D. J. (2006). Multiple EGFR ligands participate in guiding migrating border cells. *Dev. Biol.* **296**, 94–103.

McKeown, S. J., Wallace, A. S. and Anderson, R. B. (2013). Expression and function of cell adhesion molecules during neural crest migration. *Dev. Biol.* **373**, 244–257.

McLennan, R. and Kulesa, P. M. (2007). In vivo analysis reveals a critical role for neuropilin-1 in cranial neural crest cell migration in chick. *Dev. Biol.* **301**, 227–239.

McLennan, R. and Kulesa, P. M. (2010). Neuropilin-1 interacts with the second

branchial arch microenvironment to mediate chick neural crest cell dynamics. *Dev. Dyn.* **239**, 1664–1673.

McLennan, R., Teddy, J. M., Kasemeier-Kulesa, J. C., Romine, M. H. and Kulesa, P. M. (2010). Vascular endothelial growth factor (VEGF) regulates cranial neural crest migration in vivo. *Dev. Biol.* **339**, 114–125.

McLennan, R., Dyson, L., Prather, K. W., Morrison, J. a., Baker, R. E., Maini, P. K. and Kulesa, P. M. (2012). Multiscale mechanisms of cell migration during development: theory and experiment. *Development* **139**, 2935–2944.

McLennan, R., Schumacher, L. J., Morrison, J. A., Teddy, J. M., Ridenour, D. A., Box, A. C., Semerad, C. L., Li, H., McDowell, W., Kay, D., et al. (2015). VEGF signals induce trailblazer cell identity that drives neural crest migration. *Dev. Biol.* **407**, 12–25.

McMahon, A. P., Joyner, A. L., Bradley, A. and McMahon, J. A. (1992). The midbrain-hindbrain phenotype of Wnt-1- Wnt-1- mice results from stepwise deletion of engrailed-expressing cells by 9.5 days postcoitum. *Cell* **69**, 581–595.

Mellott, D. O. and Burke, R. D. (2008a). The molecular phylogeny of eph receptors and ephrin ligands. *BMC Cell Biol.* **9**, 27.

Mellott, D. O. and Burke, R. D. (2008b). Divergent roles for Eph and ephrin in avian cranial neural crest. *BMC Dev. Biol.* **8**, 56.

Mellström, K., Höglund, A.-S., Nistér, M., Heldin, C.-H., Westermark, B. and Lindberg, U. (1983). The effect of platelet-derived growth factor on morphology and motility of human glial cells. *J. Muscle Res. {&} Cell Motil.* **4**, 589–609.

Merlot, S. and Firtel, R. A. (2003). Leading the way: Directional sensing through phosphatidylinositol 3-kinase and other signaling pathways. *J. Cell Sci.* **116**,

3471–8.

Milet, C. and Monsoro-Burq, A. H. (2012). Neural crest induction at the neural plate border in vertebrates. *Dev. Biol.* **366**, 22–33.

Minami, Y., Ikeda, W., Kajita, M., Fujito, T., Amano, H., Tamaru, Y., Kuramitsu, K., Sakamoto, Y., Monden, M. and Takai, Y. (2007). Necl-5/poliovirus receptor interacts in cis with integrin ??V??3 and regulates its clustering and focal complex formation. *J. Biol. Chem.* **282**, 18481–18496.

Mittal, A., Pulina, M., Hou, S. Y. and Astrof, S. (2010). Fibronectin and integrin alpha 5 play essential roles in the development of the cardiac neural crest. *Mech. Dev.* **127**, 472–484.

Monier-Gavelle, F. and Duband, J. L. (1997). Cross talk between adhesion molecules: Control of N-cadherin activity by intracellular signals elicited by β1 and β3 integrins in migrating neural crest cells. *J. Cell Biol.* **137**, 1663–1681.

Monsoro-Burq, A.-H., Fletcher, R. B. and Harland, R. M. (2003). Neural crest induction by paraxial mesoderm in Xenopus embryos requires FGF signals. *Development* **130**, 3111–24.

Montero, J., Kilian, B., Chan, J., Bayliss, P. E. and Heisenberg, C. (2003). Phosphoinositide 3-Kinase Is Required for Process Outgrowth and Cell Polarization of Gastrulating Mesendodermal Cells. **13**, 1279–1289.

Moore, R., Theveneau, E., Pozzi, S., Alexandre, P., Richardson, J., Merks, A., Parsons, M., Kashef, J., Linker, C. and Mayor, R. (2013). Par3 controls neural crest migration by promoting microtubule catastrophe during contact inhibition of locomotion. *Development* **140**, 4763–4775.

Morrison-Graham, K., Schatteman, G. C., Bork, T., Bowen-Pope, D. F. and Weston, J. a (1992). A PDGF receptor mutation in the mouse (Patch) perturbs the

development of a non-neuronal subset of neural crest-derived cells. *Development* **115**, 133–42.

Mui, K. L., Chen, C. S. and Assoian, R. K. (2016). The mechanical regulation of integrin-cadherin crosstalk organizes cells, signaling and forces. *J. Cell Sci.* **129**, 1093–100.

Nagasaki, T., Chapin, C. J. and Gundersen, G. G. (1992). Distribution of detyrosinated microtubules in motile NRK fibroblasts is rapidly altered upon cell-cell contact: implications for contact inhibition of locomotion. *Cell Motil. Cytoskeleton* **23**, 45–60.

Nagel, M., Tahinci, E., Symes, K. and Winklbauer, R. (2004). Guidance of mesoderm cell migration in the Xenopus gastrula requires PDGF signaling. *Development* **131**, 2727–36.

Nakagawa, S. and Takeichi, M. (1995). Neural crest cell-cell adhesion controlled by sequential and subpopulation-specific expression of novel cadherins. *Development* **121**, 1321–32.

Nakagawa, S. and Takeichi, M. (1998). Neural crest emigration from the neural tube depends on regulated cadherin expression. *Development* **125**, 2963–2971.

Nandadasa, S., Tao, Q., Menon, N. R., Heasman, J. and Wylie, C. (2009). N- and E-cadherins in Xenopus are specifically required in the neural and non-neural ectoderm, respectively, for F-actin assembly and morphogenetic movements. *Development* **136**, 1327–1338.

Nawrocki Raby, B., Polette, M., Gilles, C., Clavel, C., Strumane, K., Matos, M., Zahm, J. M., Van Roy, F., Bonnet, N. and Birembaut, P. (2001). Quantitative cell dispersion analysis: new test to measure tumor cell aggressiveness. *Int J Cancer* **93**, 644–652.

Neuner, R., Cousin, H., McCusker, C., Coyne, M. and Alfandari, D. (2009). Xenopus ADAM19 is involved in neural, neural crest and muscle development. *Mech. Dev.* **126**, 240–255.

Newgreen, D. F. (1982). Adhesion to extracellular materials by neural crest cells at the stage of initial migration. *Cell Tissue Res.* **227**, 297–317.

Newgreen, D. and Thiery, J. P. (1980). Fibronectin in early avian embryos: Synthesis and distribution along the migration pathways of neural crest cells. *Cell Tissue Res.* **211**, 269–291.

Nichols, D. H. (1981). Neural crest formation in the head of the mouse embryo as observed using a new histological technique. *J. Embryol. Exp. Morphol.* **64**, 105–20.

Nichols, D. H. (1987). Ultrastructure of neural crest formation in the midbrain/rostral hindbrain and preotic hindbrain regions of the mouse embryo. *Am. J. Anat.* **179**, 143–54.

Nieto, M. A., Sargent, M. G., Wilkinson, D. G. and Cooke, J. (1994). Control of Cell Behavior During Vertebrate Development By Slug, a Zinc-Finger Gene. *Science (80-.).* **264**, 835–839.

Nieuwkoop, N., D., P. and Faber., J. (1994). Normal Table of Xenopus laevis (Daudin)(Garland, New York).

Nimnual, A. S., Taylor, L. J. and Bar-Sagi, D. (2003). Redox-dependent downregulation of Rho by Rac. *Nat. Cell Biol.* **5**, 236–241.

Noren, N. K., Liu, B. P., Burridge, K., Kreft, B., Hill, C. and Carolina, N. (2000). p120 Catenin Regulates the Actin Cytoskeleton via Rho Family GTPases. *J. Cell Biol.* **150**, 567–579.

Ohta, Y., Hartwig, J. H. and Stossel, T. P. (2006). FilGAP, a Rho- and ROCK-regulated GAP for Rac binds filamin A to control actin remodelling. *Nat. Cell Biol.* **8**, 803–814.

Olesnicky Killian, E. C., Birkholz, D. A. and Artinger, K. B. (2009). A role for chemokine signaling in neural crest cell migration and craniofacial development. *Dev. Biol.* **333**, 161–172.

Omelchenko, T., Fetisova, E., Ivanova, O., Bonder, E. M., Feder, H., Vasiliev, J. M. and Gelfand, I. M. (2001). Contact interactions between epitheliocytes and fibroblasts: formation of heterotypic cadherin-containing adhesion sites is accompanied by local cytoskeletal reorganization. *Proc. Natl. Acad. Sci. USA* **98**, 8632–8637.

Orr-Urtreger, A. and Lonai, P. (1992). Platelet-derived growth factor-A and its receptor are expressed in separate, but adjacent cell layers of the mouse embryo. *Development* **115**, 1045.

Orrurtreger, A. and Lonai, P. (1992). Platelet-Derived Growth Factor-a and Its Receptor Are Expressed in Separate, but Adjacent Cell-Layers of the Mouse Embryo. *Development* **115**, 1045-.

Osborne, N. J., Begbie, J., Chilton, J. K., Schmidt, H. and Eickholt, B. J. (2005). Semaphorin/neuropilin signaling influences the positioning of migratory neural crest cells within the hindbrain region of the chick. *Dev. Dyn.* **232**, 939–949.

Ostman, A. and Heldin, C.-H. (2007). PDGF receptors as targets in tumor treatment. *Adv. Cancer Res.* **97**, 247–74.

Ouyang, M., Lu, S., Kim, T., Chen, C.-E., Seong, J., Leckband, D. E., Wang, F., Reynolds, A. B., Schwartz, M. A. and Wang, Y. (2013). N-cadherin regulates spatially polarized signals through distinct p120ctn and β-catenin-dependent signalling pathways. *Nat. Commun.* **4**, 1589.

Park, J., Leong, M. L. L., Buse, P., Maiyar, A. C., Firestone, G. L. and Hemmings, B. A. (1999). Serum and glucocorticoid-inducible kinase (SGK) is a target of the PI 3-kinase-stimulated signaling pathway. *EMBO J.* **18**, 3024–3033.

Pennock, S. and Kazlauskas, A. (2012). Vascular endothelial growth factor A competitively inhibits platelet-derived growth factor (PDGF)-dependent activation of PDGF receptor and subsequent signaling events and cellular responses. *Mol. Cell. Biol.* **32**, 1955–66.

Perez-Alcala, S., Nieto, M. A. and Barbas, J. a (2004). LSox5 regulates RhoB expression in the neural tube and promotes generation of the neural crest. *Development* **131**, 4455–4465.

Perris, R. and Perissinotto, D. (2000). Role of the extracellular matrix during neural crest cell migration. *Mech. Dev.* **95**, 3–21.

Pertz, O., Hodgson, L., Klemke, R. L. and Hahn, K. M. (2006). Spatiotemporal dynamics of RhoA activity in migrating cells. *Nature* **440**, 1069–72.

Peso, L. del, González-García, M., Page, C., Herrera, R. and Nuñez, G. (1997). Interleukin-3-Induced Phosphorylation of BAD Through the Protein Kinase Akt. *Science (80-.).* **278**, 687 LP-689.

Phillips, H. M., Papoutsi, T., Soenen, H., Ybot-Gonzalez, P., Henderson, D. J. and Chaudhry, B. (2012). Neural crest cell survival is dependent on Rho kinase and is required for development of the mid face in mouse embryos. *PLoS One* **7**,.

Rabadán, M. A., Herrera, A., Fanlo, L., Usieto, S., Carmona-Fontaine, C., Barriga, E. H., Mayor, R., Pons, S. and Martí, E. (2016). Delamination of neural crest cells requires transient and reversible Wnt inhibition mediated by Dact1/2. *Development* **143**, 2194–205.

Reig, G., Pulgar, E. and Concha, M. L. (2014). Cell migration: from tissue culture to

embryos. *Development* **141**, 1999–2013.

Rhee, J., Mahfooz, N. S., Arregui, C., Lilien, J., Balsamo, J. and VanBerkum, M. F. a (2002). Activation of the repulsive receptor Roundabout inhibits N-cadherin-mediated cell adhesion. *Nat. Cell Biol.* **4**, 798–805.

Richardson, W. D., Pringle, N., Mosley, M. J., Westermark, B. and Dubois-Dalcg, M. (1988). A role for platelet-derived growth factor in normal gliogenesis in the central nervous system. *Cell* **53**, 309–319.

Richarte, A. M., Mead, H. B. and Tallquist, M. D. (2007). Cooperation between the PDGF receptors in cardiac neural crest cell migration. *Dev. Biol.* **306**, 785–96.

Ridley, A. J. (2015). Rho GTPase signalling in cell migration. *Curr. Opin. Cell Biol.* **36**, 103–112.

Ridley, A. J. and Hall, A. (1992). The small GTP-binding protein rho regulates the assembly of focal adhesions and actin stress fibers in response to growth factors. *Cell* **70**, 389–399.

Ridley, A. J., Paterson, H. F., Johnston, C. L., Diekmann, D. and Hall, A. (1992). The small GTP-binding protein rac regulates growth factor-induced membrane ruffling. *Cell* **70**, 401–410.

Rinon, A., Molchadsky, A., Nathan, E., Yovel, G., Rotter, V., Sarig, R. and Tzahor, E. (2011). P53 Coordinates Cranial Neural Crest Cell Growth and Epithelial-Mesenchymal Transition/Delamination Processes. *Development* **138**, 1827–1838.

Robbins, J. R., McGuire, P. G., Wehrle-Haller, B. and Rogers, S. L. (1999). Diminished matrix metalloproteinase 2 (MMP-2) in ectomesenchyme-derived tissues of the Patch mutant mouse: regulation of MMP-2 by PDGF and effects on mesenchymal cell migration. *Dev. Biol.* **212**, 255–63.

Romashkova, J. A. and Makarov, S. S. (1999). NF-[kappa]B is a target of AKT in anti-apoptotic PDGF signalling. *Nature* **401**, 86–90.

Ross, R., Glomset, J., Kariya, B. and Harker, L. (1974). A platelet-dependent serum factor that stimulates the proliferation of arterial smooth muscle cells in vitro. *Proc. Natl. Acad. Sci. U. S. A.* **71**, 1207–10.

Rovasio, R. A., Delouvee, A., Yamada, K. M., Timpl, R. and Thiery, J. P. (1983). Neural crest cell migration: Requirements for exogenous fibronectin and high cell density. *J. Cell Biol.* **96**,.

Roycroft, A. and Mayor, R. (2015). Forcing contact inhibition of locomotion. *Trends Cell Biol.* **25**, 373–375.

Roycroft, A. and Mayor, R. (2016). Molecular basis of contact inhibition of locomotion. *Cell. Mol. Life Sci.* **73**, 1119–1130.

Rupp, P. A. and Kulesa, P. M. (2007). A role for RhoA in the two-phase migratory pattern of post-otic neural crest cells. *Dev. Biol.* **311**, 159–171.

Rupp, E., Siegbahn, A., Ronnstrand, L., Wernstedt, C., Claesson-welsh, L. and Heldin, C. (1994). A unique autophosphorylation site in the platelet-derived growth factor a-receptor from a heterodimeric receptor complex. *Eur. J. Biochem.* **225**, 29–41.

Sadaghiani, B. and Thibaud, C. H. (1987). Neural crest development in the Xenopus laevis embryo, studied by interspecific transplantation and scanning electron microscopy. *Dev. Biol.* **124**, 91–110.

Saito, D., Takase, Y., Murai, H. and Takahashi, Y. (2012). The Dorsal Aorta Initiates a Molecular Cascade That Instructs Sympatho-Adrenal Specification. *Science (80-.).* **336**, 1578–1581.

Sander, E. E., Ten Klooster, J. P., Van Delft, S., Van Der Kammen, R. A. and Collard, J. G. (1999). Rac downregulates Rho activity: Reciprocal balance between both GTPases determines cellular morphology and migratory behavior. *J. Cell Biol.* **147**, 1009–1021.

Santiago, A. and Erickson, C. A. (2002). Ephrin-B ligands play a dual role in the control of neural crest cell migration. *Development* **129**, 3621–3632.

Sauka-Spengler, T. and Bronner-Fraser, M. (2008). A gene regulatory network orchestrates neural crest formation. *Nat. Rev. Mol. Cell Biol.* **9**, 557–68.

Scarpa, E. and Mayor, R. (2016). Collective cell migration in development. *J. Cell Biol.* **212**, 143–155.

Scarpa, E., Roycroft, A., Theveneau, E., Terriac, E., Piel, M. and Mayor, R. (2013). A novel method to study contact inhibition of locomotion using micropatterned substrates.

Scarpa, E., Szabó, A., Bibonne, A., Theveneau, E., Parsons, M. and Mayor, R. (2015). Cadherin Switch during EMT in Neural Crest Cells Leads to Contact Inhibition of Locomotion via Repolarization of Forces. *Dev. Cell* **34**, 421–434.

Schatteman, G. C., Morrison-Graham, K., Van Koppen, A., Weston, J. A. and Bowen-Pope, D. F. (1992). Regulation and role of {PDGF} receptor a-subunit expression during embryogenesis. *Development* **115**, 123–131.

Schneider, C. A., Rasband, W. S. and Eliceiri, K. W. (2012). NIH Image to ImageJ: 25 years of image analysis. *Nat Meth* **9**, 671–675.

Schneller, M., Vuori, K. and Ruoslahti, E. (1997). alpha-v-beta-3 integrin associates with activated insulin and PDGF- beta receptors and potentiates the biological activity of PDGF. *EMBO J.* **16**, 5600–5607.

Schulte-Merker, S. and Stainier, D. Y. R. (2014). Out with the old, in with the new: reassessing morpholino knockdowns in light of genome editing technology. *Development* **141**, 3103–3104.

Severinsson, L., Ek, B., Mellstrom, K., Claesson-Welsh, L. and Heldin, C. H. (1990). Deletion of the kinase insert sequence of the platelet-derived growth factor beta-receptor affects receptor kinase activity and signal transduction. *Mol. Cell. Biol.* **10**, 801–809.

Shellard, A. and Mayor, R. (2016). Chemotaxis during neural crest migration. *Semin. Cell Dev. Biol.* **55**, 111–118.

Shoval, I. and Kalcheim, C. (2012). Antagonistic activities of Rho and Rac GTPases underlie the transition from neural crest delamination to migration. *Dev. Dyn.* **241**, 1155–1168.

Shoval, I., Ludwig, A. and Kalcheim, C. (2007). Antagonistic roles of full-length N-cadherin and its soluble BMP cleavage product in neural crest delamination. *Development* **134**, 491–501.

Smith, C. L. and Tallquist, M. D. (2010). PDGF function in diverse neural crest cell populations. *Cell Adh. Migr.* **4**, 561–6.

Smith, a, Robinson, V., Patel, K. and Wilkinson, D. G. (1997). The EphA4 and EphB1 receptor tyrosine kinases and ephrin-B2 ligand regulate targeted migration of branchial neural crest cells. *Curr. Biol.* **7**, 561–70.

Smith, E. M., Mitsi, M., Nugent, M. a and Symes, K. (2009). PDGF-A interactions with fibronectin reveal a critical role for heparan sulfate in directed cell migration during Xenopus gastrulation. *Proc. Natl. Acad. Sci. U. S. A.* **106**, 21683–8.

Solanas, G., Cortina, C., Sevillano, M. and Batlle, E. (2011). Cleavage of E-cadherin

by ADAM10 mediates epithelial cell sorting downstream of EphB signalling. *Nat. Cell Biol.* **13**, 1100–7.

Soriano, P. (1994). Abnormal kidney development and hematological disorders in PDGF beta-receptor mutant mice. *Genes Dev.* **8**, 1888–1896.

Soriano, P. (1997). The PDGF alpha receptor is required for neural crest cell development and for normal patterning of the somites. *Development* **124**, 2691–700.

Stephenson, D. a, Mercola, M., Anderson, E., Wang, C. Y., Stiles, C. D., Bowen-Pope, D. F. and Chapman, V. M. (1991). Platelet-derived growth factor receptor alpha-subunit gene (Pdgfra) is deleted in the mouse patch (Ph) mutation. *Proc. Natl. Acad. Sci. U. S. A.* **88**, 6–10.

Stewart, A. L., Young, H. M., Popoff, M. and Anderson, R. B. (2007). Effects of pharmacological inhibition of small GTPases on axon extension and migration of enteric neural crest-derived cells. *Dev. Biol.* **307**, 92–104.

Stocker, H., Andjelkovic, M., Oldham, S., Laffargue, M., Wymann, M. P., Hemmings, B. A. and Hafen, E. (2002). Living with Lethal PIP3 Levels: Viability of Flies Lacking PTEN Restored by a PH Domain Mutation in Akt/PKB. *Science (80-.).* **295**, 2088 LP-2091.

Stramer, B. and Mayor, R. (2016). Mechanisms and in vivo functions of contact inhibition of locomotion. *Nat. Rev. Mol. Cell Biol.* **advance on**,.

Stramer, B., Moreira, S., Millard, T., Evans, I., Huang, C. Y., Sabet, O., Milner, M., Dunn, G., Martin, P. and Wood, W. (2010). Clasp-mediated microtubule bundling regulates persistent motility and contact repulsion in Drosophila macrophages in vivo. *J. Cell Biol.* **189**, 681–689.

Sugiura, T., Taniguchi, Y., Tazaki, A., Ueno, N., Watanabe, K. and Mochii, M.

(2004). Differential gene expression between the embryonic tail bud and regenerating larval tail in Xenopus laevis. *Dev. Growth Differ.* **46**, 97–105.

Symes, K. and Mercola, M. (1996). Embryonic mesoderm cells spread in response to platelet-derived growth factor and signaling by phosphatidylinositol 3-kinase. *Proc. Natl. Acad. Sci. U. S. A.* **93**, 9641–9644.

Takakura, N., Yoshida, H., Ogura, Y., Kataoka, H., Nishikawa, S. and Nishikawa, S.-I. (1997). PDGFR Expression During Mouse Embryogenesis: Immunolocalization Analyzed by Whole-mount Immunohistostaining Using the Monoclonal Anti-mouse PDGFR Antibody APA5. *J. Histochem. Cytochem.* **45**, 883–893.

Takeichi, M. (1988). The cadherins: cell-cell adhesion molecules controlling animal morphogenesis. *Development* **102**, 639–655.

Tallquist, M. D., Weismann, K. E., Hellström, M. and Soriano, P. (2000). Early myotome specification regulates PDGFA expression and axial skeleton development. *Development* **127**, 5059–5070.

Tallquist, M. D., Tallquist, M. D. Soriano, P., Tallquist, M. D. and Soriano, P. (2003). Cell autonomous requirement for PDGFRalpha in populations of cranial and cardiac neural crest cells. *Development* **130**, 507–518.

Tanaka, M., Kuriyama, S. and Aiba, N. (2012). Nm23-H1 regulates contact inhibition of locomotion, which is affected by ephrin-B1. *J. Cell Sci.* **125**, 4343–53.

Taneyhill, L. a, Coles, E. G. and Bronner-Fraser, M. (2007). Snail2 directly represses cadherin6B during epithelial-to-mesenchymal transitions of the neural crest. *Development* **134**, 1481–1490.

Teddy, J. M. and Kulesa, P. M. (2004). In vivo evidence for short- and long-range cell communication in cranial neural crest cells. *Development* **131**, 6141–6151.

Testaz, S. and Duband, J. L. (2001). Central role of the alpha4beta1 integrin in the coordination of avian truncal neural crest cell adhesion, migration, and survival. *Dev. Dyn.* **222**, 127–140.

Theveneau, E. and Mayor, R. (2012). Neural crest delamination and migration: from epithelium-to-mesenchyme transition to collective cell migration. *Dev. Biol.* **366**, 34–54.

Theveneau, E., Marchant, L., Kuriyama, S., Gull, M., Moepps, B., Parsons, M. and Mayor, R. (2010). Collective chemotaxis requires contact-dependent cell polarity. *Dev. Cell* **19**, 39–53.

Theveneau, E., Steventon, B., Scarpa, E., Garcia, S., Trepat, X., Streit, A. and Mayor, R. (2013). Chase-and-run between adjacent cell populations promotes directional collective migration. *Nat. Cell Biol.* **15**, 763–72.

Théveneau, E., Duband, J.-L. and Altabef, M. (2007). Ets-1 confers cranial features on neural crest delamination. *PLoS One* **2**, e1142.

Thiery, J. P. and Sleeman, J. P. (2006). Complex networks orchestrate epithelial-mesenchymal transitions. *Nat. Rev. Mol. Cell Biol.* **7**, 131–42.

Thiery, J. P., Acloque, H., Huang, R. Y. J. and Nieto, M. A. (2009). Epithelial-mesenchymal transitions in development and disease. *Cell* **139**, 871–90.

Thomas, P. S., Kim, J., Nunez, S., Glogauer, M. and Kaartinen, V. (2010). Neural crest cell-specific deletion of Rac1 results in defective cell-matrix interactions and severe craniofacial and cardiovascular malformations. *Dev. Biol.* **340**, 613–625.

Turlo, K. A., Noel, O. D. V, Vora, R., LaRussa, M., Fassler, R., Hall-Glenn, F. and Iruela-Arispe, M. L. (2012). An essential requirement for beta1 integrin in the assembly of extracellular matrix proteins within the vascular wall. *Dev. Biol.*

365, 23–35.

Valius, M. and Kazlauskas, A. (1993). Phospholipase C-??1 and phosphatidylinositol 3 kinase are the downstream mediators of the PDGF receptor's mitogenic signal. *Cell* **73**, 321–334.

Van Den Akker, N. M. S., Winkel, L. C. J., Nisancioglu, M. H., Maas, S., Wisse, L. J., Armulik, A., Poelmann, R. E., Lie-Venema, H., Betsholtz, C. and Gittenberger-De Groot, A. C. (2008). PDGF-B signaling is important for murine cardiac development: Its role in developing atrioventricular valves, coronaries, and cardiac innervation. *Dev. Dyn.* **237**, 494–503.

Vasudevan, H. N., Mazot, P., He, F. and Soriano, P. (2015). Receptor tyrosine kinases modulate distinct transcriptional programs by differential usage of intracellular pathways. *Elife* **4**, 1–22.

Veevers-Lowe, J., Ball, S. G., Shuttleworth, A. and Kielty, C. M. (2011). Mesenchymal stem cell migration is regulated by fibronectin through α5β1-integrin-mediated activation of PDGFR-β and potentiation of growth factor signals. *J. Cell Sci.* **124**, 1288–1300.

Veselý, P. and Weiss, R. (1973). Cell locomotion and contact inhibition of normal and neoplastic rat cells. *Int. J. Cancer* **76**, 64–76.

Villar-Cerviño, V., Molano-Mazón, M., Catchpole, T., Valdeolmillos, M., Henkemeyer, M., Martínez, L. M., Borrell, V. and Marín, O. (2013). Contact Repulsion Controls the Dispersion and Final Distribution of Cajal-Retzius Cells. *Neuron* **77**, 457–471.

Vivanco, I. and Sawyers, C. (2002). The phosphatidylinositol 3-Kinase-AKT pathway in human cancer. *Nat. Rev. - Cancer* **2**, 489–501.

Wehrle-Haller, B. (2003). The role of Kit-ligand in melanocyte development and

epidermal homeostasis. *Pigment cell Res.* **16**, 287–296.

Wehrle-Haller, B., Morrison-Graham, K. and Weston, J. a (1996). Ectopic c-kit Expression Affects the Fate of Melanocyte Precursors inPatchMutant Embryos. *Dev. Biol.* **177**, 463–474.

Welch, H., Eguinoa, A., Stephens, L. R. and Hawkins, P. T. (1998). Protein kinase B and Rac are activated in parallel within a phosphatidylinositide 30H-kinase-controlled signaling pathway. *J. Biol. Chem.* **273**, 11248–11256.

Wennstrom, S., Siegbahn, A., Yokote, K., Arvidsson, A. K., Heldin, C. H., Mori, S. and Claesson-Welsh, L. (1994). Membrane ruffling and chemotaxis transduced by the PDGF beta-receptor require the binding site for phosphatidylinositol 3' kinase. *Oncogene* **9**, 651–660.

Wennström, S., Hawkins, P., Cooke, F., Hara, K., Yonezawa, K., Kasuga, M., Jackson, T., Claesson-Welsh, L. and Stephens, L. (1994). Activation of phosphoinositide 3-kinase is required for PDGF-stimulated membrane ruffling. *Curr. Biol.* **4**, 385–393.

Wilson, P. a and Melton, D. a (1994). Mesodermal patterning by an inducer gradient depends on secondary cell-cell communication. *Curr Biol* **4**, 676–86.

Winklbauer, R., Nagel, M., Selchow, A. and Wacker, S. (1996). Mesoderm migration in the Xenopus gastrula. *Int. J. Dev. Biol.* **40**, 305–311.

Woodard, a S., García-Cardeña, G., Leong, M., Madri, J. a, Sessa, W. C. and Languino, L. R. (1998). The synergistic activity of alphavbeta3 integrin and PDGF receptor increases cell migration. *J. Cell Sci.* **111 (Pt 4**, 469–478.

Woods, M. L., Carmona-Fontaine, C., Barnes, C. P., Couzin, I. D., Mayor, R. and Page, K. M. (2014). Directional collective cell migration emerges as a property of cell interactions. *PLoS One* **9**,.

Wu, Q., Hou, X., Xia, J., Qian, X., Miele, L., Sarkar, F. H. and Wang, Z. (2013). Emerging roles of PDGF-D in EMT progression during tumorigenesis. *Cancer Treat. Rev.* **39**, 640–6.

Xu, X., Li, W. E. I., Huang, G. Y., Meyer, R., Chen, T., Luo, Y., Thomas, M. P., Radice, G. L. and Lo, C. W. (2001). Modulation of mouse neural crest cell motility by N-cadherin and connexin 43 gap junctions. *J. Cell Biol.* **154**, 217–229.

Xue, G. and Hemmings, B. A. (2013). PKB/akt-dependent regulation of cell motility. *J. Natl. Cancer Inst.* **105**, 393–404.

Yamaguchi, N., Mizutani, T., Kawabata, K. and Haga, H. (2015). Leader cells regulate collective cell migration via Rac activation in the downstream signaling of integrin β1 and PI3K. *Sci. Rep.* **5**, 7656.

Yang, X., Chrisman, H. and Weijer, C. J. (2008). PDGF signalling controls the migration of mesoderm cells during chick gastrulation by regulating N-cadherin expression. **3530**, 3521–3530.

Yu, H. H. and Moens, C. B. (2005). Semaphorin signaling guides cranial neural crest cell migration in zebrafish. *Dev. Biol.* **280**, 373–385.

Zemskov, E. A., Loukinova, E., Mikhailenko, I., Coleman, R. A., Strickland, D. K. and Belkin, A. M. (2009). Regulation of platelet-derived growth factor receptor function by integrin-associated cell surface transglutaminase. *J Biol Chem* **284**, 16693–16703.

Zhou, B. P., Liao, Y., Xia, W., Zou, Y., Spohn, B. and Hung, M.-C. (2001). HER-2/neu induces p53 ubiquitination via Akt-mediated MDM2 phosphorylation. *Nat Cell Biol* **3**, 973–982.